NUMERICAL METHODS FOR PRICING PASSPORT OPTION

by

Ankur Kanaujiya

DEPARTMENT OF MATHEMATICS

INDIAN INSTITUTE OF TECHNOLOGY GUWAHATI

GUWAHATI-781039, INDIA

March, 2018

NUMERICAL METHODS FOR PRICING PASSPORT OPTION

A Thesis submitted

in partial fulfillment of the requirements

for the degree of

DOCTOR OF PHILOSOPHY

by

Ankur Kanaujiya

(Roll Number: 126123010)

to the

DEPARTMENT OF MATHEMATICS

INDIAN INSTITUTE OF TECHNOLOGY GUWAHATI

March, 2018

Declaration

I hereby declare that the work contained in this thesis entitled **"Numerical Methods for Pricing Passport Option"** was done by me, under the supervision of **Dr. Siddhartha Pratim Chakrabarty**, Associate Professor, Department of Mathematics, Indian Institute of Technology Guwahati for the award of the degree of Doctor of Philosophy and this work has not been submitted elsewhere for a degree.

March, 2018

Ankur Kanaujiya
Roll No. 126123010
Department of Mathematics
Indian Institute of Technology Guwahati

Certificate

It is certified that the work contained in this thesis entitled **"Numerical Methods for Pricing Passport Option"** by **Ankur Kanaujiya,** a student in Department of Mathematics, Indian Institute of Technology Guwahati, for the award of the degree of Doctor of Philosophy has been carried out under my supervision and this work has not been submitted elsewhere for a degree.

March, 2018

Dr. Siddhartha Pratim Chakrabarty
Associate Professor
Department of Mathematics
Indian Institute of Technology Guwahati

Dedicated

to

my Parents

Acknowledgements

I would like to acknowledge all those people who have helped me to carry out the research and shared their precious experience.

I am very grateful to my supervisor Siddhartha Pratim Chakrabarty for his generous guidance throughout these years. Also, I would like to express my deep appreciation for his patience, understanding and support. He helped me to overcome many obstacles that emerged while working on several problems. In a good way, he always used to push for better results. He was deeply involved and helped me in every possible way. His continuous encouragement and advice made it possible for me to work on this thesis. Without his guidance and persistent help, this dissertation would not have been possible.

I want to convey my sincere thanks to the doctoral committee of members Prof. Rajen K. Sinha, Prof. Anoop K. Dass, Dr. Arabin Kumar Dey and Dr. K.V. Srikanth for reviewing my research work periodically and giving valuable suggestions for improvement on the same. Also, I would like to take this opportunity to express my gratitude to all the faculty members of the Department of Mathematics who have offered help directly or indirectly at different stages during my research work.

I am also indebted to my friends and colleagues of Department of Mathematics, IIT Guwahati, who have motivated and helped me in many situations directly or indirectly. I thank my fellow students for all the fun we have had in these years. I would particularly like to thank Sougata, Swapnendu and Ashish for their friendly and wonderful company throughout my research life. I take this opportunity to thank Abhishek, Anirban, Naba Da, Jayanta, Anirudha, Hiranmoy, Swarup and Balasubramani, for their encouragement and support. I am also thankful to my seniors Dr. Dinesh Kumar and Dr. Kalyan Manna, and my junior Mr. Sonjoy Pan.

I sincerely acknowledge *Indian Institute of Technology Guwahati* for providing a very nice educational environment. I am highly grateful to the *Ministry of Human Resource Development*, Government of India for providing me financial assistance for the completion of my thesis work.

I thank our technical staff Mr. Santanu Majumdar, Mr. Pranpratim Borgohain and Mr. Pranab Jyoti Boro and office staff members Mr. Sridhar Samal, Mr. Phatik Kumar and Mr. Saurav Choudhury of the department, for their assistance in various ways during my research period.

I thank both the examiners of the thesis for their valuable comments and suggestions.

Finally, it is not possible for me to adequately express my heartfelt gratitude towards my parents (my mother Mrs. Shishu Palti and my father Mr. Hari Ram Kanaujiya) and my brother (Mr. Abhai Kanaujiya) for everything they have done for me from the very first day of my life. I can not thank them enough for their love which has been the driving force in every aspect of my life. I would also like to convey my deepest love to all my family members.

March, 2018 Ankur Kanaujiya

Abstract

Passport option is a financial derivative with the contingent claim being dependent on the value of a trading account. The valuation of the passport option can be obtained through the solution of a nonlinear backward pricing partial differential equation (PDE). In this thesis, we examine the numerical approaches to pricing the passport option, by solving the pricing PDE for both the symmetric case as well as the non-symmetric case.

A general introduction and description of the passport option, both theoretical and numerical, along with the pricing PDE and the holder's optimal trading strategy for European passport option is presented. In the symmetric case (when the cost of carry is identical to the risk-free rate), it is observed that the pricing PDE becomes linear parabolic for which a closed form solution exists. The absence of the same in the non-symmetric case motivated the focus on the numerical approaches as presented in this thesis.

A radial basis function approach, along with grid refinement in spatial direction is proposed for European type passport option. The scheme which is first and second order accurate in time and space, respectively, is numerically presented for both the symmetric and non-symmetric case. Next, we consider a three time level scheme that is amenable for non-smooth payoffs and does not produce oscillation for larger time steps (especially in case of Greeks for the symmetric case, which are also derived in the thesis). This scheme is second order accurate in both time and space. Numerical results using three time level scheme for both the cases are presented. We then undertake the numerical valuation of American passport option using three time level schemes with the resulting discretized system of inequalities being solved using the Brennan-Schwartz algorithm and projected successive over-relaxation (PSOR) method.

Finally, we present the higher order compact (HOC) schemes, for both European and American style passport options, with second and fourth order accuracy in time and space, respectively. However, basic numerical approach was able to achieve only second order accuracy in space, which was then improved up to third order in space by making use of grid stretching near the zero accumulated gain, giving higher order compact scheme with grid stretching (HOCGS). The numerical results using HOC and HOCGS schemes for European (both the cases) and American (non-symmetric case) passport options are presented.

Contents

List of Figures

List of Tables

Chapter 1

Introduction

1.1 Brief background

Financial markets in general and derivative markets in particular, have undergone significant growth both in terms of volume as well as the variety of derivative products that are traded in such markets. The valuation of financial derivatives involves several mathematical and computational complexities, which in turn has led to significant amount of work in the area of mathematical finance. Trading of derivatives serve a wide variety of financial requirements, especially hedging, arbitrage and speculation and are usually executed through an exchange or over the counter, with the latter typically taking place between large financial institutions [1]. This thesis will focus on one of the most widely analyzed financial derivative, namely, options. An option is a derivative which gives the holder or buyer of the option the right but not the obligation to buy or sell the underlying security on or before a pre-determined future date for a pre-specified price, with the obligation being assigned to the writer or seller of the option. Depending on whether the holder of the option has right to buy or sell the asset, the option is classified as being call or put respectively. The pre-determined future date on which the option can be exercised (classified as European) or before which the option is exercised (classified as American) is called the expiration date. The pre-specified price, which could be fixed or could be dependent on the asset price movement of the underlying security during the duration of the option, is called the strike price. Since an option confers a right without obligation on the holder, with a corresponding obligation without right for the writer, the holder has to pay a premium to the writer of the option for the leverage resulting from this arrangement. In the parlance of financial derivatives, this premium is referred

to as the price or value of the option. Clearly, the price of an American option will at least be the price of a European option.

In this thesis, the thrust of the work is on numerical approaches to the pricing of a particular option, namely, the passport option. This option belongs to a specific category of the financial derivatives, namely, an option on actively managed funds and was designed by Hyer et al. [2] at the Bankers Trust in 1997. While traditional financial derivatives typically have stocks or bonds as the underlying security, the more exotic ones can potentially include trading accounts as the underlying. The accumulated wealth of a trading account which is the result of gains and losses incurred by the securities of the trading account can by itself be treated as the underlying security of the option on this trading account. Clearly, the payoff or contingent claim, in this case, would be the accumulated gain value.

Passport option, which belongs to the class of trading account dependent option serves the purpose of protecting the underlying trading account, wherein the holder pays a premium to the writer, in exchange of being compensated for any loss incurred by the trading account, while retaining the profits made by the trading account [3, 4]. Such an arrangement clearly offers greater flexibility in terms of hedging the managed portfolios against adverse events, as compared to a standardized derivative on an index-linked portfolio. However, in order to limit the exposure risk of writers of such option, limitations on trading strategies for the trading account such as caps, floors and barriers are usually put in place. Thus the arrangement also serves the additional purpose of retaining a reasonable price level for the options.

Hyer et al. [2] at the time of designing and pricing passport option, considered a trading account (as the underlying) whose value was contingent on a traded security, modelled using the geometric Brownian motion (GBM). They demonstrate the existence of a risk-free hedging strategy with the optimal strategy being determined by a stochastic control problem. The arbitrage-free price of the passport option is ascertained using the strategy of maximizing the wealth, resulting in the Hamilton Jacobi Bellman (HJB) equation. The solution of the HJB equation, which is a backward partial differential equation (PDE) provides the price of the passport option. In order to analytically price the passport option for the symmetric case (when the risk-free rate is identical to the cost of the carry), the HJB equation is transformed to a heat equation, which is then solved

for by making use of the Green's function [2]. However, no analytic solution exists when the symmetric restriction is removed and consequently numerical results for this non-symmetric case was presented.

Andersen et al. [3] also examined the problem of valuation of passport option. While their model was motivated by [2], it is slightly different in that they considered the payoff function to be dependent on the gain from an investment strategy as opposed to the uninvested wealth accruing interest at a specific rate [5]. They established that the price of a passport option is the solution to a Markov control problem, by making an appropriate change to the numeraire. They derived a nonlinear PDE for the asset deflated option price and presented a closed form pricing formula for the symmetric case making use of Laplace transformation. The absence of closed form solution in the non-symmetric case, prompted them to resort to numerical PDE approaches using mixed implicit/explicit finite difference scheme and in particular they used the Crank-Nicholson scheme in actual implementation for determination of the passport option price. They further carried out the numerical study of several extensions of the passport option, namely, American exercise, discrete passport option and non-convex price function.

Nagayama [6] studied more generalized passport option and developed a numerical algorithm for the non-symmetric case, in addition to presenting an explicit formula for the valuation problem in the case when the risk-free rate is zero. In a technical report, Chan [7] presented a linear complementarity formulation to the problem for American passport option, wherein the optimal stopping time problem was decomposed into several variational inequality formulations. This problem was numerically approached using the Crank-Nicholson scheme and complementarity solver PATH (due to Dirkse and Feris [8]). Ahn et.al. [9] considered the pricing problem for passport option with the underlying trading account consisting of multiple assets, with the pricing problem being reduced to HJB equation. They also included discrete constraints for the problem which requires the solution to a linear complementarity problem. The utility aspect (in case of both the holder and seller) of trading a passport option and the gains made through the sale of passport option was also examined, with all these aspects being numerically illustrated. In a subsequent article [10], the authors, studied several exotic extension of the passport option, namely, chooser, barrier, smooth trader, reset, double stake, magic portion and switch passport option, with the corresponding HJB pricing equation along with the boundary

conditions being presented, which could potentially be solved using numerical methods.

Henderson and Hobson [11] making use of *Tanaka's formula* and the *Skorokhod Lemma* derived a simplified approach to pricing passport option by associating it with the price of lookback option. They further obtained the optimal strategy for a wide class of price processes. Subsequently, they [12] considered the problem by taking stochastic volatility into account with the volatility process being modeled through an autonomous stochastic differential equation (SDE). In [12], it was shown that the optimal strategy will remain unaffected, provided the Brownian motions, driving the asset pricing GBM model and the one in the volatility SDE, are independent of each other. The models used for numerical illustration were the ones due to Hull and White [13] and Stein and Stein [14]. The importance of this work lay in that the optimal strategy is unaffected by the variations in model specifications.

Shreve and Vecer in their article [15] proposed a broader class of option rather than just the passport option and introduced the concept of "options on traded account", wherein the restrictions on the trading strategy adopted by the option holder were removed, thereby allowing for the position taken by the holder to be arbitrary. The resulting optimal strategy was determined using Hajek's mean comparison theorem [16]. It turned out that the strategy reduces to that of passport option as a particular case. This enabled the option price to be reduced to a function of single non-temporal variable as opposed to a function of two non-temporal variables. Delbaen and Yor [17] applied the martingale theory and the theory of Bessel processes to price the passport option. They also discussed the discrete version of the passport option and established that the price of the passport option on two different norms on a continuous martingale are equal.

Finite element method using collocation approach was used in the numerical implication of the pricing problem in the thesis of Topper [4]. The resulting system of the nonlinear equation was solved using Newton's method along with finite difference methods for the purpose of time integration, both American and exotic types. Numerical methods for nonlinear equations in the option pricing problems are discussed by Pooley in his thesis [18]. In particular, the thesis examines trader compensation strategy making use of passport option. The problem of pricing passport option using a jump-diffusion model (which addresses some of the drawbacks of GBM) for the underlying traded security was

considered by Baojun and Yang in [19] where the pricing equation was obtained along with several other results including uniqueness of viscosity solution of the related HJB equations. Subsequently, [20] used the dynamic programming principle (DPP) to derive nonlinear pricing equation. Kampen [21] considered a multivariate passport option in order to ascertain the optimal strategy, which turned out to be dependent on correlations of returns as well as Greeks. The interested reader may refer to [5, 22] for a comprehensive review on passport option in both discrete (binomial) and continuous time setting, wherein it is observed that the optimal strategy for passport option for both these models are identical and that the binomial model converges to the continuous time model.

1.2 The passport option

We begin with the formulation of pricing problem for European passport option [2–4], with the underlying trading account comprising of a traded security, whose price process is assumed to follow the GBM,

$$dS(t) = \mu S(t)dt + \sigma S(t)dW(t), \tag{1.2.1}$$

where μ and σ are the drift and volatility respectively. Further, $W(t)$ is the Wiener process under the risk-neutral measure $\mathbb{P}^*$. The cost of carry which is deducted (added) from the trading account when the option trader takes a long (short) position on the asset is denoted by γ, which results in the following modified asset pricing model,

$$dS(t) = (\mu - \gamma)S(t)dt + \sigma S(t)dW(t). \tag{1.2.2}$$

Under $\mathbb{P}^*$, $\mu = r$, where r is the risk-free rate. Further, we consider a bond or a money-market account, whose price $B(t)$, at time t, for every unit investment is $B(t) = e^{rt}$. The trading strategy for the option holder is an adapted process $\{u(t)\}_{0\leq t\leq T}$ [3]. Let T is the expiration of the option and $0 = t_0 < t_1 < t_2 \cdots < t_N = T$ be the instances at which the option holder changes strategy. If $u(t) \in [-1, 1]$ is the trading position of the holder at time t, then $u(t_i)$ denotes the position initiated at time t_i and held up to the next change in position at time t_{i+1}. The resulting gain for the trader for these two consecutive time points is $u(t_i)[S(t_{i+1}) - S(t_i)]$. Consequently the accumulated gain over the $[0, T]$ is

$$w(T) = \sum_{i=0}^{N-1} u(t_i)[S(t_{i+1}) - S(t_i)].$$

In the continuous time setup, the accumulated gain at time t is

$$w(t) = \int_0^t u(\tau) dS(\tau),$$

or equivalently

$$dw(t) = u(t)dS(t) \text{ with } w(0) = 0.$$

For a European passport option, the payoff is

$$[w(T)]^+ = \max(w(T), 0).$$

One can now use a hedging argument [2,4] to obtain the following Black-Scholes type pricing PDE for the passport option value $V(S(t), t, w(t))$

$$\frac{\partial V}{\partial t} + (r-\gamma)S\left(\frac{\partial V}{\partial S} + u^*\frac{\partial V}{\partial w}\right) + \frac{1}{2}\sigma^2 S^2\left(\frac{\partial^2 V}{\partial S^2} + 2u^*\frac{\partial^2 V}{\partial s \partial w} + (u^*)^2\frac{\partial^2 V}{\partial w^2}\right) = rV,$$

with the final condition

$$V(S(T), T, w(T)) = [w(T)]^+.$$

The transformation $x = w/S$ [2,4] then results in the following PDE

$$\frac{\partial v}{\partial t} + (u^* - x)(r-\gamma)\frac{\partial v}{\partial x} + \frac{1}{2}(u^* - x)^2\sigma^2\frac{\partial^2 v}{\partial x^2} = \gamma v, \tag{1.2.3}$$

where u^* is the optimal holding strategy for the holder and is given by

$$u^*(x,t) = \text{sign}\left((r-\gamma)\frac{\partial v}{\partial x} - x\sigma^2\frac{\partial^2 v}{\partial x^2}\right) \tag{1.2.4}$$

with $v(x,t)$ being the transformed option price. The proof for the optimal holding strategy is as follows [3]. Applying the HJB equation [23] we obtain,

$$\sup_{h\in[-1,1]}\left\{\frac{\partial v}{\partial t} + (h-x)(r-\gamma)\frac{\partial v}{\partial x} + \frac{1}{2}(h-x)^2\sigma^2\frac{\partial^2 v}{\partial x^2} - \gamma v\right\} = 0$$

The supremum is attained at $h = u^*(x(t), t)$. Taking

$$C_1 = (r-\gamma)\frac{\partial v}{\partial x}, \quad C_2 = \frac{1}{2}\sigma^2\frac{\partial^2 v}{\partial x^2}, \quad C_3 = \frac{\partial v}{\partial t} - x(r-\gamma)\frac{\partial v}{\partial x} + \frac{1}{2}x^2\sigma^2\frac{\partial^2 v}{\partial x^2} - \gamma v,$$

the problem reduces to

$$\sup_{h\in[-1,1]}\left\{C_3 + h(C_1 - 2xC_2) + h^2 C_2\right\} = 0.$$

Since $\dfrac{\partial^2 v}{\partial x^2} \geq 0$, this expression represents the upward parabola with the *sup* at the end points of the domain. Thus $h = 1$ or -1. It is easy to see that,

$$u^*(x(t), t) = \text{sign}\,(C_1 - 2xC_2) = \text{sign}\left((r-\gamma)\frac{\partial v}{\partial x} - x\sigma^2\frac{\partial^2 v}{\partial x^2}\right).$$

Then the instantaneous hedge ratio, Δ [2–4] is given by,

$$\Delta = \frac{\partial V}{\partial S} + u^*\frac{\partial V}{\partial w} = v + (u^* - x)\frac{\partial v}{\partial x}.$$

The equivalent formulation of the pricing PDE is given by

$$\begin{aligned} &\frac{\partial v}{\partial t} - x(r-\gamma)\frac{\partial v}{\partial x} + \frac{1}{2}(1+x^2)\sigma^2\frac{\partial^2 v}{\partial x^2} + u^*\left((r-\gamma)\frac{\partial v}{\partial x} - x\sigma^2\frac{\partial^2 v}{\partial x^2}\right) = \gamma v \\ \Rightarrow\quad &\frac{\partial v}{\partial t} - x(r-\gamma)\frac{\partial v}{\partial x} + \frac{1}{2}(1+x^2)\sigma^2\frac{\partial^2 v}{\partial x^2} + \left|(r-\gamma)\frac{\partial v}{\partial x} - x\sigma^2\frac{\partial^2 v}{\partial x^2}\right| = \gamma v, \end{aligned}$$

with the final condition

$$v(x, T) = [x(T)]^+.$$

Note that

$$\text{sign}(x) = \begin{cases} -1, & \text{if } x < 0 \\ 1, & \text{if } x \geq 0. \end{cases}$$

Further, the pricing equation for European passport option, in the symmetric case of $r = \gamma$ is given by the following linear parabolic PDE [3]

$$\frac{\partial v}{\partial t} + \frac{1}{2}(1+|x|)^2\sigma^2\frac{\partial^2 v}{\partial x^2} = \gamma v, \tag{1.2.5}$$

with the final condition

$$v(x, T) = [x(T)]^+. \tag{1.2.6}$$

In this case, the optimal holding strategy is

$$u^*(x(t), t) = -\text{sign}(x(t)) = -\text{sign}(w(t)).$$

The analytic solution for the above linear parabolic PDE is [3]:

$$\begin{aligned} v(x,t) = e^{-\gamma(T-t)}\Bigg[&x^+ + \frac{1}{2}[d\sigma\sqrt{T-t}+1]\mathcal{N}(d) \\ &- \frac{1}{2}(1+|x|)\mathcal{N}(d-\sqrt{T-t}) + \frac{1}{2}\sigma\sqrt{T-t}\mathcal{N}'(d)\Bigg], \end{aligned} \tag{1.2.7}$$

with

$$d = -\frac{\ln(1+|x|)}{\sigma\sqrt{T-t}} + \frac{1}{2}\sigma\sqrt{T-t}, \tag{1.2.8}$$

where $\mathcal{N}$ and $\mathcal{N}'$ denote the cumulative and density function of the normal distribution respectively.

1.3 Outline of the thesis

The thesis has been arranged into six chapters as briefly outlined below. The literature review and problem background along with the problem formulation have been presented in the introductory Chapter 1. In Chapter 2, we describe the radial basis function approach using a mesh refinement algorithm to price European passport option, both for the symmetric and the non-symmetric case. In Chapter 3, we derive three Greeks, namely, Delta, Gamma and Theta for the symmetric case. We also present the three time level scheme for pricing the European passport option as well as the Greeks for both the cases. Chapter 4 describes the formulation for American passport option problem as a sequence of linear complementarity problem using three time level scheme with the numerical implementation being carried out using Brennan-Schwartz and projected successive over-relaxation (PSOR) algorithm. Chapter 5 dwells upon HOC schemes with grid stretching near zero accumulated gain for numerical valuation of both European and American passport option. Finally, the concluding chapter summarizes the work carried out in this thesis along with the roadmap for future work.

Chapter 2

Pricing of European passport option using radial basis function

In this chapter, we will seek the solution to the pricing problem in case of European passport option as outlined in Section 1.2 of Chapter 1, by using radial basis functions (RBFs) and point interpolation method (PIM) [24]. RBFs, which are typically functions of distance variables [25] offers several advantages, such as easier implementation and dimensionality independence [26,27]. It has been seen that globally supported RBFs are accurate, converge exponentially, are applicable to problems in higher dimension and are meshless. However, it does have its share of disadvantages including ill-conditioned interpolating matrix and results becoming dependent on the choice of shape parameters, which potentially leads to increased computational costs for large scale problems in particular [25]. Further, PIM involves the functional evaluation at a specified point in the domain through approximation by interpolation at the scattered nodes [28–30]. The shape function used in case of PIM is the Kronecker delta function, which makes it amenable for the imposition of the boundary condition [31]. Despite its efficiency, this approach could lead to singularities, in the event that the scattered nodes spacing is inconsistent with the order of the polynomial. This problem of singularity was resolved in [29], by using the local radial point interpolation method (LPRIM) which makes use of RBF for interpolation.

2.1 Radial basis function

A function $\phi : \mathbb{R}^n \to \mathbb{R}$ is said to be radial if there exists a function $\psi : [0, \infty) \to \mathbb{R}$ such that $\phi(x) = \psi(\|x\|)$, where $\|\cdot\|$ is some norm on $\mathbb{R}^n$ [32]. In order to use PIM [28,29,31], a real-valued function $f(x)$ is sought to be approximated at some $x \in [x_{\min}, x_{\max}]$ through interpolation of functional values at the points (nodes), namely, $x_{\min} = x_1 < x_2 < \cdots < x_n < x_{n+1} = x_{\max}$. Consequently, we will use the radial basis point interpolation (RBPI) method, wherein the interpolating function comprises of a combination of polynomials and RBFs. If $f_{RBPIM}(x)$ denotes the interpolating function for $f(x)$, then [31],

$$f_{RBPIM}(x) = \sum_{i=1}^{n+1} A_i(x)a_i + \sum_{j=1}^{m+1} B_j(x)b_j. \tag{2.1.1}$$

Here the functions $A_i(x)$ is the RBF and $B_j(x) = x^{j-1}, j = 1\ldots, m+1$. The goal is to ascertain the unknown coefficients $\{a_i\}_{i=1}^{n+1}$ and $\{b_j\}_{j=1}^{m+1}$. For the implementation purpose in our problem, we use $m = 1$ [31]. Choices for the RBF $A_i(x)$ include polyharmonic spline, thin plate splines, multiquadric, inverse multiquadric and Gaussian [25, 31–33]. Examples for these commonly used RBF's are listed in Table 2.1 [25], where $[k]$ is the largest integer less than or equal to k and c is a positive constant known as the shape parameter. Also the column with the header "CPD order (m)" in Table 2.1 denotes the m-order conditionally positive definite functions.

RBFs	$\phi(x)$	CPD order (m)
Polyharmonic spline	$\begin{cases} r^{2k-1}, & k \in \mathbb{N} \\ r^{2k}\ln(r), & k \in \mathbb{N} \end{cases}$	$[k/2]+1$
Thin plate splines	$r^2\ln(r)$	2
Multiquadric	$(r^2+c^2)^k, k>0, k \notin \mathbb{N}$	$[k]+1$
Inverse Multiquadric	$(r^2+c^2)^{-k}, k>0, k \notin \mathbb{N}$	0
Gaussian	$e^{-\left(\frac{r^2}{c^2}\right)}$	0

Table 2.1: Commonly used globally-supported RBF's and their order with $r = |x - x_i|$ [25].

The choice of the latter three RBFs, namely, multiquardic, inverse multiquardic and Gaussian are less desirable, since they could result in an ill-conditioned system resulting from their dependence on a free shape parame-

ter [31]. Unfortunately, a systematic protocol for determining the values of the shape parameter was not found in literature. Consequently, the approach for methods and algorithms for determining the appropriate shape parameter often becomes contingent on the specific problem under consideration. In our case, we will use the polyharmonic spline, using the argument (after [31]), that does not have any free shape parameter, with the specific choice of the RBF $A_i(x)$ being

$$A_i(x) = (x - x_i)^4 \log(|x - x_i|), \ i = 1, 2, \ldots, n+1.$$

Enforcing the interpolation condition(at the nodes),

$$f_{RBPIM}(x_i) = f(x_i), \ i = 1, 2, \ldots, n+1$$

in equation (2.1.1) results on $(n+1)$ linear equations in $n+m+2$ unknowns, namely, $\{a_i\}_{i=1}^{n+1}$ and $\{b_j\}_{j=1}^{m+1}$. Further, the following additional $(m+1)$ conditions required to obtain unique solution are imposed [31].

$$\sum_{i=1}^{n+1} a_i B_j(x_i) = 0, \ j = 1, 2, \ldots, m+1. \tag{2.1.2}$$

Evaluating (2.1.1) at $x = x_i$ along with (2.1.2) gives,

$$\begin{bmatrix} R & P \\ P^\top & O \end{bmatrix} \begin{bmatrix} \vec{a} \\ \vec{b} \end{bmatrix} = \begin{bmatrix} \vec{U} \\ \vec{0} \end{bmatrix}, \tag{2.1.3}$$

with

$$R = \begin{bmatrix} A_1(x_1) & A_2(x_1) & \ldots & \ldots & A_{n+1}(x_1) \\ A_1(x_2) & A_2(x_2) & \ldots & \ldots & A_{n+1}(x_2) \\ \vdots & \vdots & & & \vdots \\ \vdots & \vdots & & & \vdots \\ A_1(x_{n+1}) & A_2(x_{n+1}) & \ldots & \ldots & A_{n+1}(x_{n+1}) \end{bmatrix}, \tag{2.1.4}$$

$$P = \begin{bmatrix} B_1(x_1) & B_2(x_1) & \ldots & \ldots & B_{m+1}(x_1) \\ B_1(x_2) & B_2(x_2) & \ldots & \ldots & B_{m+1}(x_2) \\ \vdots & \vdots & & & \vdots \\ \vdots & \vdots & & & \vdots \\ B_1(x_{n+1}) & B_2(x_{n+1}) & \ldots & \ldots & B_{m+1}(x_{n+1}) \end{bmatrix}, \tag{2.1.5}$$

$$\vec{a} = [a_1, a_2, \ldots, a_{n+1}]^\top, \tag{2.1.6}$$
$$\vec{b} = [b_1, b_2, \ldots, b_{m+1}]^\top, \tag{2.1.7}$$
$$\vec{U} = [u_1, u_2, \ldots, u_{n+1}]^\top = [f(x_1), f(x_2), \ldots, f(x_{n+1})]^\top \tag{2.1.8}$$

and $\vec{0}$ is a $m+1$ dimensional zero vector. Also O is a $(m+1)\times(m+1)$ zero matrix. Defining

$$G = \begin{bmatrix} R & P \\ P^\top & O \end{bmatrix}, \tag{2.1.9}$$

the coefficients $\{a_i\}_{i=1}^{n+1}$ and $\{b_j\}_{j=1}^{m+1}$ can be obtained from equation (2.1.3) as follows,

$$\begin{bmatrix} \vec{a} \\ \vec{b} \end{bmatrix} = G^{-1} \begin{bmatrix} \vec{U} \\ \vec{0} \end{bmatrix}. \tag{2.1.10}$$

Using equation (2.1.1) and (2.1.10) we get

$$f_{RBPIM}(x) = [R^\top(x) \quad P^\top(x)] G^{-1} \begin{bmatrix} \vec{U} \\ \vec{0} \end{bmatrix}, \tag{2.1.11}$$

where $R^\top(x) = \begin{bmatrix} A_1(x) & \ldots & A_{n+1}(x) \end{bmatrix}$ and $P^\top(x) = \begin{bmatrix} B_1(x) & \ldots & B_{m+1}(x) \end{bmatrix}$. Now equation (2.1.11) can be written in the form

$$f_{RBPIM}(x) = \sum_{i=1}^{n+1} u_i \phi_i(x), \tag{2.1.12}$$

where

$$\phi_k(x) = \sum_{i=1}^{n+1} A_i(x) G^{-1}_{i,k} + \sum_{j=1}^{m+1} B_j(x) G^{-1}_{n+j+1,k}, \ k = 1, 2, \ldots, n+1. \tag{2.1.13}$$

Note that $G^{-1}_{i,k}$ is the (i,k)-th element of matrix G^{-1}. It is easy to see that the shape function defined by (2.1.13) satisfies the Kronecker property.

2.2 Numerical implementation for the symmetric case

Recall that the valuation PDE for the European passport option in the symmetric case ($r = \gamma$) is given by equation (1.2.5). The boundary conditions at the boundaries, $x_{\min} = -\exp(4\sigma\sqrt{T})$ and $x_{\max} = \exp(4\sigma\sqrt{T})$ along with the final condition are as follows [4]:

$$v(x_{\min}, t) = 0, \tag{2.2.1}$$
$$v_x(x_{\max}, t) = e^{-r(T-t)}, \tag{2.2.2}$$
$$v(x, T) = \max(x, 0). \tag{2.2.3}$$

Equation (1.2.5) can be rewritten as

$$\frac{\partial v}{\partial t} + \mathcal{A}(x)\frac{\partial^2 v}{\partial x^2} - \gamma v = 0, \tag{2.2.4}$$

where

$$\mathcal{A}(x) = \frac{1}{2}\left(1 + |x|\right)^2 \sigma^2.$$

The uniform discretization is now carried out as follows. The time interval $[0, T]$ is discretized into N uniform subintervals ($N+1$ temporal nodes) each with length $\Delta t = T/N$ with k-th temporal grid point being $t_k = (k-1)\Delta t,\ k = 1, 2, \ldots N+1$. Accordingly, we define $v^k(x) = v(x, t_k), k = 1, 2, \ldots, N+1$. Thus, the temporal semi-discretization of (2.2.4) using the θ-method results in

$$\begin{aligned}&\frac{1}{\Delta t}\left[v^{k+1}(x) - v^k(x)\right] + \theta\mathcal{A}(x)v_{xx}^{k+1}(x)\\ &+ (1-\theta)\mathcal{A}(x)v_{xx}^{k}(x) - \gamma\theta v^{k+1}(x) - \gamma(1-\theta)v^k(x) = 0.\end{aligned} \tag{2.2.5}$$

Note that $\theta = 0$, $\theta = 1/2$ and $\theta = 1$ lead to *backward*, *Crank-Nicholson* and *forward* schemes respectively. Substituting $\theta = 0$ in equation (2.2.5) results in the following backward scheme:

$$\frac{1}{\Delta t}v^{k+1}(x) = -\mathcal{A}(x)v_{xx}^k(x) + \left(\frac{1}{\Delta t} + \gamma\right)v^k(x). \tag{2.2.6}$$

For the spatial discretization, we proceed with the RBPI discretization. Accordingly, spatial domain $(x_{\min}, x_{\max})$ is divided into M uniform subintervals ($M+1$ spatial nodes) of length $\Delta x = \dfrac{x_{\max} - x_{\min}}{M}$ with the i-th spatial grid point being, $x_i = x_{\min} + (i-1)\Delta x,\ i = 1, 2, \ldots, M+1$. Accordingly, the RBPI approximation of $v^k(x)$ [31] is given by

$$v_{RBPIM}^k(x) = \sum_{j=1}^{M+1}\lambda_j^k\phi_j(x), k = 1, 2, \ldots, (N+1). \tag{2.2.7}$$

Substituting (2.2.7) in (2.2.6) we get

$$\frac{1}{\Delta t}\left[\sum_{j=1}^{M+1}\lambda_j^{k+1}\phi_j(x)\right] = -\mathcal{A}(x)\frac{\partial^2}{\partial x^2}\left[\sum_{j=1}^{M+1}\lambda_j^k\phi_j(x)\right] + \left(\frac{1}{\Delta t} + \gamma\right)\left[\sum_{j=1}^{M+1}\lambda_j^k\phi_j(x)\right]. \tag{2.2.8}$$

We now define $\Lambda^k = \left[\lambda_1^k, \lambda_2^k \ldots \lambda_{M+1}^k\right]^\top$ and $\vec{\psi}_i = \vec{\psi}\ (x_i)$ where $\vec{\psi}\ (x) = [\phi_1(x), \phi_2(x) \ldots \phi_{M+1}(x)]$. Then we rewrite equation (2.2.8) in terms of the newly defined vectors as

$$\frac{1}{\Delta t}\vec{\psi}\ (x)\Lambda^{k+1} = -\mathcal{A}(x)\frac{\partial^2}{\partial x^2}\left[\vec{\psi}\ (x)\Lambda^k\right] + \left(\frac{1}{\Delta t} + \gamma\right)\left[\vec{\psi}\ (x)\Lambda^k\right]. \tag{2.2.9}$$

Further, the discretized version of the boundary conditions given in (2.2.1) and (2.2.2) is given by $\overrightarrow{\psi}\ (x_1)\Lambda^k = 0$ and $\overrightarrow{\psi}_x\ (x_{M+1})\Lambda^k = e^{-r(T-t_k)}$ for $k = 1, 2, \ldots, N+1$. The scheme (2.2.9) at the interior points along with the boundary conditions can be written in the compact matrix form as

$$\frac{1}{\Delta t}\Phi_1\Lambda^{k+1} + H^k = \left(\mathcal{P}(D^2\Phi_1) + \left(\frac{1}{\Delta t} + \gamma\right)\Phi_1 + \Phi_2\right)\Lambda^k, \tag{2.2.10}$$

where

$$\Phi_1 = \begin{bmatrix} 0 & 0 & \ldots & \ldots & 0 & 0 \\ \phi_1(x_2) & \phi_2(x_2) & \ldots & \ldots & \phi_M(x_2) & \phi_{M+1}(x_2) \\ \vdots & \vdots & & & \vdots & \vdots \\ \vdots & \vdots & & & \vdots & \vdots \\ \phi_1(x_M) & \phi_2(x_M) & \ldots & \ldots & \phi_M(x_M) & \phi_{M+1}(x_M) \\ 0 & 0 & \ldots & \ldots & 0 & 0 \end{bmatrix},$$

$$H^k = \left[0, 0, \ldots, e^{-r(T-t_k)}\right]^\top,$$

$$\mathcal{P} = \text{diag}(0, -\mathcal{A}(x_2), -\mathcal{A}(x_3), \ldots, -\mathcal{A}(x_M), 0),$$

$$D^2\Phi_1 = \begin{bmatrix} 0 & 0 & \ldots & \ldots & 0 & 0 \\ \frac{\partial^2}{\partial x^2}(\phi_1(x_2)) & \frac{\partial^2}{\partial x^2}(\phi_2(x_2)) & \ldots & \ldots & \frac{\partial^2}{\partial x^2}(\phi_M(x_2)) & \frac{\partial^2}{\partial x^2}(\phi_{M+1}(x_2)) \\ \vdots & \vdots & & & \vdots & \vdots \\ \vdots & \vdots & & & \vdots & \vdots \\ \frac{\partial^2}{\partial x^2}(\phi_1(x_M)) & \frac{\partial^2}{\partial x^2}(\phi_2(x_M)) & \ldots & \ldots & \frac{\partial^2}{\partial x^2}(\phi_M(x_M)) & \frac{\partial^2}{\partial x^2}(\phi_{M+1}(x_M)) \\ 0 & 0 & \ldots & \ldots & 0 & 0 \end{bmatrix},$$

$$\Phi_2 = \begin{bmatrix} \phi_1(x_1) & \phi_2(x_1) & \ldots & \phi_M(x_1) & \phi_{M+1}(x_1) \\ 0 & 0 & \ldots & \ldots & 0 \\ \vdots & \vdots & & & \vdots \\ \vdots & \vdots & & & \vdots \\ 0 & 0 & \ldots & \ldots & 0 \\ \frac{\partial}{\partial x}\phi_1(x_{M+1}) & \frac{\partial}{\partial x}\phi_2(x_{M+1}) & \ldots & \frac{\partial}{\partial x}\phi_M(x_{M+1}) & \frac{\partial}{\partial x}\phi_{M+1}(x_{M+1}) \end{bmatrix}.$$

Further, (2.2.10) can be written as

$$A\Lambda^k = B\Lambda^{k+1} + H^k,$$

where

$$A = \mathcal{P}(D^2\Phi_1) + \left(\frac{1}{\Delta t} + \gamma\right)\Phi_1 + \Phi_2,$$
$$B = \frac{1}{\Delta t}\Phi_1.$$

The contingent claim or payoff for the passport option is non-smooth and hence a refined mesh is used near the mesh point zero (corresponding to the zero accumulated gain) in order to improve the computational efficiency. Let the spatial mesh points be stored as an array x of length l. Algorithm 1 outlines the method used for mesh refinement near the mesh point "zero".

Algorithm 1 Algorithm for mesh refinement near the mesh point zero

procedure MESH REFINEMENT
mm = number of mesh refinement points
if mm is even
set $dx_0 = \Delta x$
    for $i = 1$ to $l/2$ **do**
        $x(l + mm - i) = x(l + 1 - i)$
    end for
kk = 1
repeat until kk =4
$dx_1 = \frac{4}{mm+1} dx_0$
    for $i = 1$ to mm **do**
        $x\left(\frac{l+1}{2} + i - 1\right) = -2dx_0 + idx_1$
    end for
$kk \leftarrow kk + 1$
$dx_0 \leftarrow dx_1$
end repeat
else
set $dx_0 = \Delta x$
    for $i = 1$ to $l/2$ **do**
        $x(l + mm + 1 - i) = x(l + 1 - i)$
    end for
kk = 1
repeat until kk =4
$dx_1 = \frac{4}{mm+1} dx_0$
    for $i = 1$ to mm **do**
        $x\left(\frac{l}{2} + i\right) = -2dx_0 + idx_1$
    end for
$kk \leftarrow kk + 1$
$dx_0 \leftarrow dx_1$
end repeat
end procedure

Spatial steps (M) with	Temporal Steps (N)						
3 refinement points	25	50	100	200	400	800	1600
50	5.3524	5.3735	5.3840	5.394	5.5605	7.2547	13.1400
100	12.3706	12.4011	12.4170	12.4250	12.4290	12.4311	12.4321
200	13.5543	13.5798	13.5925	13.5989	13.6020	13.6036	13.6044
400	267.4509	208.7102	186.7632	177.1704	172.6748	170.4974	169.4257

Table 2.2: Even odd average value of the European passport option with $S(t) = 100, r = 0, \gamma = 0, \sigma = 30\%, T - t = 1$ and $w(t) = 0$ with 3 refinement points.

Spatial steps (M) with	Temporal Steps (N)						
4 refinement points	25	50	100	200	400	800	1600
50	13.1587	13.1876	13.2021	13.2094	13.2130	13.2148	13.2157
100	13.0971	13.1265	13.1412	13.1486	13.1523	13.1541	13.1550
200	13.0833	13.1128	13.1275	13.1349	13.1386	13.1405	13.1414
400	13.0801	13.1096	13.1244	13.1317	13.1354	13.1373	13.1382

Table 2.3: Even odd average value of the European passport option with $S(t) = 100, r = 0, \gamma = 0, \sigma = 30\%, T - t = 1$ and $w(t) = 0$ with 4 refinement points.

We now present the numerical results for the RBPI method detailed in equation (2.2.5)–(2.2.10). For the purpose of illustration and comparison, several different numbers of refinements points in the spatial direction are used. The model parameter used in this symmetric case ($r = \gamma$) are the ones used in [3] (during the implementation using Crank-Nicholson implicit method), namely, $S(t) = 100$, $r = 0$, $\gamma = 0$, $\sigma = 30\%$, $T - t = 1$ and $w(t) = 0$. The computation was implemented using MatLab™ . In Table 2.3, the results for the European passport option are presented with 4 refinement points for several different sets of number of spatial and temporal grid points. While the computation was carried out in case of both M and $M + 1$ number of spatial grid points, the result presented in Table 2.3 are the averaging of option prices obtained using M and $M + 1$ spatial grid points for several different temporal grid points. Similar averaged values of option prices for the same set of spatial and temporal grid points with $3, 5$ and 6 refinement points are presented in Table 2.2, 2.4 and 2.5 respectively. It is interesting to note that the results obtained for $3, 5$ and 6 refinement points are further away from the analytical solution of 13.1381 as

Spatial steps (M) width	Temporal Steps (N)						
5 refinement points	25	50	100	200	400	800	1600
50	13.0327	13.0622	13.0770	13.0844	13.0881	13.0900	13.0909
100	13.0650	13.0945	13.1092	13.1166	13.1203	13.1222	13.1231
200	13.0752	13.1047	13.1195	13.1269	13.1306	13.1324	13.1333
400	13.0781	13.1075	13.1223	13.1297	13.1334	13.1352	13.1362

Table 2.4: Even odd average value of the European passport option with $S(t) = 100, r = 0, \gamma = 0, \sigma = 30\%, T - t = 1$ and $w(t) = 0$ with 5 refinement points.

Spatial steps (M) with	Temporal Steps (N)						
6 refinement points	25	50	100	200	400	800	1600
50	13.0440	13.0735	13.0882	13.0956	13.0993	13.1012	13.1021
100	13.0679	13.0974	13.1121	13.1195	13.1232	13.1251	13.1260
200	13.0760	13.1054	13.1202	13.1276	13.1313	13.1331	13.1341
400	13.0783	13.1078	13.1225	13.1299	13.1336	13.1355	13.1364

Table 2.5: Even odd average value of the European passport option with $S(t) = 100, r = 0, \gamma = 0, \sigma = 30\%, T - t = 1$ and $w(t) = 0$ with 6 refinement points.

compared to the case when 4 refinement points were used. This apparent discrepancy can be attributed to the extent to which the interpolation matrix G (given by equation (2.1.9)) is ill-conditioned (which is determined by using MatLab™ 's inbuilt reciprocal condition number `rcond(G)`). The matrix G is said to be well-conditioned (ill-conditioned) depending on whether `rcond(G)` is near to 1.0 (0). The `rcond(G)` for $3, 4, 5$ and 6 refinement points in case of several spatial steps are tabulated in Table 2.6. We note that `rcond(G)` is dependent only on the number of spatial steps and not contingent on the number of temporal steps. Accordingly, the results presented in Table 2.6 are only for $N = 50$, with similar trends being obtained for other values of N. It is observed that for refinement 3, `rcond(G)` is quite close to zero which suggest that either the interpolation matrix G is singular or ill-conditioned, which leads to the non-convergence of solution. Further, inaccurate result are also observed in case of $M = 800$ for refinements 3, 4, 5 and 6 due to the `rcond(G)` being close to zero. Also, `rcond(G)` values for 4 refinement are larger as compared to $3, 5$ and 6 refinement, which is suggestive of better results in case of 4 refinement. In particular, we observe that in the

Spatial steps	Refinement 3	Refinement 4	Refinement 5	Refinement 6
50	1.2360370e-23	1.4591501e-10	9.7688699e-12	7.6735077e-13
100	2.3576136e-20	4.7155679e-12	3.1632510e-13	2.4896555e-14
200	4.9717853e-21	1.4989538e-13	1.0065644e-14	7.9305516e-16
400	4.1343007e-21	4.7244502e-15	3.1740150e-16	2.4994231e-17
800	6.6849856e-21	1.4800087e-16	9.9423207e-18	7.7672310e-19

Table 2.6: Reciprocal condition number of matrix G for $r = \gamma$ case with $N = 50$

case of $M = 400$ and $N = 1600$ with 4 refinement points, the option price is 13.1382 which is very close to the analytic value of 13.1381 as compared to the numerical value of 13.1387 as reported in [4] and 13.1371 based on the algorithm in [3].

The exponential growth in the condition number of the interpolation matrix could lead to numerical instabilities resulting in inaccurate results. Such instabilities can be remedied through the usage of pre-conditioner or more appropriate basis in the approximation space [34].

2.3 Numerical implementation for the non-symmetric case

Recall that the valuation PDE for the European passport option in the non-symmetric case ($r \neq \gamma$) is given by equation (1.2.3), with final and boundary conditions being the same as in the symmetric case and given by equation (2.2.1)–(2.2.3). Equation (1.2.3) can be written as

$$\frac{\partial v}{\partial t} = \mathcal{A}(x)\frac{\partial^2 v}{\partial x^2} + \mathcal{B}(x)\frac{\partial v}{\partial x} + \gamma v, \tag{2.3.1}$$

where $\mathcal{A}(x) = -\frac{1}{2}(u^* - x)^2\sigma^2$ and $\mathcal{B}(x) = -(u^* - x)(r - \gamma)$. We use the same temporal discretization as used in the case $r = \gamma$ in Section 2.2 over $[0, T]$. The temporal semi-discretization of (2.3.1) using the θ-method results in

$$\begin{aligned}\frac{1}{\Delta t}\left[v^{k+1}(x) - v^k(x)\right] &= \theta\mathcal{A}^k(x)v_{xx}^{k+1}(x) + (1-\theta)\mathcal{A}^k(x)v_{xx}^k(x) + \theta\mathcal{B}^k(x)v_x^{k+1}(x) \\ &\quad + (1-\theta)\mathcal{B}^k(x)v_x^k(x) + \gamma\theta v^{k+1}(x) + \gamma(1-\theta)v^k(x).\end{aligned} \tag{2.3.2}$$

Substituting $\theta = 0$ in equation (2.3.2) results in the following backward scheme,

$$\frac{1}{\Delta t}v^{k+1}(x) = \mathcal{A}^k(x)v_{xx}^k(x) + \mathcal{B}^k(x)v_x^k(x) + \left(\frac{1}{\Delta t} + \gamma\right)v^k(x). \tag{2.3.3}$$

As done previously, the RBPI approximation

$$v^k_{RBPIM}(x) = \sum_{j=1}^{M+1} \lambda^k_j \phi_j(x), k = 1, 2, \ldots, N+1,$$

after being substituted in (2.3.3) results in

$$\frac{1}{\Delta t}\left[\sum_{j=1}^{M+1} \lambda_j^{k+1}\phi_j(x)\right] = \mathcal{A}^k(x)\frac{\partial^2}{\partial x^2}\left[\sum_{j=1}^{M+1} \lambda_j^{k}\phi_j(x)\right] + \mathcal{B}^k(x)\frac{\partial}{\partial x}\left[\sum_{j=1}^{M+1} \lambda_j^{k}\phi_j(x)\right] + \left(\frac{1}{\Delta t} + \gamma\right)\left[\sum_{j=1}^{M+1} \lambda_j^{k}\phi_j(x)\right]. \quad (2.3.4)$$

Equation (2.3.4) can be rewritten in the vector form as

$$\frac{1}{\Delta t}\vec{\psi}\,(x)\Lambda^{k+1} = \mathcal{A}^k(x)\frac{\partial^2}{\partial x^2}\left[\vec{\psi}\,(x)\Lambda^{k}\right] + \mathcal{B}^k(x)\frac{\partial}{\partial x}\left[\vec{\psi}\,(x)\Lambda^{k}\right] + \left(\frac{1}{\Delta t} + \gamma\right)\left[\vec{\psi}\,(x)\Lambda^{k}\right]. \quad (2.3.5)$$

Further, the boundary conditions are given as,

$$\vec{\psi}\,(x_1)\Lambda^k = 0 \text{ and } \vec{\psi}_x\,(x_{M+1})\Lambda^k = e^{-r(T-t_k)},\ k = 1, 2, \ldots, N+1.$$

The scheme (2.3.5) at the interior points along with the boundary conditions can be written in the compact matrix form as

$$\frac{1}{\Delta t}\Phi_1\Lambda^{k+1} + H^k = \left(\mathcal{P}^k(D^2\Phi_1) + \mathcal{Q}^k(D\Phi_1) + \left(\frac{1}{\Delta t} + \gamma\right)\Phi_1 + \Phi_2\right)\Lambda^k. \quad (2.3.6)$$

where,

$$\Phi_1 = \begin{bmatrix} 0 & 0 & \ldots & \ldots & 0 & 0 \\ \phi_1(x_2) & \phi_2(x_2) & \ldots & \ldots & \phi_M(x_2) & \phi_{M+1}(x_2) \\ \vdots & \vdots & & & \vdots & \vdots \\ \vdots & \vdots & & & \vdots & \vdots \\ \phi_1(x_M) & \phi_2(x_M) & \ldots & \ldots & \phi_M(x_M) & \phi_{M+1}(x_M) \\ 0 & 0 & \ldots & \ldots & 0 & 0 \end{bmatrix},$$

$$H^k = \left[0, 0, \ldots, e^{-r(T-t_k)}\right]^\top,$$
$$\mathcal{P}^k = \text{diag}(0, \mathcal{A}^k(x_2), \mathcal{A}^k(x_3), \ldots, \mathcal{A}^k(x_M), 0),$$
$$\mathcal{Q}^k = \text{diag}(0, \mathcal{B}^k(x_2), \mathcal{B}^k(x_3), \ldots, \mathcal{B}^k(x_M), 0),$$

$$D^2\Phi_1 = \begin{bmatrix} 0 & 0 & \ldots & \ldots & 0 & 0 \\ \frac{\partial^2}{\partial x^2}(\phi_1(x_2)) & \frac{\partial^2}{\partial x^2}(\phi_2(x_2)) & \ldots & \ldots & \frac{\partial^2}{\partial x^2}(\phi_M(x_2)) & \frac{\partial^2}{\partial x^2}(\phi_{M+1}(x_2)) \\ \vdots & \vdots & & & \vdots & \vdots \\ \vdots & \vdots & & & \vdots & \vdots \\ \frac{\partial^2}{\partial x^2}(\phi_1(x_M)) & \frac{\partial^2}{\partial x^2}(\phi_2(x_M)) & \ldots & \ldots & \frac{\partial^2}{\partial x^2}(\phi_M(x_M)) & \frac{\partial^2}{\partial x^2}(\phi_{M+1}(x_M)) \\ 0 & 0 & \ldots & \ldots & 0 & 0 \end{bmatrix},$$

$$D\Phi_1 = \begin{bmatrix} 0 & 0 & \ldots & \ldots & 0 & 0 \\ \frac{\partial}{\partial x}(\phi_1(x_2)) & \frac{\partial}{\partial x}(\phi_2(x_2)) & \ldots & \ldots & \frac{\partial}{\partial x}(\phi_M(x_2)) & \frac{\partial}{\partial x}(\phi_{M+1}(x_2)) \\ \vdots & \vdots & & & \vdots & \vdots \\ \vdots & \vdots & & & \vdots & \vdots \\ \frac{\partial}{\partial x}(\phi_1(x_M)) & \frac{\partial}{\partial x}(\phi_2(x_M)) & \ldots & \ldots & \frac{\partial}{\partial x}(\phi_M(x_M)) & \frac{\partial}{\partial x}(\phi_{M+1}(x_M)) \\ 0 & 0 & \ldots & \ldots & 0 & 0 \end{bmatrix},$$

$$\Phi_2 = \begin{bmatrix} \phi_1(x_1) & \phi_2(x_1) & \ldots & \phi_M(x_1) & \phi_{M+1}(x_1) \\ 0 & 0 & \ldots & \ldots & 0 \\ \vdots & \vdots & & & \vdots \\ \vdots & \vdots & & & \vdots \\ 0 & 0 & \ldots & \ldots & 0 \\ \frac{\partial}{\partial x}\phi_1(x_{M+1}) & \frac{\partial}{\partial x}\phi_2(x_{M+1}) & \ldots & \frac{\partial}{\partial x}\phi_M(x_{M+1}) & \frac{\partial}{\partial x}\phi_{M+1}(x_{M+1}) \end{bmatrix}.$$

Further (2.3.6) can be written as

$$A\Lambda^k = B\Lambda^{k+1} + H^k,$$

where

$$\begin{aligned} A &= \mathcal{P}^k(D^2\Phi_1) + \mathcal{Q}^k(D\Phi_1) + \left(\frac{1}{\Delta t} + \gamma\right)\Phi_1 + \Phi_2, \\ B &= \frac{1}{\Delta t}\Phi_1. \end{aligned}$$

Using the RBPI approximation in (1.2.4) we obtain,

$$(u^*)^k(x) = \text{sign}\left((r-\gamma)\frac{\partial}{\partial x}\left[\sum_{j=1}^{M+1}\lambda_j^k\phi_j(x)\right] - x\sigma^2\frac{\partial^2}{\partial x^2}\left[\sum_{j=1}^{M+1}\lambda_j^k\phi_j(x)\right]\right). \tag{2.3.7}$$

At $x = x_i$

$$(u^*)^k(x_i) = \text{sign}\left((r-\gamma)\left[\frac{\partial}{\partial x}\overrightarrow{\psi}(x_i)\right]\Lambda^k - x_i\sigma^2\left[\frac{\partial^2}{\partial x^2}\overrightarrow{\psi}(x_i)\right]\Lambda^k\right), \quad i = 1, 2, \ldots, M+1. \tag{2.3.8}$$

We now present the numerical results for the RBPI method detailed in equation (2.3.2)–(2.3.8) for the non-symmetric case. The model parameters used in this non-symmetric case of $r \neq \gamma$ are the ones used in [3], namely, $S(t) = 100, r = 5\%, \gamma = 4.5\%, \sigma = 30\%$ and $T - t = 2$. The computation was implemented using MatLab™ . The computation was carried out for several mesh sizes as well as refinement points, as was done in the case $r = \gamma$. However, we present here only the results for the accumulated gains $\overrightarrow{w}(t) = [20, 10, 0, -10, -20]$ since results available in [3] and [4] are only for this set of accumulated gains. The option price computed for $M = 200, N = 200$ for the above $\overrightarrow{w}(t)$ and refinement 4 in spatial direction are presented in Table 2.7. It is seen that the values tabulated in Table 2.7 are very close to those reported in [3] and [4]. Also, the results for refinement 3, 5 and 6 are presented in Table 2.8. Finally, the reciprocal condition number, `rcond(G)` for all the four refinements with $N = 50$ are tabulated in Table 2.9. Based on `rcond(G)` reported in Table 2.9, we observe that in case of refinements $3, 5$ and 6, the interpolation matrix G is either singular or ill-conditioned.

2.4 Conclusion

In this chapter, we solved the pricing problem for the European passport option using the radial basis function for both the symmetric and non-symmetric case. To solve the problem numerically we used the radial basis point interpolation in spatial direction and backward finite difference scheme in temporal direction. The numerical scheme is first order accurate in time and second order accurate in space. We also presented an algorithm for the grid refinement in the spatial direction near zero accumulated gain, in order to improve the numerical results.

$w(t)$	Andersen et al. [3]	Topper [4]	RBPI with mesh (200×200) and 4 refinement points
20	28.2277	28.2249	28.2360
10	22.3741	22.3734	22.3755
0	17.4323	17.4423	17.4298
-10	13.5100	13.5113	13.5121
-20	10.4261	10.4293	10.4381

Table 2.7: Price of the European passport option with $S(t) = 100, r = 5\%, \gamma = 4.5\%, \sigma = 30\%$ and $T - t = 2$.

.

$w(t)$	3 refinement points	4 refinement points	5 refinement points	6 refinement points
20	22.236879	28.236001	28.230911	28.230726
10	16.425990	22.375512	22.369428	22.369911
0	11.509562	17.429765	17.416672	17.418147
-10	7.479582	13.512093	13.506332	13.506436
-20	4.294891	10.438097	10.433186	10.432745

Table 2.8: Price of the European passport option with mesh size (200×200), $S(t) = 100, r = 5\%, \gamma = 4.5\%, \sigma = 30\%, T - t = 2$.

Spatial steps	Refinement 3	Refinement 4	Refinement 5	Refinement 6
50	1.5415e-34	5.3224e-10	3.5980e-10	5.9290e-13
100	9.4060e-21	3.6459e-12	2.4452e-13	1.9241e-14
200	3.8161e-22	1.1589e-13	7.7811e-15	6.1299e-16
400	1.4434e-21	3.6524e-15	2.4540e-16	1.9362e-17
800	8.3666e-24	1.1436e-16	7.6707e-18	6.1316e-19

Table 2.9: Reciprocal condition number of matrix G for $r \neq \gamma$ case with $N = 50$.

Chapter 3

Pricing and estimates of Greeks for European passport option using three time level scheme

In this chapter, we examine the numerical approach for the symmetric case and the non-symmetric case for European type passport option using three time level scheme. In addition to solving the pricing equation for both the cases, we also evaluate the first and second derivative of the option value, that is, the Delta, Gamma and Theta for symmetric case [35]. This evaluation is critical in case of passport option, since the optimal holding strategy depends upon the Greeks, namely, Delta and Gamma. It has been noticed that widely applied numerical schemes such as Crank-Nicholson scheme is not very suitable for the pricing problem under consideration unless a large number of appropriate time steps are used for the numerical implementation, in absence of which small oscillatory errors in the solution could arise from the non-smooth initial data. This particular concern would be addressed in this chapter by using a three time level finite difference scheme, wherein one can use larger time steps (*i.e.,* lesser number of time points) while ensuring the accuracy of the solution to the valuation PDE along with the evaluation of the Greeks, namely, Delta, Gamma and Theta. The analytic value of the Greeks are also derived in this chapter.

Numerical PDE problems with discontinuous or non-smooth initial data have several numerical approaches, formulated with the goal of effective dampening of the oscillation that is typical of such problems. A list of 14 such difference schemes is presented in the book of Richtmyer and Morton [36]. In case of non-

smooth initial data, the authors recommended the application of schemes 9, 11 and 13 (see pp. 189 – 191 of [36]). Recall that the diffusion term for the passport option pricing PDE (both symmetric and non-symmetric case) is non-smooth. Accordingly, we will make use scheme 9 (as noted above), which is akin to a three time level version of the Crank-Nicholson scheme. Note that both the spatial and temporal accuracy of the three time level scheme is of second order.

3.1 Three time level scheme for the symmetric case

We seek to solve the backward valuation PDE (1.2.5) for the European passport option in the symmetric case along with the boundary conditions (2.2.1–2.2.2) and final condition (2.2.3). Defining a new temporal variable $\tau_1 = T - t$, equation (1.2.5) can be rewritten as

$$\frac{\partial v}{\partial \tau_1} = \mathcal{A}(x)\frac{\partial^2 v}{\partial x^2} - \gamma v, \tag{3.1.1}$$

where

$$\mathcal{A}(x) = \frac{1}{2}\left(1 + |x|\right)^2 \sigma^2.$$

The spatial domain discretization is the same as the one in Section 2.2 in Chapter 2. Further, the time interval $[0, T]$ is discretized into N uniform subintervals ($N+1$ points) each of length $\Delta\tau_1 = \dfrac{T}{N}$. Accordingly, the grid point $\left(x_i, \tau_1^j\right)$ is defined by $x_i = x_{\min} + (i-1)\Delta x,\ i = 1, 2, \ldots, M+1$ (as in Chapter 2) and $\tau_1^j = (j-1)\Delta\tau_1,\ j = 1, 2, \ldots, N+1$. Consequently, we let v_i^j denote the approximate value of $v(x, \tau_1)$ at the above discretization point $\left(x_i, \tau_1^j\right)$. Thus, three time level scheme [36–38] applied to the PDE (3.1.1) yields,

$$\frac{3}{2}\left(\frac{v_i^{j+1} - v_i^j}{\Delta\tau_1}\right) - \frac{1}{2}\left(\frac{v_i^j - v_i^{j-1}}{\Delta\tau_1}\right) = \mathcal{A}(x_i)\left(\frac{v_{i+1}^{j+1} - 2v_i^{j+1} + v_{i-1}^{j+1}}{(\Delta x)^2}\right) - \gamma v_i^{j+1}, \tag{3.1.2}$$

and can be written as

$$\mathcal{A}(x_i)p\left(v_{i+1}^{j+1} + v_{i-1}^{j+1}\right) - \left(2\mathcal{A}(x_i)p + \frac{3}{2} + \gamma\Delta\tau_1\right)v_i^{j+1} = -2v_i^j + \frac{1}{2}v_i^{j-1}, \tag{3.1.3}$$

where $p = \dfrac{\Delta\tau_1}{(\Delta x)^2}$. Since we now have three time levels, so information is required at two preceding time levels in order to numerically evaluate the value at the current time level. Clearly, this approach cannot be applied when one evaluates the value at time level $j = 2$, since information is available from only

one preceding time level, namely $j = 1$. Accordingly, for this scenario we make use of the Crank-Nicholson scheme [36, 37] given below,

$$\begin{aligned} & -\frac{1}{2}\mathcal{A}(x_i)p\left(v_{i+1}^{j+1}+v_{i-1}^{j+1}\right)+\left(1+\frac{1}{2}\gamma\Delta\tau_1+p\mathcal{A}(x_i)\right)v_i^{j+1} \\ = \; & \frac{1}{2}\mathcal{A}(x_i)p\left(v_{i+1}^{j}+v_{i-1}^{j}\right)+\left(1-\frac{1}{2}\gamma\Delta\tau_1-p\mathcal{A}(x_i)\right)v_i^{j}. \end{aligned} \tag{3.1.4}$$

3.2 Three time level scheme for the non-symmetric case

The pricing PDE in this case is given by equation (1.2.3) along with the boundary and final condition being given by (2.2.1)–(2.2.3). Now equation (1.2.3) can be rewritten as,

$$\frac{\partial v}{\partial t}+\mathcal{A}(x,u^*)\frac{\partial v}{\partial x}+\mathcal{B}(x,u^*)\frac{\partial^2 v}{\partial x^2}=\gamma v. \tag{3.2.1}$$

where $\mathcal{A}(x,u^*)=(u^*-x)(r-\gamma)$ and $\mathcal{B}(x,u^*)=\frac{1}{2}(u^*-x)^2\sigma^2$. Using, $\tau_1 = T-t$, equation (3.2.1) can be rewritten as

$$\frac{\partial v}{\partial \tau_1}=\mathcal{A}(x,u^*)\frac{\partial v}{\partial x}+\mathcal{B}(x,u^*)\frac{\partial^2 v}{\partial x^2}-\gamma v. \tag{3.2.2}$$

The discretization for the PDE (3.2.2) using three time level finite difference scheme [36–38] is given by

$$\begin{aligned} & \frac{3}{2}\left(\frac{v_i^{j+1}-v_i^{j}}{\Delta\tau_1}\right)-\frac{1}{2}\left(\frac{v_i^{j}-v_i^{j-1}}{\Delta\tau_1}\right)=\mathcal{A}(x_i,(u^*)_i^{j+1})\left(\frac{v_{i+1}^{j+1}-v_{i-1}^{j+1}}{2\Delta x}\right) \\ & +\mathcal{B}(x_i,(u^*)_i^{j+1})\left(\frac{v_{i+1}^{j+1}-2v_i^{j+1}+v_{i-1}^{j+1}}{(\Delta x)^2}\right)-\gamma v_i^{j+1}, \end{aligned} \tag{3.2.3}$$

and can be written as

$$\begin{aligned} & \left(-\frac{1}{2}q\mathcal{A}\left(x_i,(u^*)_i^{j+1}\right)-p\mathcal{B}\left(x_i,(u^*)_i^{j+1}\right)\right)v_{i+1}^{j+1} \\ & +\left(\frac{3}{2}+\gamma\Delta\tau_1+2p\mathcal{B}\left(x_i,(u^*)_i^{j+1}\right)\right)v_i^{j+1} \\ & +\left(\frac{1}{2}q\mathcal{A}\left(x_i,(u^*)_i^{j+1}\right)-p\mathcal{B}\left(x_i,(u^*)_i^{j+1}\right)\right)v_{i-1}^{j+1}=2v_i^{j}-\frac{1}{2}v_i^{j-1}, \end{aligned} \tag{3.2.4}$$

where $p=\dfrac{\Delta\tau_1}{(\Delta x)^2}$ and $q=\dfrac{\Delta\tau_1}{\Delta x}$. In order to move from time level $j=1$ to $j=2$, we use the following Crank-Nicholson scheme instead of three time level

scheme [36, 37] (for reasons similar to the symmetric case), which is given as follows,

$$\begin{aligned}
&\left(-\frac{1}{4}q\mathcal{A}\left(x_i,(u^*)_i^{j+1}\right)-\frac{1}{2}p\mathcal{B}\left(x_i,(u^*)_i^{j+1}\right)\right)v_{i+1}^{j+1}\\
&+\left(1+\frac{1}{2}\gamma\Delta\tau_1+p\mathcal{B}\left(x_i,(u^*)_i^{j+1}\right)\right)v_i^{j+1}\\
&+\left(\frac{1}{4}q\mathcal{A}\left(x_i,(u^*)_i^{j+1}\right)-\frac{1}{2}p\mathcal{B}\left(x_i,(u^*)_i^{j+1}\right)\right)v_{i-1}^{j+1}\\
&=\left(\frac{1}{4}q\mathcal{A}\left(x_i,(u^*)_i^{j+1}\right)+\frac{1}{2}p\mathcal{B}\left(x_i,(u^*)_i^{j+1}\right)\right)v_{i+1}^{j}\\
&+\left(1-\frac{1}{2}\gamma\Delta\tau_1-p\mathcal{B}\left(x_i,(u^*)_i^{j+1}\right)\right)v_i^{j}\\
&+\left(-\frac{1}{4}q\mathcal{A}\left(x_i,(u^*)_i^{j+1}\right)+\frac{1}{2}p\mathcal{B}\left(x_i,(u^*)_i^{j+1}\right)\right)v_{i-1}^{j}. \qquad (3.2.5)
\end{aligned}$$

The option value (resulting from solving the valuation PDE) at initial time level τ_1^1, is denote by $\overrightarrow{v}^1$, which is turn is used to evaluate $\overrightarrow{v}^2$ at time τ_1^2. The procedure for calculating $\overrightarrow{v}^2$ for both the symmetric and the non-symmetric case is illustrated in Figure 3.1. The implementation is done by first applying Crank-Nicholson scheme with $\Delta\tau_1 \to \dfrac{\Delta\tau_1}{4}$, and subsequent use of three time level scheme with $\Delta\tau_1 \to \dfrac{\Delta\tau_1}{4}$ and $\Delta\tau_1 \to \dfrac{\Delta\tau_1}{2}$. Once $\overrightarrow{v}^2$ is determined, the values form $\overrightarrow{v}^3$ onwards are determined by using three time level scheme. Finally, the optimal holding strategy given in (1.2.4) is discretized as follows,

$$(u^*)_i^{j+1} = \text{sign}\left[(r-\gamma)\left(\frac{v_{i+1}^{j+1}-v_{i-1}^{j+1}}{2\Delta x}\right)-x_i\sigma^2\left(\frac{v_{i+1}^{j+1}-2v_i^{j+1}+v_{i-1}^{j+1}}{(\Delta x)^2}\right)\right]. \qquad (3.2.6)$$

To discretize the Neumann boundary condition (2.2.2), we used the second order central difference approximation for v_x.

3.3 Valuation of Greeks: Delta, Gamma and Theta

Recall that analytic solution of the European passport option for the particular symmetric case of $r = \gamma = 0$, due to Andersen et al. [3] (*see Appendix B of [3]*) is,

$$f(x,\tau) = x^+ + \mathcal{N}(z(\tau)) - (1+|x|)\mathcal{N}(z(\tau)-\sqrt{\tau}) + \frac{1}{4}\int_0^\tau \mathcal{N}(z(u))du, \qquad (3.3.1)$$

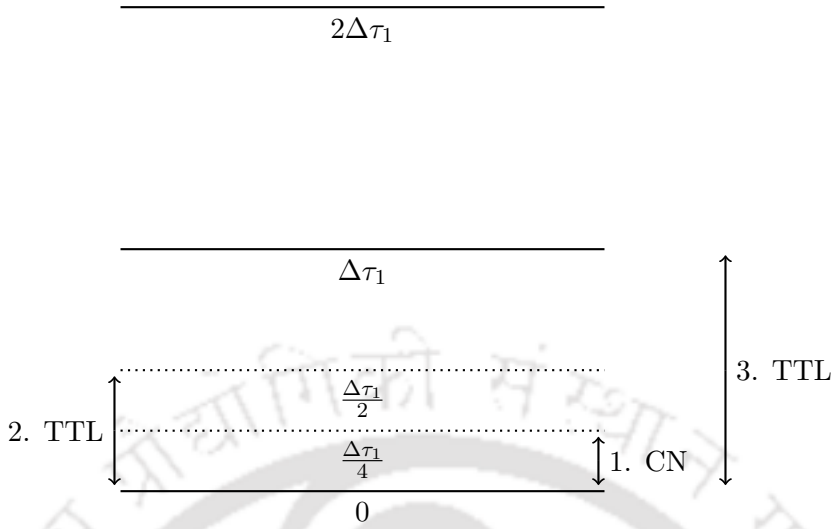

Figure 3.1: Procedure to calculate $\vec{v}^2$

with

$$z(\tau) = -\frac{\ln(1+|x|)}{\sqrt{\tau}} + \frac{1}{2}\sqrt{\tau}, \tag{3.3.2}$$

and the integral in (3.3.1) being explicitly represented by,

$$\frac{1}{2}\int_0^\tau \mathcal{N}(z(u))du = \left[z(\tau)\sqrt{\tau} - 1\right]\mathcal{N}(z(\tau)) + e^{\tau/2 - z(\tau)\sqrt{\tau}}\mathcal{N}(z(\tau) - \sqrt{\tau}) + \sqrt{\tau}\mathcal{N}'(z(\tau)). \tag{3.3.3}$$

Here $\tau = \sigma^2(T-t)$ and $v(x,t) = f(x,\tau)$, where $v(x,t)$ is the analytic solution of (1.2.5) for $r = \gamma = 0$. Also, $\mathcal{N}'$ denotes the density function of the normal distribution. We will now further simplify the solution (3.3.1) given above. Accordingly, from (3.3.2) we obtain,

$$e^{\tau/2 - z(\tau)\sqrt{\tau}} = (1+|x|).$$

Using this expression in (3.3.3) and the substituting the resulting expression in (3.3.1) we obtain the solution as,

$$\begin{aligned} f(x,\tau) &= x^+ + \mathcal{N}(z(\tau)) - (1+|x|)\mathcal{N}(z(\tau) - \sqrt{\tau}) + \frac{1}{2}\left[z(\tau)\sqrt{\tau} - 1\right]\mathcal{N}(z(\tau)) \\ &+ \frac{1}{2}(1+|x|)\mathcal{N}(z(\tau) - \sqrt{\tau}) + \frac{1}{2}\sqrt{\tau}\mathcal{N}'(z(\tau)), \end{aligned}$$

which can be further simplified to obtain,

$$f(x,\tau) = x^+ + \frac{1}{2}\left[z(\tau)\sqrt{\tau} + 1\right]\mathcal{N}(z(\tau)) - \frac{1}{2}(1+|x|)\mathcal{N}(z(\tau) - \sqrt{\tau}) + \frac{1}{2}\sqrt{\tau}\mathcal{N}'(z(\tau)). \tag{3.3.4}$$

For the non particular symmetric case, that is $r = \gamma \neq 0$, we note that if $v(x,t)$ is the solution to equation (1.2.5) when $r = \gamma = 0$, then $v(x,t)e^{-\gamma(T-t)}$ is the solution to equation (1.2.5) when $r = \gamma \neq 0$, *i.e.,*

$$v(x,t) = e^{-\gamma(T-t)}\left[x^+ + \frac{1}{2}[z(\tau)\sqrt{\tau}+1]\mathcal{N}(z(\tau)) - \frac{1}{2}(1+|x|)\mathcal{N}(z(\tau)-\sqrt{\tau}) + \frac{1}{2}\sqrt{\tau}\mathcal{N}'(z(\tau))\right], \tag{3.3.5}$$

where, as before,

$$\tau = \sigma^2(T-t).$$

As for the Greeks, we first consider the particular case $r = \gamma = 0$ and derive the Delta (Δ) and Gamma (Γ) when $x > 0$, $x < 0$ and $x = 0$ in Subsections 3.3.1, 3.3.2 and 3.3.3 respectively. The expression for Theta (Θ) in this case is derived in Subsection 3.3.4. Eventually, the Greeks for the non-particular case of $r = \gamma \neq 0$ is given in Subsection 3.3.5.

3.3.1 Δ and Γ for $r = \gamma = 0$ (Case 1: $x > 0$)

In this case, from equation (3.3.4) and (3.3.2) we obtain

$$\begin{aligned} f(x,\tau) &= x + \frac{1}{2}[z(\tau)\sqrt{\tau}+1]\mathcal{N}(z(\tau)) - \frac{1}{2}(1+x)\mathcal{N}(z(\tau)-\sqrt{\tau}) + \frac{1}{2}\sqrt{\tau}\mathcal{N}'(z(\tau)). \\ z(\tau) &= -\frac{\ln(1+x)}{\sqrt{\tau}} + \frac{1}{2}\sqrt{\tau}. \end{aligned}$$

Differentiating the above equations with respect to x, we obtain

$$\Delta = \frac{\partial f}{\partial x} = 1 + \frac{1}{2}[z(\tau)\sqrt{\tau}+1]\mathcal{N}'(z(\tau))\frac{\partial z}{\partial x} + \left(\frac{1}{2}\sqrt{\tau}\frac{\partial z}{\partial x}\right)\mathcal{N}(z(\tau)) - \frac{1}{2}(1+x)\mathcal{N}'(z(\tau)-\sqrt{\tau})\frac{\partial z}{\partial x} - \frac{1}{2}\mathcal{N}(z(\tau)-\sqrt{\tau}) + \frac{1}{2}\sqrt{\tau}\mathcal{N}''(z(\tau))\frac{\partial z}{\partial x}. \tag{3.3.6}$$

$$\frac{\partial z}{\partial x} = -\frac{1}{(1+x)\sqrt{\tau}}. \tag{3.3.7}$$

Differentiating equations (3.3.6) and (3.3.7), again, with respect to x, we obtain,

$$\Gamma = \frac{\partial^2 f}{\partial x^2} = \frac{1}{2}\sqrt{\tau}\left(\frac{\partial z}{\partial x}\right)^2\mathcal{N}'(z(\tau)) + \frac{1}{2}[z(\tau)\sqrt{\tau}+1]\mathcal{N}''(z(\tau))\left(\frac{\partial z}{\partial x}\right)^2 + \frac{1}{2}[z(\tau)\sqrt{\tau}+1]\mathcal{N}'(z(\tau))\frac{\partial^2 z}{\partial x^2} + \left(\frac{1}{2}\sqrt{\tau}\frac{\partial^2 z}{\partial x^2}\right)\mathcal{N}(z(\tau)) + \frac{1}{2}\sqrt{\tau}\left(\frac{\partial z}{\partial x}\right)^2\mathcal{N}'(z(\tau)) - \frac{1}{2}\mathcal{N}'(z(\tau)-\sqrt{\tau})\frac{\partial z}{\partial x}$$

$$
\begin{aligned}
&- \frac{1}{2}(1+x)\mathcal{N}''(z(\tau)-\sqrt{\tau})\left(\frac{\partial z}{\partial x}\right)^2 \\
&- \frac{1}{2}(1+x)\mathcal{N}'(z(\tau)-\sqrt{\tau})\frac{\partial^2 z}{\partial x^2} - \frac{1}{2}\mathcal{N}'(z(\tau)-\sqrt{\tau})\frac{\partial z}{\partial x} \\
&+ \frac{1}{2}\sqrt{\tau}\mathcal{N}'''(z(\tau))\left(\frac{\partial z}{\partial x}\right)^2 + \frac{1}{2}\sqrt{\tau}\mathcal{N}''(z(\tau))\frac{\partial^2 z}{\partial x^2}. \qquad (3.3.8)
\end{aligned}
$$

$$
\frac{\partial^2 z}{\partial x^2} = \frac{1}{(1+x)^2\sqrt{\tau}}. \qquad (3.3.9)
$$

In addition,

$$
\mathcal{N}'(z(\tau)) = \frac{1}{\sqrt{2\pi}}e^{-\frac{1}{2}(z(\tau))^2}, \qquad (3.3.10)
$$

$$
\mathcal{N}''(z(\tau)) = -z(\tau)\mathcal{N}'(z(\tau)), \qquad (3.3.11)
$$

$$
\mathcal{N}'''(z(\tau)) = ((z(\tau))^2 - 1)\mathcal{N}'(z(\tau)). \qquad (3.3.12)
$$

3.3.2 Δ and Γ for $r = \gamma = 0$ (Case 2: $x < 0$)

In this case, from equation (3.3.4) and (3.3.2) we obtain,

$$
\begin{aligned}
f(x,\tau) &= \frac{1}{2}[z(\tau)\sqrt{\tau}+1]\mathcal{N}(z(\tau)) - \frac{1}{2}(1-x)\mathcal{N}(z(\tau)-\sqrt{\tau}) + \frac{1}{2}\sqrt{\tau}\mathcal{N}'(z(\tau)). \\
z(\tau) &= -\frac{\ln(1-x)}{\sqrt{\tau}} + \frac{1}{2}\sqrt{\tau}.
\end{aligned}
$$

Proceeding as in Case 1 ($x > 0$), we obtain,

$$
\begin{aligned}
\Delta = \frac{\partial f}{\partial x} &= \frac{1}{2}[z(\tau)\sqrt{\tau}+1]\mathcal{N}'(z(\tau))\frac{\partial z}{\partial x} + \left(\frac{1}{2}\sqrt{\tau}\frac{\partial z}{\partial x}\right)\mathcal{N}(z(\tau)) \\
&- \frac{1}{2}(1-x)\mathcal{N}'(z(\tau)-\sqrt{\tau})\frac{\partial z}{\partial x} + \frac{1}{2}\mathcal{N}(z(\tau)-\sqrt{\tau}) \\
&+ \frac{1}{2}\sqrt{\tau}\mathcal{N}''(z(\tau))\frac{\partial z}{\partial x}. \qquad (3.3.13)
\end{aligned}
$$

$$
\begin{aligned}
\Gamma = \frac{\partial^2 f}{\partial x^2} &= \frac{1}{2}\sqrt{\tau}\mathcal{N}'(z(\tau))\left(\frac{\partial z}{\partial x}\right)^2 + \frac{1}{2}[z(\tau)\sqrt{\tau}+1]\mathcal{N}''(z(\tau))\left(\frac{\partial z}{\partial x}\right)^2 \\
&+ \frac{1}{2}[z(\tau)\sqrt{\tau}+1]\mathcal{N}'(z(\tau))\frac{\partial^2 z}{\partial x^2} + \left(\frac{1}{2}\sqrt{\tau}\frac{\partial^2 z}{\partial x^2}\right)\mathcal{N}(z(\tau)) \\
&+ \frac{1}{2}\sqrt{\tau}\left(\frac{\partial z}{\partial x}\right)^2\mathcal{N}'(z(\tau)) + \frac{1}{2}\mathcal{N}'(z(\tau)-\sqrt{\tau})\frac{\partial z}{\partial x} \\
&- \frac{1}{2}(1-x)\mathcal{N}''(z(\tau)-\sqrt{\tau})\left(\frac{\partial z}{\partial x}\right)^2 \\
&- \frac{1}{2}(1-x)\mathcal{N}'(z(\tau)-\sqrt{\tau})\frac{\partial^2 z}{\partial x^2} + \frac{1}{2}\mathcal{N}'(z(\tau)-\sqrt{\tau})\frac{\partial z}{\partial x} \\
&+ \frac{1}{2}\sqrt{\tau}\mathcal{N}'''(z(\tau))\left(\frac{\partial z}{\partial x}\right)^2 + \frac{1}{2}\sqrt{\tau}\mathcal{N}''(z(\tau))\frac{\partial^2 z}{\partial x^2}. \qquad (3.3.14)
\end{aligned}
$$

Here,

$$\frac{\partial z}{\partial x} = \frac{1}{(1-x)\sqrt{\tau}}, \tag{3.3.15}$$

$$\frac{\partial^2 z}{\partial x^2} = \frac{1}{(1-x)^2\sqrt{\tau}}, \tag{3.3.16}$$

and $\mathcal{N}'(z(\tau))$, $\mathcal{N}''(z(\tau))$ and $\mathcal{N}'''(z(\tau))$ are the same as in the case when $x > 0$ (*i.e,* (3.3.10), (3.3.11) and (3.3.12) respectively).

3.3.3 Δ and Γ for $r = \gamma = 0$ (Case 3: $x = 0$)

In order to study the behaviour of equation (3.3.4) around $x = 0$, we first observe from (3.3.2) and (3.3.4)

$$z(\tau) = \frac{1}{2}\sqrt{\tau} - \frac{|x|}{\sqrt{\tau}} + \frac{x^2}{2\sqrt{\tau}} + O(x^3). \tag{3.3.17}$$

and

$$f(0,\tau) = \left(\frac{1}{4}\tau + \frac{1}{2}\right)\mathcal{N}\left(\frac{1}{2}\sqrt{\tau}\right) - \frac{1}{2}\mathcal{N}\left(-\frac{1}{2}\sqrt{\tau}\right) + \frac{1}{2}\sqrt{\tau}\mathcal{N}'\left(\frac{1}{2}\sqrt{\tau}\right).$$

which can be further simplified to,

$$f(0,\tau) = \left(1 + \frac{1}{4}\tau\right)\mathcal{N}\left(\frac{1}{2}\sqrt{\tau}\right) + \frac{1}{2}\sqrt{\tau}\mathcal{N}'\left(\frac{1}{2}\sqrt{\tau}\right) - \frac{1}{2}. \tag{3.3.18}$$

We will now introduce the following notations,

$$\alpha = \frac{1}{2}\sqrt{\tau}, \qquad \beta = -\frac{|x|}{\sqrt{\tau}} + \frac{x^2}{2\sqrt{\tau}} + O(x^3). \tag{3.3.19}$$

Then,

$$\beta^2 = \frac{x^2}{\tau} + O(x^3), \tag{3.3.20}$$

$$\alpha\beta = -\frac{|x|}{2} + \frac{x^2}{4} + O(x^3), \tag{3.3.21}$$

$$(\alpha\beta)^2 = \frac{x^2}{4} + O(x^3). \tag{3.3.22}$$

Consider,

$$\begin{aligned}
\frac{1}{\sqrt{2\pi}}e^{-\frac{1}{2}(\alpha+\beta)^2} &= \frac{1}{\sqrt{2\pi}}e^{-\frac{1}{2}\alpha^2}e^{-\frac{1}{2}\beta^2}e^{-\alpha\beta} \\
&= \mathcal{N}'(\alpha)\left(1 - \frac{1}{2}\beta^2 + O(x^3)\right)\left(1 - \alpha\beta + \frac{(\alpha\beta)^2}{2} + O(x^3)\right) \\
&= \mathcal{N}'(\alpha)\left(1 - \frac{x^2}{2\tau} + O(x^3)\right)\left(1 + \frac{|x|}{2} - \frac{x^2}{4} + \frac{x^2}{8} + O(x^3)\right) \\
&= \mathcal{N}'(\alpha)\left(1 + \frac{|x|}{2} - \frac{x^2}{8} - \frac{x^2}{2\tau}\right) + O(x^3).
\end{aligned} \tag{3.3.23}$$

Similarly,

$$\begin{aligned}\frac{1}{\sqrt{2\pi}}e^{-\frac{1}{2}(-\alpha+\beta)^2} &= \frac{1}{\sqrt{2\pi}}e^{-\frac{1}{2}\alpha^2}e^{-\frac{1}{2}\beta^2}e^{\alpha\beta}\\ &= \mathcal{N}'(\alpha)\left(1-\frac{1}{2}\beta^2+O(x^3)\right)\left(1+\alpha\beta+\frac{(\alpha\beta)^2}{2}+O(x^3)\right)\\ &= \mathcal{N}'(\alpha)\left(1-\frac{x^2}{2\tau}+O(x^3)\right)\left(1-\frac{|x|}{2}+\frac{x^2}{4}+\frac{x^2}{8}+O(x^3)\right)\\ &= \mathcal{N}'(\alpha)\left(1-\frac{|x|}{2}+\frac{3x^2}{8}-\frac{x^2}{2\tau}\right)+O(x^3). \qquad (3.3.24)\end{aligned}$$

We will now derive the expression for $\mathcal{N}(z(\tau))$,

$$\begin{aligned}\mathcal{N}(z(\tau)) &= \frac{1}{\sqrt{2\pi}}\int_{-\infty}^{z(\tau)} e^{-\frac{1}{2}t^2}dt\\ &= \frac{1}{\sqrt{2\pi}}\int_{-\infty}^{\alpha+\beta} e^{-\frac{1}{2}t^2}dt\\ &= \frac{1}{\sqrt{2\pi}}\int_{-\infty}^{\alpha} e^{-\frac{1}{2}t^2}dt+\frac{1}{\sqrt{2\pi}}\int_{\alpha}^{\alpha+\beta} e^{-\frac{1}{2}t^2}dt\\ &= \mathcal{N}(\alpha)+\frac{1}{\sqrt{2\pi}}\int_{\alpha}^{\alpha+\beta} e^{-\frac{1}{2}t^2}dt. \qquad (3.3.25)\end{aligned}$$

Using the transformation $t=\alpha+y$, the integral term in (3.3.25) can be written as

$$\frac{1}{\sqrt{2\pi}}\int_{\alpha}^{\alpha+\beta} e^{-\frac{1}{2}t^2}dt=\frac{1}{\sqrt{2\pi}}\int_{0}^{\beta} e^{-\frac{1}{2}(\alpha+y)^2}dy. \qquad (3.3.26)$$

which upon expansion (using integration by parts), gives,

$$\begin{aligned}\frac{1}{\sqrt{2\pi}}\int_{0}^{\beta} e^{-\frac{1}{2}(\alpha+y)^2}dy &= \frac{1}{\sqrt{2\pi}}\beta e^{-\frac{1}{2}(\alpha+\beta)^2}+\frac{1}{\sqrt{2\pi}}\int_{0}^{\beta} y(\alpha+y)e^{-\frac{1}{2}(\alpha+y)^2}dy\\ &= \frac{1}{\sqrt{2\pi}}\beta e^{-\frac{1}{2}(\alpha+\beta)^2}+\frac{1}{\sqrt{2\pi}}\beta^2\left(\frac{\alpha}{2}+\frac{\beta}{3}\right)e^{-\frac{1}{2}(\alpha+\beta)^2}\\ &\quad+\frac{1}{\sqrt{2\pi}}\int_{0}^{\beta}\left(\frac{\alpha y^2}{2}+\frac{y^3}{3}\right)(\alpha+y)e^{-\frac{1}{2}(\alpha+y)^2}dy\\ &= \frac{1}{\sqrt{2\pi}}\beta e^{-\frac{1}{2}(\alpha+\beta)^2}+\frac{1}{\sqrt{2\pi}}\beta^2\left(\frac{\alpha}{2}+\frac{\beta}{3}\right)e^{-\frac{1}{2}(\alpha+\beta)^2}+O(x^3).\end{aligned} \qquad (3.3.27)$$

Using (3.3.17) to (3.3.22) and (3.3.23) we obtain

$$\frac{1}{\sqrt{2\pi}}\int_0^{\beta} e^{-\frac{1}{2}(\alpha+y)^2}dy = \mathcal{N}'(\alpha)\left(1+\frac{|x|}{2}-\frac{x^2}{8}-\frac{x^2}{2\tau}\right)\left(-\frac{|x|}{\sqrt{\tau}}+\frac{x^2}{2\sqrt{\tau}}\right)$$
$$+\mathcal{N}'(\alpha)\frac{x^2}{\tau}\left(1+\frac{|x|}{2}-\frac{x^2}{8}-\frac{x^2}{2\tau}\right)\left(\frac{\sqrt{\tau}}{4}-\frac{|x|}{3\sqrt{\tau}}+\frac{x^2}{6\sqrt{\tau}}\right)+O(x^3)$$
$$=-\frac{|x|}{\sqrt{\tau}}\mathcal{N}'(\alpha)+\frac{x^2}{4\sqrt{\tau}}\mathcal{N}'(\alpha)+O(x^3). \tag{3.3.28}$$

Substituting this integral value in (3.3.25) we obtain

$$\mathcal{N}(z(\tau)) = \mathcal{N}\left(\frac{1}{2}\sqrt{\tau}\right)-\frac{|x|}{\sqrt{\tau}}\mathcal{N}'\left(\frac{1}{2}\sqrt{\tau}\right)+\frac{x^2}{4\sqrt{\tau}}\mathcal{N}'\left(\frac{1}{2}\sqrt{\tau}\right)+O(x^3). \tag{3.3.29}$$

We will now derive the expression for $\mathcal{N}(z(\tau)-\sqrt{\tau})$

$$\mathcal{N}(z(\tau)-\sqrt{\tau}) = \frac{1}{\sqrt{2\pi}}\int_{-\infty}^{z(\tau)-\sqrt{\tau}} e^{-\frac{1}{2}t^2}dt$$
$$=\frac{1}{\sqrt{2\pi}}\int_{-\infty}^{-\alpha+\beta} e^{-\frac{1}{2}t^2}dt$$
$$=\frac{1}{\sqrt{2\pi}}\int_{-\infty}^{-\alpha} e^{-\frac{1}{2}t^2}dt+\frac{1}{\sqrt{2\pi}}\int_{-\alpha}^{-\alpha+\beta} e^{-\frac{1}{2}t^2}dt$$
$$=\mathcal{N}(-\alpha)+\frac{1}{\sqrt{2\pi}}\int_{-\alpha}^{-\alpha+\beta} e^{-\frac{1}{2}t^2}dt. \tag{3.3.30}$$

Using the transformation $t=-\alpha+y$, the integral term in (3.3.30) can be written as

$$\frac{1}{\sqrt{2\pi}}\int_{-\alpha}^{-\alpha+\beta} e^{-\frac{1}{2}t^2}dt = \frac{1}{\sqrt{2\pi}}\int_0^{\beta} e^{-\frac{1}{2}(-\alpha+y)^2}dy. \tag{3.3.31}$$

which upon expansion (using integration by parts) gives,

$$\frac{1}{\sqrt{2\pi}}\int_0^{\beta} e^{-\frac{1}{2}(-\alpha+y)^2}dy = \frac{1}{\sqrt{2\pi}}\beta e^{-\frac{1}{2}(-\alpha+\beta)^2}+\frac{1}{\sqrt{2\pi}}\int_0^{\beta} y(-\alpha+y)e^{-\frac{1}{2}(-\alpha+y)^2}dy$$
$$=\frac{1}{\sqrt{2\pi}}\beta e^{-\frac{1}{2}(-\alpha+\beta)^2}+\frac{1}{\sqrt{2\pi}}\beta^2\left(-\frac{\alpha}{2}+\frac{\beta}{3}\right)e^{-\frac{1}{2}(-\alpha+\beta)^2}$$
$$+\frac{1}{\sqrt{2\pi}}\int_0^{\beta}\left(-\frac{\alpha y^2}{2}+\frac{y^3}{3}\right)(-\alpha+y)e^{-\frac{1}{2}(-\alpha+y)^2}dy$$

$$= \frac{1}{\sqrt{2\pi}}\beta e^{-\frac{1}{2}(-\alpha+\beta)^2} + \frac{1}{\sqrt{2\pi}}\beta^2\left(-\frac{\alpha}{2}+\frac{\beta}{3}\right)e^{-\frac{1}{2}(-\alpha+\beta)^2} + O(x^3). \tag{3.3.32}$$

Using (3.3.17) to (3.3.22) and (3.3.24), we obtain

$$\begin{aligned}
&\frac{1}{\sqrt{2\pi}}\int_0^\beta e^{-\frac{1}{2}(-\alpha+y)^2}dy = \mathcal{N}'(\alpha)\left(1-\frac{|x|}{2}+\frac{3x^2}{8}-\frac{x^2}{2\tau}\right)\left(-\frac{|x|}{\sqrt{\tau}}+\frac{x^2}{2\sqrt{\tau}}\right)\\
&+\mathcal{N}'(\alpha)\frac{x^2}{\tau}\left(1-\frac{|x|}{2}+\frac{3x^2}{8}-\frac{x^2}{2\tau}\right)\left(-\frac{\sqrt{\tau}}{4}-\frac{|x|}{3\sqrt{\tau}}+\frac{x^2}{6\sqrt{\tau}}\right)+O(x^3)\\
&=\left(-\frac{|x|}{\sqrt{\tau}}+\frac{x^2}{\sqrt{\tau}}\right)\mathcal{N}'(\alpha)-\frac{x^2}{4\sqrt{\tau}}\mathcal{N}'(\alpha)+O(x^3)\\
&=-\frac{|x|}{\sqrt{\tau}}\mathcal{N}'(\alpha)+\frac{3x^2}{4\sqrt{\tau}}\mathcal{N}'(\alpha)+O(x^3).
\end{aligned} \tag{3.3.33}$$

Substituting this integral value in (3.3.30) we obtain

$$\mathcal{N}(z(\tau)-\sqrt{\tau}) = \mathcal{N}\left(-\frac{1}{2}\sqrt{\tau}\right)-\frac{|x|}{\sqrt{\tau}}\mathcal{N}'\left(\frac{1}{2}\sqrt{\tau}\right)+\frac{3x^2}{4\sqrt{\tau}}\mathcal{N}'\left(\frac{1}{2}\sqrt{\tau}\right)+O(x^3). \tag{3.3.34}$$

Finally, we derive the expression for $\mathcal{N}'(z(\tau))$ (using (3.3.17) and (3.3.23))

$$\begin{aligned}
\mathcal{N}'(z(\tau)) &= \frac{1}{\sqrt{2\pi}}e^{-\frac{1}{2}(z(\tau))^2}\\
&= \frac{1}{\sqrt{2\pi}}e^{-\frac{1}{2}(\alpha+\beta)^2}\\
&= \left(1+\frac{|x|}{2}-\frac{x^2}{8}-\frac{x^2}{2\tau}\right)\mathcal{N}'(\alpha)+O(x^3).
\end{aligned} \tag{3.3.35}$$

Substituting (3.3.17), (3.3.29), (3.3.34) and (3.3.35) in (3.3.4) we get

$$\begin{aligned}
f(x,\tau) = x^+ &+ \frac{1}{2}\left(\frac{1}{2}\tau-|x|+\frac{x^2}{2}+1\right)\left[\mathcal{N}\left(\frac{1}{2}\sqrt{\tau}\right)-\frac{|x|}{\sqrt{\tau}}\mathcal{N}'\left(\frac{1}{2}\sqrt{\tau}\right)\right.\\
&\left.+\frac{x^2}{4\sqrt{\tau}}\mathcal{N}'\left(\frac{1}{2}\sqrt{\tau}\right)\right]-\frac{1}{2}(1+|x|)\left[\mathcal{N}\left(-\frac{1}{2}\sqrt{\tau}\right)-\frac{|x|}{\sqrt{\tau}}\mathcal{N}'\left(\frac{1}{2}\sqrt{\tau}\right)\right.\\
&\left.+\frac{3x^2}{4\sqrt{\tau}}\mathcal{N}'\left(\frac{1}{2}\sqrt{\tau}\right)\right]+\frac{1}{2}\sqrt{\tau}\left(1+\frac{|x|}{2}-\frac{x^2}{8}-\frac{x^2}{2\tau}\right)\mathcal{N}'\left(\frac{1}{2}\sqrt{\tau}\right)+O(x^3).
\end{aligned} \tag{3.3.36}$$

which can be further simplified to

$$\begin{aligned}
f(x,\tau) = x^+ &+ \left(\frac{1}{4}\tau-\frac{|x|}{2}+\frac{x^2}{4}+\frac{1}{2}\right)\mathcal{N}\left(\frac{1}{2}\sqrt{\tau}\right)\\
&+\left(\frac{1}{4}\tau-\frac{|x|}{2}+\frac{x^2}{4}+\frac{1}{2}\right)\left(-\frac{|x|}{\sqrt{\tau}}+\frac{x^2}{4\sqrt{\tau}}\right)\mathcal{N}'\left(\frac{1}{2}\sqrt{\tau}\right)\\
&-\left(\frac{1}{2}+\frac{|x|}{2}\right)\mathcal{N}\left(-\frac{1}{2}\sqrt{\tau}\right)-\left(\frac{1}{2}+\frac{|x|}{2}\right)\left(-\frac{|x|}{\sqrt{\tau}}+\frac{3x^2}{4\sqrt{\tau}}\right)\mathcal{N}'\left(\frac{1}{2}\sqrt{\tau}\right)
\end{aligned}$$

$$
\begin{aligned}
&+\frac{1}{2}\sqrt{\tau}\left(1+\frac{|x|}{2}-\frac{x^2}{8}-\frac{x^2}{2\tau}\right)\mathcal{N}'\left(\frac{1}{2}\sqrt{\tau}\right)+O(x^3)\\
&=x^+ +\left(\frac{1}{4}\tau-\frac{|x|}{2}+\frac{x^2}{4}+\frac{1}{2}\right)\mathcal{N}\left(\frac{1}{2}\sqrt{\tau}\right)\\
&+\left(-\frac{|x|\sqrt{\tau}}{4}-\frac{|x|}{2\sqrt{\tau}}+\frac{x^2\sqrt{\tau}}{16}+\frac{5x^2}{8\sqrt{\tau}}\right)\mathcal{N}'\left(\frac{1}{2}\sqrt{\tau}\right)\\
&-\left(\frac{1}{2}+\frac{|x|}{2}\right)\left(1-\mathcal{N}\left(\frac{1}{2}\sqrt{\tau}\right)\right)+\left(\frac{|x|}{2\sqrt{\tau}}+\frac{x^2}{8\sqrt{\tau}}\right)\mathcal{N}'\left(\frac{1}{2}\sqrt{\tau}\right)\\
&+\left(\frac{1}{2}\sqrt{\tau}+\frac{|x|\sqrt{\tau}}{4}-\frac{x^2\sqrt{\tau}}{16}-\frac{x^2}{4\sqrt{\tau}}\right)\mathcal{N}'\left(\frac{1}{2}\sqrt{\tau}\right)+O(x^3)\\
&=x^+ -\frac{1}{2}-\frac{|x|}{2}+\left(\frac{1}{4}\tau+\frac{x^2}{4}+1\right)\mathcal{N}\left(\frac{1}{2}\sqrt{\tau}\right)\\
&+\left(\frac{1}{2}\sqrt{\tau}+\frac{x^2}{2\sqrt{\tau}}\right)\mathcal{N}'\left(\frac{1}{2}\sqrt{\tau}\right)+O(x^3). \qquad (3.3.37)
\end{aligned}
$$

Using (3.3.37) and (3.3.18) we get

$$
\begin{aligned}
f(x,\tau)-f(0,\tau) &= x^+ -\frac{1}{2}-\frac{|x|}{2}+\left(\frac{1}{4}\tau+\frac{x^2}{4}+1\right)\mathcal{N}\left(\frac{1}{2}\sqrt{\tau}\right)\\
&+\left(\frac{1}{2}\sqrt{\tau}+\frac{x^2}{2\sqrt{\tau}}\right)\mathcal{N}'\left(\frac{1}{2}\sqrt{\tau}\right)-\left(1+\frac{1}{4}\tau\right)\mathcal{N}\left(\frac{1}{2}\sqrt{\tau}\right)\\
&-\frac{1}{2}\sqrt{\tau}\mathcal{N}'\left(\frac{1}{2}\sqrt{\tau}\right)+\frac{1}{2}+O(x^3)\\
&= x^+ -\frac{|x|}{2}+\frac{x^2}{4}\mathcal{N}\left(\frac{1}{2}\sqrt{\tau}\right)+\frac{x^2}{2\sqrt{\tau}}\mathcal{N}'\left(\frac{1}{2}\sqrt{\tau}\right)+O(x^3). \qquad (3.3.38)
\end{aligned}
$$

which can be written as

$$
f(x,\tau)=f(0,\tau)+\frac{x}{2}+\frac{x^2}{4}\mathcal{N}\left(\frac{1}{2}\sqrt{\tau}\right)+\frac{x^2}{2\sqrt{\tau}}\mathcal{N}'\left(\frac{1}{2}\sqrt{\tau}\right)+O(x^3). \qquad (3.3.39)
$$

From (3.3.39) we can conclude that

$$
\Delta = \frac{\partial f}{\partial x}=\frac{1}{2}, \qquad (3.3.40)
$$

$$
\Gamma = \frac{\partial^2 f}{\partial x^2}=\frac{1}{2}\mathcal{N}\left(\frac{1}{2}\sqrt{\tau}\right)+\frac{1}{\sqrt{\tau}}N'\left(\frac{1}{2}\sqrt{\tau}\right). \qquad (3.3.41)
$$

3.3.4 Θ for $r=\gamma=0$

In order to determine the expression for Theta, we differentiate (3.3.4) with respect to t to obtain,

$$
\begin{aligned}
\frac{\partial f}{\partial t} &= \frac{1}{2}\sqrt{\tau}\mathcal{N}(z(\tau))\frac{\partial z}{\partial t}+\frac{1}{4\sqrt{\tau}}z(\tau)\mathcal{N}(z(\tau))\frac{\partial \tau}{\partial t}+\frac{1}{2}z(\tau)\sqrt{\tau}\mathcal{N}'(z(\tau))\frac{\partial z}{\partial t}\\
&+ \frac{1}{2}\mathcal{N}'(z(\tau))\frac{\partial z}{\partial t}-\frac{1}{2}(1+|x|)\mathcal{N}'(z(\tau)-\sqrt{\tau})\left(\frac{\partial z}{\partial t}-\frac{1}{2\sqrt{\tau}}\frac{\partial \tau}{\partial t}\right)
\end{aligned}
$$

$$+\frac{1}{4\sqrt{\tau}}\mathcal{N}'(z(\tau))\frac{\partial \tau}{\partial t}+\frac{1}{2}\sqrt{\tau}\mathcal{N}''(z(\tau))\frac{\partial z}{\partial t}.$$

where

$$\begin{aligned}\frac{\partial \tau}{\partial t} &= -\sigma^2,\\ \frac{\partial z}{\partial t} &= \frac{-\sigma^2}{2\sqrt{\tau}}\left(\frac{\ln(1+|x|)}{\tau}+\frac{1}{2}\right).\end{aligned}$$

Upon further simplification, we get,

$$\begin{aligned}\Theta=\frac{\partial f}{\partial t} &= \left(\frac{1}{2}\sqrt{\tau}\frac{\partial z}{\partial t}+\frac{1}{4\sqrt{\tau}}z(\tau)\frac{\partial \tau}{\partial t}\right)\mathcal{N}(z(\tau))+\left(\frac{1}{2}\frac{\partial z}{\partial t}+\frac{1}{4\sqrt{\tau}}\frac{\partial \tau}{\partial t}\right)\mathcal{N}'(z(\tau))\\ &- \frac{1}{2}(1+|x|)N'(z(\tau)-\sqrt{\tau})\left(\frac{\partial z}{\partial t}-\frac{1}{2\sqrt{\tau}}\frac{\partial \tau}{\partial t}\right)\\ &= -\frac{\sigma^2}{4}\mathcal{N}(z(\tau))-\frac{\sigma^2}{4\sqrt{\tau}}\left(\frac{\ln(1+|x|)}{\tau}+\frac{3}{2}\right)\mathcal{N}'(z(\tau))\\ &+ \frac{\sigma^2}{4\sqrt{\tau}}(1+|x|)\left(\frac{\ln(1+|x|)}{\tau}-\frac{1}{2}\right)\mathcal{N}'(z(\tau)-\sqrt{\tau}). \qquad (3.3.42)\end{aligned}$$

3.3.5 Δ, Γ and Θ for $r=\gamma\neq 0$

In this case ($r=\gamma\neq 0$), we have

$$v(x,t)=e^{-\gamma(T-t)}f(x,\tau). \qquad (3.3.43)$$

Accordingly, we have the Delta, Gamma and Theta for the case $r=\gamma\neq 0$ as,

$$\Delta = \frac{\partial v}{\partial x}=e^{-\gamma(T-t)}\frac{\partial f}{\partial x}, \qquad (3.3.44)$$

$$\Gamma = \frac{\partial^2 v}{\partial x^2}=e^{-\gamma(T-t)}\frac{\partial^2 f}{\partial x^2}, \qquad (3.3.45)$$

$$\Theta = \frac{\partial v}{\partial t}=\gamma v(x,t)+e^{-\gamma(T-t)}\frac{\partial f}{\partial t}, \qquad (3.3.46)$$

where $\frac{\partial f}{\partial x}$, $\frac{\partial^2 f}{\partial x^2}$ and $\frac{\partial f}{\partial t}$ are the Δ, Γ and Θ for the case $r=\gamma=0$, and have already been derived. The results can now be summarised in the Table 3.1

3.4 Numerical results

In this section, we present the numerical implementation of the valuation of passport option as well as estimation of Greeks. For the symmetric case, in case of the particular scenario of $r=\gamma=0$, we present the results using the scheme in Section 3.1. The parameter values are the same as given in Section 2.2 of

Greek	$r = \gamma = 0$	$r = \gamma \neq 0$
Delta (Δ)	Eq. (3.3.6) (Case when $x > 0$)	Eq. (3.3.44)
	Eq. (3.3.13) (Case when $x < 0$)	
	Eq. (3.3.40) (Case when $x = 0$)	
Gamma (Γ)	Eq. (3.3.8) (Case when $x > 0$)	Eq. (3.3.45)
	Eq. (3.3.14) (Case when $x < 0$)	
	Eq. (3.3.41) (Case when $x = 0$)	
Theta (Θ)	Eq. (3.3.42)	Eq.(3.3.46)

Table 3.1: Greeks for the symmetric case when $r = \gamma$

Chapter 2. While the simulations were run in MatLab™ for several M(spatial) and N(temporal) steps, the results presented here are only for $M = 800$ and $N = 40$.

w	Analytic	Crank-Nicholson	Crank-Nicholson Error	Three time level	Three time level Error
-20	5.887568	5.886602	0.000966	5.886739	0.000829
-10	8.880836	8.879462	0.001374	8.879995	0.000841
-5	10.830686	10.829025	0.001660	10.829716	0.000970
-2	12.169565	12.167987	0.001578	12.169685	-0.000120
-1	12.646019	12.648500	-0.002481	12.645709	0.000310
0	13.138099	13.129705	0.008394	13.136881	0.001218
1	13.646019	13.648500	-0.002481	13.645709	0.000310
2	14.169565	14.167987	0.001578	14.169685	-0.000120
5	15.830686	15.829025	0.001660	15.829716	0.000970
10	18.880836	18.879462	0.001374	18.879995	0.000841
20	25.887568	25.886602	0.000966	25.886739	0.000829

Table 3.2: Price of the European passport option with $S(t) = 100, r = 0, \gamma = 0, \sigma = 30\%, T - t = 1$, $M = 800$, $N = 40$.

In Table 3.2, we have presented the values of the passport option for various values of accumulated gain (w). We compared these values with the ones obtained using Crank-Nicholson scheme [3] and three time level scheme for several values of $w \in [-20, 20]$. While the value of the passport option obtained by both the schemes is fairly accurate in comparison to the analytic values, it is observed

that for the three time level scheme, the error was 10^{-4} as compared to 10^{-3} in Crank-Nicholson scheme for values of w except $w = -20, 20$ when it was 10^{-4}. Further, near $w = 0$, it was observed to be 10^{-3} with a somewhat lesser error in case of the three time level scheme. The error plot for Crank-Nicholson scheme and three time level scheme are shown in Figure 3.2 and Figure 3.3 respectively. It is interesting to observe that in case of Crank-Nicholson scheme (Figure 3.2) sharp oscillating errors occur near $w = 0$. But such oscillating errors were not observed for three time level scheme (Figure 3.3). This clearly illustrates the advantage of the three time level scheme over Crank-Nicholson scheme, particularly, for estimating values near the $w = 0$, for larger time steps.

We now analyze the values for the Greeks that are tabulated in Tables 3.3–3.5. The values of Δ, given in Table 3.3 shows that the error using three time level has the order 10^{-3}, except at $w = 0$. More interestingly, it was observed that for the Crank-Nicholson scheme with values of $w = -2, -1, 1$ and 2, the error was 10^{-1}, which was significantly more than an order of 10^{-3} for the corresponding w values using three time level scheme, again highlighting better result using three time level scheme near $w = 0$. This advantage is more clearly observed when we analyze Table 3.4 for the Γ values for $w \in [-5, 5]$ with three time level scheme error being of the order 10^{-2} but the error going up to 10^{3} using the Crank-Nicholson scheme. Finally, for Θ values (Table 3.5) it is observed that in the range $w \in [-2, 2]$ the order is 10^{-3} using three time level scheme in contrast to the order ranging from 10^{-1} to 10^{1} using Crank-Nicholson scheme. The plots for all the three Greeks are given in Figures 3.4, 3.5, 3.6, 3.7, 3.8 and 3.9.

Finally, for the non-symmetric case of $r \neq \gamma$, we use the parameters values given in Section 2.3 of Chapter 2 (as before), for $M = 800$ and $N = 40$. The tabulated results for the option price using the Crank-Nicholson scheme and three time level schemes are given in Table 3.6. Further, the results from [3] and [4] for $w = -20, -10, 0, 10$ and 20 are tabulated for the purpose of comparison. We also present the values of Greeks for this (non-symmetric) case using the Crank-Nicholson scheme and three time level scheme in Table 3.7 and Table 3.8. Note that in both the Tables we have presented the results for several additional values of w, namely, for $w \in [-5, 5]$, similar to the symmetric case.

w	Analytic	Crank-Nicholson	Crank-Nicholson Error	Three time level	Three time level Error
-20	24.697278	24.698551	-0.001273	24.702788	-0.005510
-10	35.700396	35.701400	-0.001004	35.704551	-0.004155
-5	42.433492	42.440953	-0.007461	42.435855	-0.002363
-2	46.874930	47.017061	-0.142131	46.878546	-0.003616
-1	48.421288	48.246636	0.174652	48.423557	-0.002269
0	50.000000	50.000000	-0.000000	50.000000	-0.000000
1	51.578712	51.753364	-0.174652	51.576443	0.002269
2	53.125070	52.982939	0.142131	53.121454	0.003616
5	57.566508	57.559047	0.007461	57.564145	0.002363
10	64.299604	64.298600	0.001004	64.295449	0.004155
20	75.302722	75.301449	0.001273	75.297212	0.005510

Table 3.3: Delta (Δ) for the European passport option with $S(t) = 100, r = 0, \gamma = 0, \sigma = 30\%, T - t = 1$, $M = 800$, $N = 40$.

w	Analytic	Crank-Nicholson	Crank-Nicholson Error	Three time level	Three time level Error
-20	94.397786	94.397796	-0.000010	94.399427	-0.001641
-10	126.276343	126.298902	-0.022559	126.251732	0.024611
-5	143.055007	144.664243	-1.609236	143.018580	0.036426
-2	153.004559	212.785939	-59.781380	152.960696	0.043863
-1	156.260608	-23.632573	179.893182	156.216298	0.044311
0	159.473995	485.870330	-326.396335	159.431300	0.042695
1	156.260608	-23.632573	179.893182	156.216298	0.044311
2	153.004559	212.785939	-59.781380	152.960696	0.043863
5	143.055007	144.664243	-1.609236	143.018580	0.036426
10	126.276343	126.298902	-0.022559	126.251732	0.024611
20	94.397786	94.397796	-0.000010	94.399427	-0.001641

Table 3.4: Gamma (Γ) for the European passport option with $S(t) = 100, r = 0, \gamma = 0, \sigma = 30\%, T - t = 1$, $M = 800$, $N = 40$.

w	Analytic	Crank-Nicholson	Crank-Nicholson Error	Three time level	Three time level Error
-20	-6.116977	-6.116672	-0.000304	-6.116917	-0.000059
-10	-6.875747	-6.874837	-0.000910	-6.874321	-0.001426
-5	-7.097317	-7.092456	-0.004860	-7.095469	-0.001848
-2	-7.163367	-6.997160	-0.166208	-7.160927	-0.002440
-1	-7.173065	-7.762702	0.589637	-7.170778	-0.002287
0	-7.176330	-6.081327	-1.095002	-7.174409	-0.001921
1	-7.173065	-7.762702	0.589637	-7.170778	-0.002287
2	-7.163367	-6.997160	-0.166208	-7.160927	-0.002440
5	-7.097317	-7.092456	-0.004860	-7.095469	-0.001848
10	-6.875747	-6.874837	-0.000910	-6.874321	-0.001426
20	-6.116977	-6.116672	-0.000304	-6.116917	-0.000059

Table 3.5: Theta (Θ) for the European passport option with $S(t) = 100, r = 0, \gamma = 0, \sigma = 30\%, T - t = 1,\ M = 800,\ N = 40$.

w	Anderson et al. [3]	Topper [4]	Crank-Nicholson	Three time level
-20	10.4261	10.4293	10.427921	10.432338
-10	13.5100	13.5113	13.508944	13.514268
0	17.4323	17.4423	17.435007	17.442783
10	22.3741	22.3734	22.371212	22.377016
20	28.2277	28.2249	28.225034	28.230189

Table 3.6: Price of the European passport option with $S(t) = 100, r = 5\%, \gamma = 4.5\%, \sigma = 30\%, T - t = 2,\ M = 800, N = 40$.

.

w	Price	Delta	Gamma	Theta
-20	10.427921	27.140605	68.246932	-4.115058
-10	13.508944	34.770677	84.645747	-4.195941
-5	15.357117	39.215016	90.190765	-4.176121
-2	16.578253	42.132478	81.283541	-4.206566
-1	17.004120	43.060747	75.290057	-4.206532
0	17.435007	44.135347	176.527558	-3.743239
1	17.886694	45.255233	81.927855	-4.137834
2	18.344259	46.249159	89.108106	-4.097518
5	19.778059	49.407580	98.823492	-3.930423
10	22.371212	54.245622	91.933461	-3.703986
20	28.225034	62.507636	73.750364	-3.129258

Table 3.7: Price and Greeks for the European passport option with $S(t) = 100, r = 5\%, \gamma = 4.5\%, \sigma = 30\%, T - t = 2,\ M = 800, N = 40$ using the Crank-Nicholson scheme.

.

w	Price	Delta	Gamma	Theta
-20	10.432338	27.147470	68.237007	-4.114607
-10	13.514268	34.776898	84.712313	-4.195143
-5	15.362458	39.235528	93.695734	-4.162591
-2	16.582578	42.130158	99.264913	-4.115419
-1	17.008325	43.131283	101.143554	-4.094907
0	17.442783	44.148715	103.030651	-4.072198
1	17.891299	45.191969	104.928401	-4.045941
2	18.348975	46.247610	106.229700	-4.017377
5	19.783762	49.391745	102.135086	-3.916951
10	22.377016	54.242598	91.990209	-3.702919
20	28.230189	62.503378	73.681949	-3.128569

Table 3.8: Price and Greeks for the European passport option with $S(t) = 100, r = 5\%, \gamma = 4.5\%, \sigma = 30\%$ and $T - t = 2,\ M = 800, N = 40$ using three time level scheme.

.

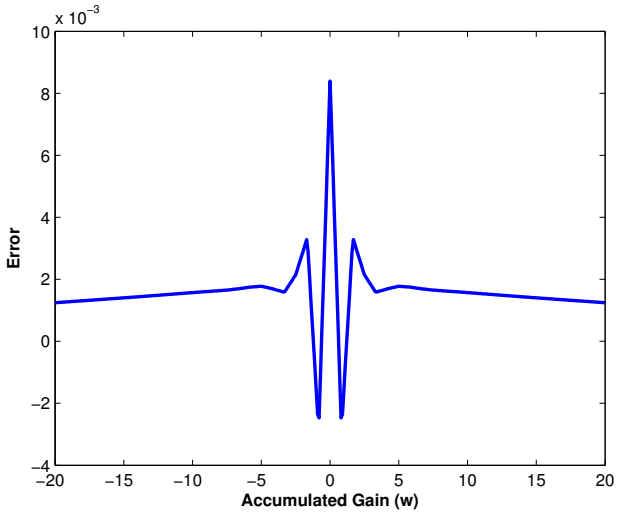

Figure 3.2: Error plot of price for the European passport option with $S(t) = 100, r = 0, \gamma = 0, \sigma = 30\%, T - t = 1,\ M = 800,\ N = 40$ using the Crank-Nicholson scheme.

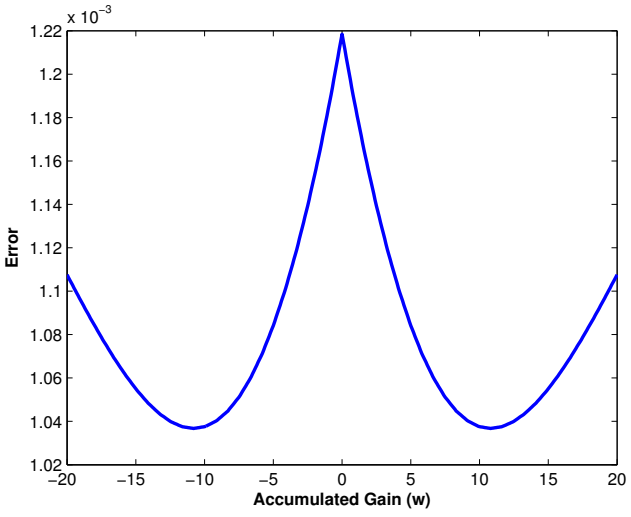

Figure 3.3: Error plot of price for the European passport option with $S(t) = 100, r = 0, \gamma = 0, \sigma = 30\%, T - t = 1,\ M = 800,\ N = 40$ using three time level scheme.

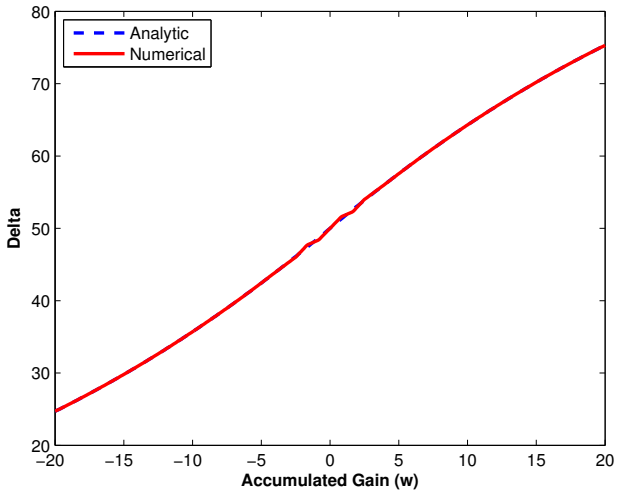

Figure 3.4: Delta (Δ) for the European passport option with $S(t) = 100, r = 0, \gamma = 0, \sigma = 30\%, T - t = 1$, $M = 800$, $N = 40$ using the Crank-Nicholson scheme.

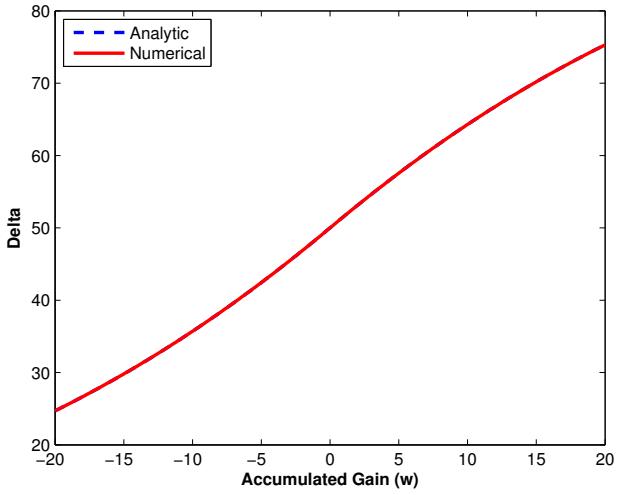

Figure 3.5: Delta (Δ) for the European passport option with $S(t) = 100, r = 0, \gamma = 0, \sigma = 30\%, T - t = 1$, $M = 800$, $N = 40$ using three time level scheme.

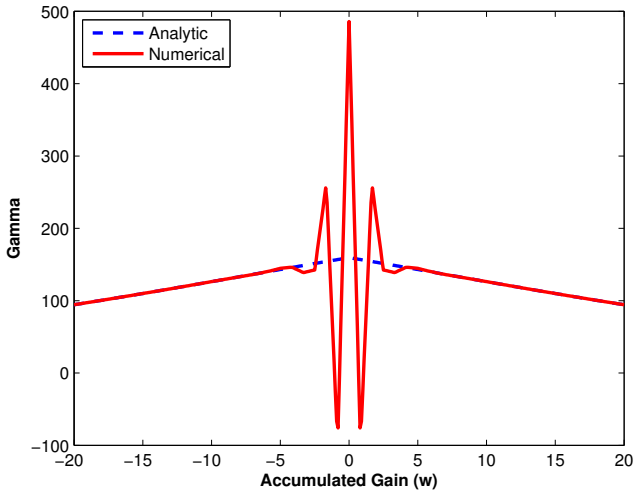

Figure 3.6: Gamma (Γ) for the European passport option with $S(t) = 100, r = 0, \gamma = 0, \sigma = 30\%, T - t = 1,\ M = 800,\ N = 40$ using the Crank-Nicholson scheme.

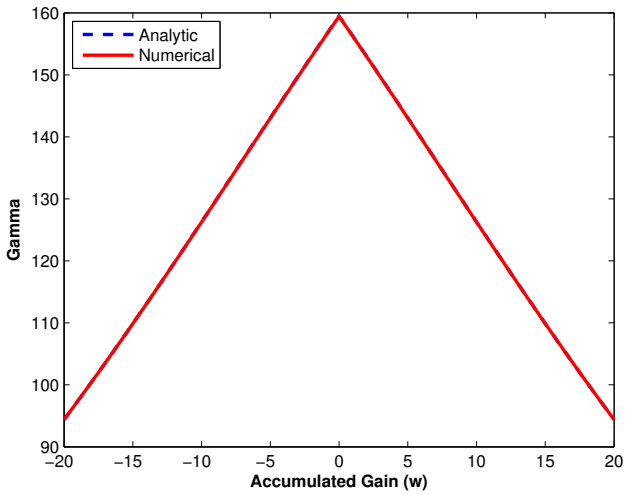

Figure 3.7: Gamma (Γ) for the European passport option with $S(t) = 100, r = 0, \gamma = 0, \sigma = 30\%, T - t = 1,\ M = 800,\ N = 40$ using three time level scheme.

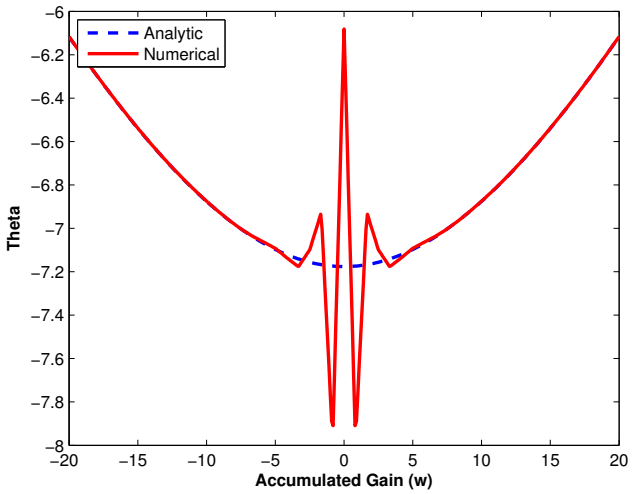

Figure 3.8: Theta (Θ) for the European passport option with $S(t) = 100, r = 0, \gamma = 0, \sigma = 30\%, T - t = 1$, $M = 800$, $N = 40$ using the Crank-Nicholson scheme.

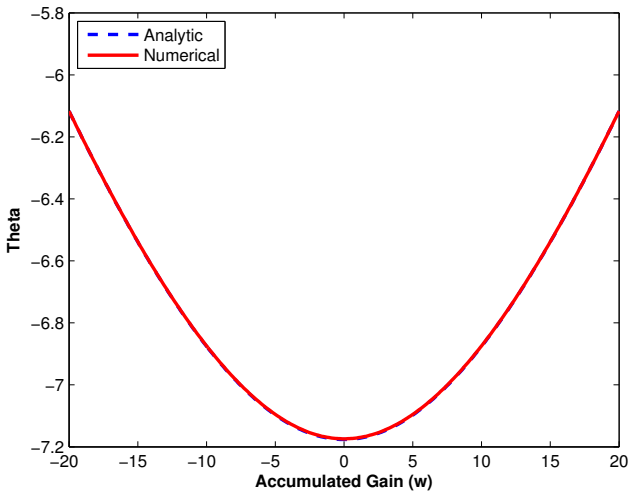

Figure 3.9: Theta (Θ) for the European passport option with $S(t) = 100, r = 0, \gamma = 0, \sigma = 30\%, T - t = 1$, $M = 800$, $N = 40$ using three time level scheme.

3.5 Conclusion

In this chapter, we considered the problem of pricing and estimation of the Greeks for the European passport option and solved it numerically using three time level scheme for the larger time steps, for both the symmetric and non-symmetric case. The numerical scheme is second order accurate in both temporal and spatial direction. We also derived the analytic value of three Greeks, namely Delta, Gamma and Theta, in the symmetric case. Finally, we observe three time level scheme giving better results as compared to the classical Crank-Nicholson scheme, near the zero accumulated gain, for the large time steps. The advantage of the three time level scheme is more evident when we numerically evaluated the Greeks, particularly Gamma and Theta near the zero accumulated gain.

Chapter 4

Pricing of American passport option using three time level scheme

In this chapter, the problem of pricing American passport option is considered. American options are more flexible than European options since they can be exercised at any time on or before the expiration date of T. For American passport option, the holder has the choice of liquidating the trading account and retaining the accumulated gain at any time on or before the expiration T [7]. The rule for such early pre-expiration exercise of an American option is the maximization of the conditional expected value (under $\mathbb{P}^*$) of the discounted payoff [39]. Accordingly, for the (x,t) domain, the region of continuation or holding (when the option is not exercised) is determined by $v(x,t) > x^+$ and the region of stopping or exercise (when the option is exercised) is determined by $v(x,t) = x^+$ [39, 40]. Therefore the option value $v(x,t)$, satisfies the following,

$$\mathcal{L}v(x,t) = \gamma v(x,t), v(x,t) > x^+ \text{ for } (x,t) \in \mathcal{R}_c,$$
$$\mathcal{L}v(x,t) \leq \gamma v(x,t), v(x,t) = x^+ \text{ for } (x,t) \in \mathcal{R}_s,$$

where

$$\mathcal{L}v(x,t) = \frac{\partial v}{\partial t} + (u^* - x)(r - \gamma)\frac{\partial v}{\partial x} + \frac{1}{2}(u^* - x)^2\sigma^2\frac{\partial^2 v}{\partial x^2}.$$

Also $\mathcal{R}_c = \left\{(x,t) \in \mathbb{R} \times [0,T] : v(x,t) > x^+\right\}$
and $\mathcal{R}_s = \left\{(x,t) \in \mathbb{R} \times [0,T] : v(x,t) = x^+\right\}$ are the continuation and stopping region respectively. The spatial domain $[x_{\min}, x_{\max}]$ has the boundary conditions $v(x_{\min}, t) = 0$ and $v(x_{\max}, t) = x_{\max}$ for all $t \in [0,T]$ [7]. Thus, the complementarity problem for the value $v(x,t)$ of American passport option for the domain

$\mathcal{R} = \{(x,t) \in [x_{\min}, x_{\max}] \times [0,T]\}$ is given by

$$\begin{cases} (\mathcal{L}v(x,t) - \gamma v(x,t)) \cdot (v(x,t) - x^+) = 0, \\ \mathcal{L}v(x,t) \leq \gamma v(x,t) \text{ and } \ v(x,t) \geq x^+, \\ v(x,T) = x^+, \text{ for all } x \in (x_{\min}, x_{\max}), \\ v(x_{\min},t) = 0 \text{ and } v(x_{\max},t) = x_{\max} \text{ for all } t \in [0,T]. \end{cases} \tag{4.0.1}$$

Using the transformation $\tau = T - t$, the above complimentary problem for the domain, $\mathcal{R}_\tau = \{(x,\tau) \in [x_{\min}, x_{\max}] \times [0,T]\}$ becomes,

$$\begin{cases} (\mathcal{L}_\tau v(x,\tau) - \gamma v(x,\tau)) \cdot (v(x,\tau) - x^+) = 0, \\ \mathcal{L}_\tau v(x,\tau) \leq \gamma v(x,\tau) \text{ and } v(x,\tau) \geq x^+, \\ v(x,0) = x^+, \text{ for all } x \in (x_{\min}, x_{\max}), \\ v(x_{\min},\tau) = 0 \text{ and } v(x_{\max},\tau) = x_{\max} \text{ for all } \tau \in [0,T]. \end{cases} \tag{4.0.2}$$

where

$$\mathcal{L}_\tau v(x,\tau) = -\frac{\partial v}{\partial \tau} + (u^* - x)(r - \gamma)\frac{\partial v}{\partial x} + \frac{1}{2}(u^* - x)^2\sigma^2\frac{\partial^2 v}{\partial x^2}.$$

4.1 Numerical implementation

The discretization in the spatial and temporal direction are the same as already given in Chapter 2 and Chapter 3, *i.e.*, $x_i = x_{\min} + (i-1)\Delta x$ $(i = 1, 2, \ldots, M+1)$ and $\tau^j = (j-1)\Delta\tau$ $(j = 1, 2, \ldots, N+1)$, with $\Delta x = \dfrac{x_{\max} - x_{\min}}{M}$ and $\Delta\tau = \dfrac{T}{N}$. We will use the Crank-Nicholson and three time level scheme [36–38] as discussed in Chapter 3 to discretize the problem (4.0.2). As done previously $v(x,\tau)$ at the grid point $\left(x_i, \tau^j\right)$ is denoted by v_i^j.

4.1.1 Crank-Nicholson scheme

The discretization of (4.0.2) using Crank-Nicholson scheme is as follows

$$\begin{cases} \text{For } i = 2, 3, \ldots, M, \ j = 1, 2, \ldots, N \\ \left((\mathcal{L}_\tau v)_i^j - \frac{\gamma}{2}(v_i^j + v_i^{j+1})\right) \cdot \left(v_i^j - x_i^+\right) = 0, \\ (\mathcal{L}_\tau v)_i^j \leq \frac{\gamma}{2}(v_i^j + v_i^{j+1}) \text{ and } v_i^j \geq x_i^+, \\ v_i^1 = x_i^+, \text{for } i = 1, 2, \ldots, M+1, \\ v_1^j = 0 \text{ and } v_{M+1}^j = x_{\max} \text{ for } j = 1, 2, \ldots, N+1. \end{cases} \tag{4.1.1}$$

where

$$(\mathcal{L}_\tau v)_i^j = -\frac{v_i^{j+1} - v_i^j}{\Delta\tau} + \frac{1}{2}(r-\gamma)\left((u^*)_i^j - x_i\right)\left[\frac{v_{i+1}^j - v_{i-1}^j}{2\Delta x} + \frac{v_{i+1}^{j+1} - v_{i-1}^{j+1}}{2\Delta x}\right] + \frac{1}{4}\sigma^2\left((u^*)_i^j - x_i\right)^2\left[\frac{v_{i-1}^j - 2v_i^j + v_{i+1}^j}{(\Delta x)^2} + \frac{v_{i-1}^{j+1} - 2v_i^{j+1} + v_{i+1}^{j+1}}{(\Delta x)^2}\right]. \tag{4.1.2}$$

In order to represent (4.1.1) in the matrix form, we define, $V^j = [v_2^j, v_3^j, \ldots, v_M^j]^\top$ with the initial value vector (payoff vector) being given by $V^1 = \Pi = [x_2^+, x_3^+, \ldots, x_M^+]^\top$. Let A^j and B^j be tridiagonal matrices with lower diagonal entries $(a_1)_i^j, (b_1)_i^j$, diagonal entries $(a_2)_i^j, (b_2)_i^j$ and upper diagonal entries $(a_3)_i^j, (b_3)_i^j$ respectively, being given by

$$\begin{aligned}
(a_1)_i^j &= -\frac{p}{4}\sigma^2(\alpha_i^j)^2 + \frac{q}{4}(r-\gamma)\alpha_i^j,\\
(a_2)_i^j &= 1 + \frac{\gamma\Delta\tau}{2} + \frac{p}{2}\sigma^2(\alpha_i^j)^2,\\
(a_3)_i^j &= -\frac{p}{4}\sigma^2(\alpha_i^j)^2 - \frac{q}{4}(r-\gamma)\alpha_i^j,\\
(b_1)_i^j &= \frac{p}{4}\sigma^2(\alpha_i^j)^2 - \frac{q}{4}(r-\gamma)\alpha_i^j,\\
(b_2)_i^j &= 1 - \frac{\gamma\Delta\tau}{2} - \frac{p}{2}\sigma^2(\alpha_i^j)^2,\\
(b_3)_i^j &= \frac{p}{4}\sigma^2(\alpha_i^j)^2 + \frac{q}{4}(r-\gamma)\alpha_i^j,
\end{aligned}$$

where $\alpha_i^j = ((u^*)_i^j - x_i)$, $p = \dfrac{\Delta\tau}{(\Delta x)^2}$ and $q = \dfrac{\Delta\tau}{\Delta x}$. Using the above notation, (4.1.1) can now be written as sequence of linear complementarity problem as follows

$$\begin{aligned}
&\text{For } j = 1, 2, \ldots, N\\
&(A^j V^{j+1} - B^j V^j - g^j)\cdot(V^j - \Pi) = 0,\\
&A^j V^{j+1} \geq B^j V^j + g^j,\\
&V^j \geq \Pi,
\end{aligned} \tag{4.1.3}$$

where

$$g^j = \left[0, 0, \ldots, (b_3)_M^j v_{M+1}^j - (a_3)_M^j v_{M+1}^{j+1}\right]^\top.$$

4.1.2 Three time level scheme

As observed in Chapter 3, the coefficient of the diffusion term for (4.0.2) being non-smooth, we will use Scheme 9 [36] (pp. 190), which is essentially a three

time level scheme. The discretized version of (4.0.2) using three time level finite difference scheme [35–37] (as discussed in Chapter 3) can be written as,

$$\begin{cases} \text{For } i = 2, 3, \ldots, M,\ j = 2, 3, \ldots, N \\ \left((\mathcal{G}_\tau v)_i^{j+1} - \gamma v_i^{j+1}\right) \cdot \left(v_i^{j+1} - x_i^+\right) = 0. \\ (\mathcal{G}_\tau v)_i^{j+1} \leq \gamma v_i^{j+1} \text{and } v_i^{j+1} \geq x_i^+ \\ v_i^1 = x_i^+, \text{ for } i = 1, 2, \ldots, M+1 \\ v_1^j = 0 \text{ and } v_{M+1}^j = x_{\max} \text{ for } j = 1, 2, \ldots, N+1. \end{cases} \tag{4.1.4}$$

where

$$\begin{aligned} (\mathcal{G}_\tau v)_i^{j+1} = &-\frac{3}{2}\left(\frac{v_i^{j+1} - v_i^j}{\Delta\tau}\right) + \frac{1}{2}\left(\frac{v_i^j - v_i^{j-1}}{\Delta\tau}\right) \\ &+ (r-\gamma)\left((u^*)_i^j - x_i\right)\left[\frac{v_{i+1}^{j+1} - v_{i-1}^{j+1}}{2\Delta x}\right] \\ &+ \frac{1}{2}\sigma^2\left((u^*)_i^j - x_i\right)^2\left[\frac{v_{i-1}^{j+1} - 2v_i^{j+1} + v_{i+1}^{j+1}}{(\Delta x)^2}\right]. \end{aligned} \tag{4.1.5}$$

Defining the tridiagonal matrix C^j with lower diagonal entries $(c_1)_i^j$, diagonal entries $(c_2)_i^j$ and upper diagonal entries $(c_3)_i^j$ being given by

$$\begin{aligned} (c_1)_i^j &= -\frac{p}{2}\sigma^2(\alpha_i^j)^2 + \frac{q}{2}(r-\gamma)\alpha_i^j, \\ (c_2)_i^j &= \frac{3}{2} + \gamma\Delta\tau + p\sigma^2(\alpha_i^j)^2, \\ (c_3)_i^j &= -\frac{p}{2}\sigma^2(\alpha_i^j)^2 - \frac{q}{2}(r-\gamma)\alpha_i^j, \end{aligned}$$

we can write (4.1.1) as sequence of linear complementarity problem as follows

$$\begin{aligned} &\text{For } j = 2, \ldots, N \\ &(C^j V^{j+1} - 2V^j + \frac{1}{2}V^{j-1} - h^j) \cdot (V^{j+1} - \Pi) = 0, \\ &C^j V^{j+1} \geq 2V^j - \frac{1}{2}V^{j-1} + h^j, \\ &V^{j+1} \geq \Pi, \end{aligned} \tag{4.1.6}$$

where

$$h^j = \left[0, 0, \ldots, -(c_3)_M^j v_{M+1}^{j+1}\right]^\top.$$

However, for reasons already justified in Chapter 3, we will use the Crank-Nicholson when estimating the value $\vec{v}^2$ using $\vec{v}^1$ as discussed in Figure 3.1. Further, the discretization of u^* is same as equation (3.2.6) in Chapter 3.

The discretized pricing problem will now be solved through both the scheme outlined, using the Brennan-Schwartz algorithm [41, 42] and the PSOR method [40, 43]. *i.e.,* using the four algorithms (outlined below). Hence Algorithm (2) and Algorithm (4) is used to solve linear complementarity problem (4.1.3) using the Brennan-Schwartz algorithm and the PSOR method respectively. Brennan-Schwartz algorithm is used to solve the matrix form of linear complementarity problem arising from the implicit discretization of linear complementarity problem. This algorithm is analog of Thomas algorithm for solving the system of linear equations. The main idea here is to transform the tridiagonal system to a lower bidiagonal system and then solving this system by imposing the early exercise condition. PSOR is the variation of SOR obtained by incorporating the early exercise condition. Analogously, Algorithm (3) and Algorithm (5) are used to solve the linear complementarity problem (4.1.6) using the Brennan-Schwartz algorithm and the PSOR method respectively. We note that the implementation of Algorithm (4) and (5) requires the over-relaxation parameter ω to lie between 0 and 2. For the purpose of this work, it is chosen to be $\omega = 1.5$.

Algorithm 2 Crank-Nicholson Brennan-Schwartz Algorithm

procedure START
  $V^1 \leftarrow \Pi$
  for $j = 1, 2, \ldots, N$ **do**
    $\Phi^j \leftarrow B^j V^j + g^j$
    $(\hat{a_2})_1^j \leftarrow (a_2)_2^j$
    $(\hat{\Phi})_1^j \leftarrow (\Phi)_1^j$
    for $k = 3, 4, \ldots, M$ **do**
      $(\hat{a_2})_{k-1}^j \leftarrow (a_2)_k^j - (a_3)_{k-1}^j \left(\frac{(a_1)_k^j}{(\hat{a_2})_{k-2}^j} \right)$
      $(\hat{\Phi})_{k-1}^j \leftarrow (\Phi)_{k-1}^j - (\hat{\Phi})_{k-2}^j \left(\frac{(a_1)_k^j}{(\hat{a_2})_{k-2}^j} \right)$
    end for
    $v_M^j \leftarrow \max \left(x_M^+, \frac{(\hat{\Phi})_{M-1}^j}{(\hat{a_2})_{M-1}^j} \right)$
    for $k = M-1, M-2, \ldots, 2$ **do**
      $v_k^j \leftarrow \max \left(x_k^+, \frac{(\hat{\Phi})_{k-1}^j - (a_3)_k^j v_{k+1}^{j+1}}{(\hat{a_2})_{k-1}^j} \right)$
    end for
    $V^{j+1} \leftarrow V^j$
  end for
end procedure

Algorithm 3 Three Time Level Brennan-Schwartz Algorithm

procedure START
  $V^1 \leftarrow \Pi$
  $V^2 \leftarrow$ Calculated as discussed in Section (4.1.2) using Algorithm (2)
  for $j = 2, 3, \ldots, N$ **do**
    $\Phi^j \leftarrow 2V^j - \frac{1}{2}V^{j-1} + h^j$
    $(\hat{c_2})_1^j \leftarrow (c_2)_2^j$
    $(\hat{\Phi})_1^j \leftarrow (\Phi)_1^j$
    for $k = 3, 4, \ldots, M$ **do**
      $(\hat{c_2})_{k-1}^j \leftarrow (c_2)_k^j - (c_3)_{k-1}^j \left(\frac{(c_1)_k^j}{(\hat{c_2})_{k-2}^j}\right)$
      $(\hat{\Phi})_{k-1}^j \leftarrow (\Phi)_{k-1}^j - (\hat{\Phi})_{k-2}^j \left(\frac{(c_1)_k^j}{(\hat{c_2})_{k-2}^j}\right)$
    end for
    $v_M^{j+1} \leftarrow \max\left(x_M^+, \frac{(\hat{\Phi})_{M-1}^j}{(\hat{c_2})_{M-1}^j}\right)$
    for $k = M-1, M-2, \ldots, 2$ **do** $v_k^{j+1} \leftarrow \max\left(x_k^+, \frac{(\hat{\Phi})_{k-1}^j - (c_3)_k^j v_{k+1}^{j+1}}{(\hat{c_2})_{k-1}^j}\right)$
    end for
  end for
end procedure

Algorithm 4 Crank-Nicholson PSOR Algorithm

procedure START
  $V^1 \leftarrow \Pi$
  for $j = 1, 2, \ldots, N$ **do**
    $\nu \leftarrow 0$
    $V^{j+1,\nu} \leftarrow \Pi$
    repeat
      $\Phi^j \leftarrow B^j V^j + g^j$
      for $i = 2, 3, \ldots, M$ **do**
        $\Gamma_{i-1}^{\nu+1} \leftarrow \frac{1}{A_{ii}^j}\left(\Phi_{i-1}^j - \sum_{k=2,k>i}^{M} A_{ik}^j V_i^{j+1,\nu} - \sum_{k=2,k<i}^{M} A_{ik}^j V_i^{j+1,\nu+1}\right)$
        $V_{i-1}^{j+1,\nu+1} \leftarrow \max\left(x_i^+, V_{i-1}^{j+1,\nu} + \omega\left(\Gamma_{i-1}^{\nu+1} - V_{i-1}^{j+1,\nu}\right)\right)$
      end for
      $\nu \leftarrow \nu + 1$
    until $\|V^{j+1,\nu+1} - V^{j+1,\nu}\|_2 <$ Tolerance, Tolerance $= 10^{-6}$
    $V^{j+1} \leftarrow V^{j+1,\nu+1}$
  end for
end procedure

Algorithm 5 Three Time Level PSOR Method

procedure START
  $V^1 \leftarrow \Pi$
  $V^2 \leftarrow$ Calculated as discussed in Section (4.1.2) using Algorithm (4)
  for $j = 2, 3, \ldots, N$ **do**
    $\nu \leftarrow 0$
    $V^{j+1,\nu} \leftarrow \Pi$
    repeat
      $\Phi^j \leftarrow 2V^j - \frac{1}{2}V^{j-1} + h^j$
      for $i = 2, 3, \ldots, M$ **do**

$$\Gamma_{i-1}^{\nu+1} \leftarrow \frac{1}{C_{ii}^j}\left(\Phi_{i-1}^j - \sum_{k=2,k>i}^{M} C_{ik}^j V_i^{j+1,\nu} - \sum_{k=2,k<i}^{M} C_{ik}^j V_i^{j+1,\nu+1}\right)$$

$$V_{i-1}^{j+1,\nu+1} \leftarrow \max\left(x_i^+, V_{i-1}^{j+1,\nu} + \omega\left(\Gamma_{i-1}^{\nu+1} - V_{i-1}^{j+1,\nu}\right)\right)$$

      end for
      $\nu \leftarrow \nu + 1$
    until $\|V^{j+1,\nu+1} - V^{j+1,\nu}\|_2 <$ Tolerance, Tolerance $= 10^{-6}$
    $V^{j+1} \leftarrow V^{j+1,\nu+1}$
  end for
end procedure

4.2 Numerical results

The numerical results using both the Crank-Nicholson and three time level scheme for the European and American passport option are illustrated here. The spatial domain chosen for the numerical simulation is $[x_{\min}, x_{\max}] = [-4, 4]$ with expiration $T = 2$ [7]. The model parameters chosen are the same as used in Chapter 2 and Chapter 3 [3, 4, 7] for the non-symmetric case. Note that we do not present the results for the symmetric case since the values of American passport option is the same as European option for the symmetric case. In the absence of any known analytic solution for American passport option, we compared our results to that of [3, 4, 7] using a smaller grid size of 200×25. The implementation was carried out using Algorithms 2–5. The results for the option price along with the comparative percentage difference from the results in [3,4,7] are tabulated in Table 4.1.

Finally, the value of American passport option for the range $(0.5\% - 50\%)$ of volatilities σ are illustrated in Figure 4.1, where it is clearly observed that the prices increase as a result of the increase in the volatility using Algorithms 2–5.

Table 4.1: Comparison of values of two-year European and American passport option for $S(t) = 100, r = 5.0\%, \gamma = 4.5\%, \sigma = 30\%$, using a 200×25 grid.

w		-20	-10	0	10	20
Andersen et al. [3]	European	10.4261	13.5100	17.4323	22.3741	28.2277
Grid: 800×100	American	10.6031	13.7776	17.8418	23.0050	29.1764
Topper [4]	European	10.4320	13.5135	17.4438	22.3760	28.2295
Grid: 400×800	American	10.6150	13.7902	17.8668	23.0298	29.2135
Chan [7]	European	9.8227	13.1341	17.3495	22.5645	28.6424
Grid: 200×25	American	9.9953	13.4065	17.7788	23.2348	29.8568
Algorithm 2	European	10.3844	13.4585	17.3819	22.3106	28.1623
	% [3]	0.40	0.38	0.29	0.28	0.23
	% [4]	0.46	0.41	0.35	0.29	0.24
	% [7]	-5.72	-2.47	-0.19	1.13	1.68
	American	10.5972	13.7701	17.8457	23.0092	29.1957
	% [3]	0.06	0.05	-0.02	-0.02	-0.07
	% [4]	0.17	0.15	0.12	0.09	0.06
	% [7]	-6.02	-2.71	-0.38	0.97	2.21
Algorithm 3	European	10.4022	13.4791	17.4046	22.3342	28.1859
	% [3]	0.23	0.23	0.16	0.18	0.15
	% [4]	0.29	0.25	0.22	0.19	0.15
	% [7]	-5.90	-2.63	-0.32	1.02	1.59
	American	10.6040	13.7785	17.8550	23.0186	29.2044
	% [3]	-0.01	-0.01	-0.08	-0.06	-0.10
	% [4]	0.10	0.08	0.07	0.05	0.03
	% [7]	-6.09	-2.77	-0.43	0.93	2.19
Algorithm 4	European	10.3844	13.4585	17.3819	22.3106	28.1623
	% [3]	0.40	0.38	0.29	0.28	0.23
	% [4]	0.46	0.41	0.35	0.29	0.24
	% [7]	-5.72	-2.47	-0.19	1.13	1.68
	American	10.5720	13.7422	17.8161	22.9795	29.1675
	% [3]	0.29	0.26	0.14	0.11	0.03
	% [4]	0.41	0.35	0.28	0.22	0.16
	% [7]	-5.77	-2.50	-0.21	1.10	2.31
Algorithm 5	European	10.4022	13.4791	17.4046	22.3342	28.1859
	% [3]	0.23	0.23	0.16	0.18	0.15
	% [4]	0.29	0.25	0.22	0.19	0.15
	% [7]	- 5.90	-2.63	-0.32	1.02	1.59
	American	10.5940	13.7673	17.8430	23.0064	29.1927
	% [3]	0.09	0.07	-0.01	-0.01	-0.06
	% [4]	0.20	0.17	0.13	0.10	0.07
	% [7]	-5.99	-2.69	-0.36	0.98	2.22

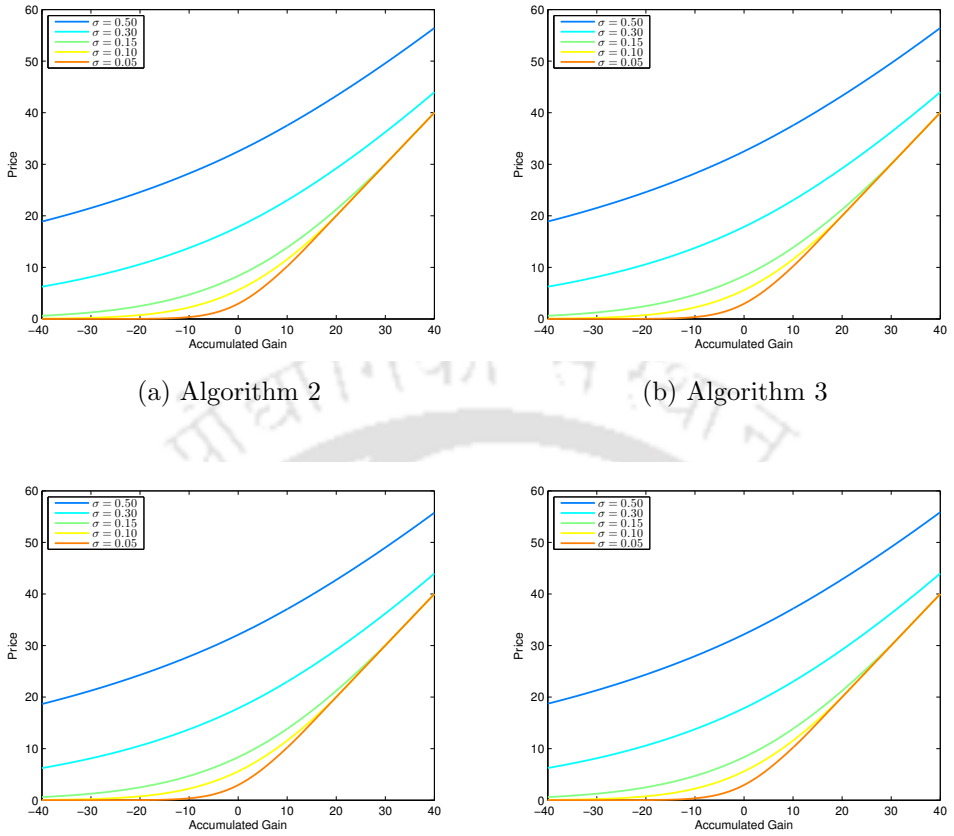

(a) Algorithm 2

(b) Algorithm 3

(c) Algorithm 4

(d) Algorithm 5

Figure 4.1: Price of an American passport option with $S(t) = 100, r = 5.0\%, \gamma = 4.5\%$ and $T - t = 2$ for $\sigma = 5\% - 50\%$, using a 200×25 grid.

4.3 Conclusion

In this chapter, we considered the problem for pricing American passport option using three time level scheme. The discretization of the pricing PDE naturally leads to a sequence of linear complementarity problems, the solution to which is obtained using the Brennan-Schwartz algorithm and PSOR method. The advantage of three time level scheme as compared to the classical Crank-Nicholson scheme in case of European passport option was detailed in the preceding chapter and the similar advantage was observed for the American passport option in this chapter.

Chapter 5

Higher order compact schemes in pricing of passport options

In this chapter, we seek to obtain more precise and accurate solution for the pricing PDE (1.2.3) on a compact stencil through higher order compact (HOC) schemes. Taking into account the specific type of PDE for the passport option, we focus on those HOC schemes, for which the coefficient of the PDE need not be smooth [44–47]. We considered a set of fourth order HOC schemes for solving the equation (1.2.3) with the boundary and final conditions as given in (2.2.1)–(2.2.3) to obtain the price for passport option (both European and American). Equation (1.2.3) can be written as

$$\frac{\partial v}{\partial t} + \mathcal{A}(x, u^*)\frac{\partial v}{\partial x} + \mathcal{B}(x, u^*)\frac{\partial^2 v}{\partial x^2} = \gamma v, \tag{5.0.1}$$

where $\mathcal{A}(x, u^*) = (u^* - x)(r - \gamma)$ and $\mathcal{B}(x, u^*) = \frac{1}{2}(u^* - x)^2\sigma^2$.

5.1 The higher order compact schemes

We present the compact difference schemes both for the interior as well as the boundary points, following the approach in [44]. Accordingly, let Δt denote the uniform temporal mesh size with the m-th time point being $t^m = m\Delta t,\ m = 0, 1, \ldots, N$, where N is the number of temporal intervals and $\Delta t = \frac{T}{N}$. For the spatial uniform mesh, we consider M spatial points $x_j = x_{\min} + (j-1)\Delta x,\ j = 1, 2, \ldots, M$, with the mesh size being $\Delta x = \dfrac{x_{\max} - x_{\min}}{(M-1)}$. The approximation of $v(x,t)$, $v_x(x,t)$, $v_{xx}(x,t)$ and $u^*(x,t)$ at the point (x_j, t^m) are denoted by v_j^m, $(v_x)_j^m$, $(v_{xx})_j^m$ and $(u^*)_j^m$ respectively. We note that the temporal semi-discretization of equation (5.0.1) using the Crank-Nicholson implicit method

(CNIM) is given by,

$$\frac{v_j^{m+1}-v_j^m}{\Delta t}+\mathcal{A}\left(x_j,(u^*)_j^{m+1}\right)\left[\frac{(v_x)_j^{m+1}+(v_x)_j^m}{2}\right]$$
$$+\mathcal{B}\left(x_j,(u^*)_j^{m+1}\right)\left[\frac{(v_{xx})_j^{m+1}+(v_{xx})_j^m}{2}\right]=\gamma\left[\frac{v_j^{m+1}+v_j^m}{2}\right]. \tag{5.1.1}$$

We now construct the fourth-order approximation for the term $(v_x)_j^m$ and $(v_{xx})_j^m$.

5.1.1 The interior points

We first consider all the interior points (x_j,t^m), where $j=3,4,\ldots,M-2$ and $m=0,1,\ldots,N-1$. The following compact schemes [46, 47] are used to derive a fourth-order approximation to $(v_x)_j^m$

$$a_1(v_x)_{j+1}^m+b_1(v_x)_j^m+c_1(v_x)_{j-1}^m=\frac{v_{j+1}^m-v_{j-1}^m}{2\Delta x}, \tag{5.1.2}$$

where the coefficients a_1,b_1 and c_1 have to be determined. In order to determine these coefficients, Taylor series expansion for the terms $(v_x)_{j+1}^m$ and $(v_x)_{j-1}^m$ about the point (x_j,t^m) is carried out as follows.

$$(v_x)_{j\pm1}^m=(v_x)_j^m\pm\Delta x(v_{xx})_j^m+\frac{(\Delta x)^2}{2}(v_{xxx})_j^m\pm\frac{(\Delta x)^3}{6}(v_{xxxx})_j^m+O((\Delta x)^4). \tag{5.1.3}$$

Similarly, the Taylor series expansion for the terms v_{j+1}^m and v_{j-1}^m about the point (x_j,t^m) are given by

$$v_{j\pm1}^m=v_j^m\pm\Delta x(v_x)_j^m+\frac{(\Delta x)^2}{2}(v_{xx})_j^m\pm\frac{(\Delta x)^3}{6}(v_{xxx})_j^m+O((\Delta x)^4). \tag{5.1.4}$$

Using (5.1.3) and (5.1.4) in (5.1.2) leads to

$$(a_1+b_1+c_1)(v_x)_j^m+(a_1-c_1)\Delta x(v_{xx})_j^m+(a_1+c_1)\frac{(\Delta x)^2}{2}(v_{xxx})_j^m$$
$$+(a_1-c_1)\frac{(\Delta x)^3}{6}(v_{xxxx})_j^m+O((\Delta x)^4)=(v_x)_j^m+\frac{(\Delta x)^2}{6}(v_{xxx})_j^m+O((\Delta x)^4).$$

Comparing the corresponding coefficients of $(\Delta x)^0,(\Delta x)^1,(\Delta x)^2$ and $(\Delta x)^3$ on both sides, we get,

$$a_1+b_1+c_1=1,\quad a_1-c_1=0,\quad \frac{a_1+c_1}{2}=\frac{1}{6}.$$

On solving the above linear system of equations, we get,

$$a_1=c_1=\frac{1}{6},\quad b_1=\frac{2}{3}.$$

Substituting these values in (5.1.2) we obtain

$$\frac{1}{4}(v_x)_{j+1}^m + (v_x)_j^m + \frac{1}{4}(v_x)_{j-1}^m = \frac{3}{2}\left[\frac{v_{j+1}^m - v_{j-1}^m}{2\Delta x}\right],$$
$$j = 3, 4, \ldots, M-2,\ m = 0, 1, \ldots, N-1. \tag{5.1.5}$$

Now we will derive fourth-order approximation to $(v_{xx})_j^m$ on the lines of $(v_x)_j^m$ as follows [46, 47],

$$a_2(v_{xx})_{j+1}^m + b_2(v_{xx})_j^m + c_2(v_{xx})_{j-1}^m = \frac{v_{j+1}^m - 2v_j^m + v_{j-1}^m}{(\Delta x)^2}, \tag{5.1.6}$$

where the coefficients a_2, b_2 and c_2 have to be determined. In order to determine these coefficients, Taylor series expansion for the terms $(v_{xx})_{j+1}^m$ and $(v_{xx})_{j-1}^m$ about the point (x_j, t^m) is carried out as follows.

$$(v_{xx})_{j\pm1}^m = (v_{xx})_j^m \pm \Delta x(v_{xxx})_j^m + \frac{(\Delta x)^2}{2}(v_{xxxx})_j^m \pm \frac{(\Delta x)^3}{6}(v_{xxxxx})_j^m + O((\Delta x)^4). \tag{5.1.7}$$

Using (5.1.4) and (5.1.7) in (5.1.6) leads to

$$(a_2 + b_2 + c_2)(v_{xx})_j^m + (a_2 - c_2)\Delta x(v_{xxx})_j^m + (a_2 + c_2)\frac{(\Delta x)^2}{2}(v_{xxxx})_j^m$$
$$+(a - c)\frac{(\Delta x)^3}{6}(v_{xxxxx})_j^m + O((\Delta x)^4) = (v_{xx})_j^m + \frac{(\Delta x)^4}{12}(v_{xxxx})_j^m + O((\Delta x)^4).$$

Comparing the corresponding coefficients of $(\Delta x)^0, (\Delta x)^1, (\Delta x)^2$ and $(\Delta x)^3$ on both sides we get

$$a_2 + b_2 + c_2 = 1, \quad a_2 - c_2 = 0, \quad \frac{a_2 + c_2}{2} = \frac{1}{12}.$$

On solving the above linear system of equations, we get

$$a_2 = c_2 = \frac{1}{12}, b_2 = \frac{5}{6}.$$

Substituting these values in (5.1.6) we obtain,

$$\frac{1}{10}(v_{xx})_{j+1}^m + (v_{xx})_j^m + \frac{1}{10}(v_{xx})_{j-1}^m = \frac{6}{5}\left[\frac{v_{j+1}^m - 2v_j^m + v_{j-1}^m}{(\Delta x)^2}\right],$$
$$j = 3, 4, \ldots, M-2,\ m = 0, 1, \ldots, N-1. \tag{5.1.8}$$

5.1.2 The boundary points

We next consider the fourth order approximation to $(v_x)_2^m$, $(v_{xx})_2^m$, $(v_x)_{M-1}^m$, and $(v_{xx})_{M-1}^m$ near the actual boundary points x_1 and x_M. At the left boundary

(x_1, t^m) we have the *Dirichlet* boundary condition, $v(x_1, t^m) = 0$. The following compact schemes are used to derive a fourth-order approximation to $(v_x)_2^m$ for $m = 0, 1, \ldots, N-1$,

$$d_1(v_x)_2^m + e_1(v_x)_3^m = \frac{1}{\Delta x}\left(f_1 v_1^m + g_1 v_2^m + h_1 v_3^m\right), \tag{5.1.9}$$

where the constants, d_1, e_1, f_1, g_1 and h_1 have to be determined. Note that v_1^m is the known boundary condition. Multiplying both sides of (5.1.9) with Δx, we get

$$d_1\Delta x(v_x)_2^m + e_1\Delta x(v_x)_3^m = \left(f_1 v_1^m + g_1 v_2^m + h_1 v_3^m\right). \tag{5.1.10}$$

By Taylor series expansion of each of the terms about the point (x_1, t^m), we get

$$\begin{aligned}
v_2^m &= v_1^m + (\Delta x)(v_x)_1^m + \frac{(\Delta x)^2}{2}(v_{xx})_1^m + \frac{(\Delta x)^3}{6}(v_{xxx})_1^m + O((\Delta x)^4),\\
v_3^m &= v_1^m + (2\Delta x)(v_x)_1^m + \frac{(2\Delta x)^2}{2}(v_{xx})_1^m + \frac{(2\Delta x)^3}{6}(v_{xxx})_1^m + O((\Delta x)^4),\\
(v_x)_2^m &= (v_x)_1^m + (\Delta x)(v_{xx})_1^m + \frac{(\Delta x)^2}{2}(v_{xxx})_1^m + O((\Delta x)^3),\\
(v_x)_3^m &= (v_x)_1^m + (2\Delta x)(v_{xx})_1^m + \frac{(2\Delta x)^2}{2}(v_{xxx})_1^m + O((\Delta x)^3).
\end{aligned}$$

Substituting these expansions in (5.1.10) and after simplification we get,

$$\begin{aligned}
&(d_1 + e_1)(\Delta x)(v_x)_1^m + (d_1 + 2e_1)(\Delta x)^2(v_{xx})_1^m + (d_1 + 4e_1)\frac{(\Delta x)^3}{2}(v_{xxx})_1^m\\
&+ O((\Delta x)^4) = (f_1 + g_1 + h_1)v_1^m + (g_1 + 2h_1)(\Delta x)(v_x)_1^m\\
&+ (g_1 + 4h_1)\frac{(\Delta x)^2}{2}(v_{xx})_1^m + (g_1 + 8h_1)\frac{(\Delta x)^3}{6}(v_{xxx})_1^m + O((\Delta x)^4).
\end{aligned} \tag{5.1.11}$$

Comparing the corresponding coefficient of $(\Delta x)^0, (\Delta x)^1, (\Delta x)^2$ and $(\Delta x)^3$ on both sides, we get,

$$f_1+g_1+h_1 = 0, \quad d_1+e_1 = g_1+2h_1, \quad d_1+2e_1 = \frac{g_1+4h_1}{2}, \quad \frac{d_1+4e_1}{2} = \frac{g_1+8h_1}{6},$$

which gives,

$$d_1 = 2e_1, \quad f_1 = -e_1/2, \quad g_1 = -2e_1, \quad h_1 = (5/2)e_1.$$

The value of e_1 being free, we choose $e_1 = 2$ which gives,

$$d_1 = 4, \quad e_1 = 2, \quad f_1 = -1, \quad g_1 = -4, \quad h_1 = 5.$$

Substituting these values in (5.1.9) we obtain,

$$4(v_x)_2^m + 2(v_x)_3^m = \frac{1}{\Delta x}\left(-v_1^m - 4v_2^m + 5v_3^m\right). \tag{5.1.12}$$

The following compact schemes are used to derive a fourth-order approximation to $(v_{xx})_2^m$ for $m = 0, 1, \ldots, N-1$,

$$(v_{xx})_2^m + k(v_{xx})_3^m = \frac{1}{(\Delta x)^2}\left(k_1 v_1^m + k_2 v_2^m + k_3 v_3^m + k_4 v_4^m + k_5 v_5^m + k_6 v_6^m\right), \tag{5.1.13}$$

where the constants $k, k_1, k_2, k_3, k_4, k_5$ and k_6 are constants to be determined. By Taylor series expansion of each of the terms about the point (x_1, t^m), we get,

$$\begin{aligned}
v_2^m &= v_1^m + (\Delta x)(v_x)_1^m + \frac{(\Delta x)^2}{2}(v_{xx})_1^m + \frac{(\Delta x)^3}{6}(v_{xxx})_1^m + \frac{(\Delta x)^4}{24}(v_{xxxx})_1^m \\
&\quad + \frac{(\Delta x)^5}{120}(v_{xxxxx})_1^m + O((\Delta x)^6), \\
v_3^m &= v_1^m + (2\Delta x)(v_x)_1^m + \frac{(2\Delta x)^2}{2}(v_{xx})_1^m + \frac{(2\Delta x)^3}{6}(v_{xxx})_1^m \\
&\quad + \frac{(2\Delta x)^4}{24}(v_{xxxx})_1^m + \frac{(2\Delta x)^5}{120}(v_{xxxxx})_1^m + O((\Delta x)^6), \\
v_4^m &= v_1^m + (3\Delta x)(v_x)_1^m + \frac{(3\Delta x)^2}{2}(v_{xx})_1^m + \frac{(3\Delta x)^3}{6}(v_{xxx})_1^m \\
&\quad + \frac{(3\Delta x)^4}{24}(v_{xxxx})_1^m + \frac{(3\Delta x)^5}{120}(v_{xxxxx})_1^m + O((\Delta x)^6), \\
v_5^m &= v_1^m + (4\Delta x)(v_x)_1^m + \frac{(4\Delta x)^2}{2}(v_{xx})_1^m + \frac{(4\Delta x)^3}{6}(v_{xxx})_1^m + \frac{(4\Delta x)^4}{24}(v_{xxxx})_1^m \\
&\quad + \frac{(4\Delta x)^5}{120}(v_{xxxxx})_1^m + O((\Delta x)^6), \\
v_6^m &= v_1^m + (5\Delta x)(v_x)_1^m + \frac{(5\Delta x)^2}{2}(v_{xx})_1^m + \frac{(5\Delta x)^3}{6}(v_{xxx})_1^m + \frac{(5\Delta x)^4}{24}(v_{xxxx})_1^m \\
&\quad + \frac{(5\Delta x)^5}{120}(v_{xxxxx})_1^m + O((\Delta x)^6), \\
(v_{xx})_2^m &= (v_{xx})_1^m + (\Delta x)(v_{xxx})_1^m + \frac{(\Delta x)^2}{2}(v_{xxxx})_1^m + \frac{(\Delta x)^3}{6}(v_{xxxxx})_1^m + O((\Delta x)^4), \\
(v_{xx})_3^m &= (v_{xx})_1^m + (2\Delta x)(v_{xxx})_1^m + \frac{(2\Delta x)^2}{2}(v_{xxxx})_1^m + \frac{(2\Delta x)^3}{6}(v_{xxxxx})_1^m + O((\Delta x)^4).
\end{aligned}$$

Substituting these expansions in (5.1.13) and after simplification we get

$$\begin{aligned}
&(1+k)(v_{xx})_1^m + (1+2k)(\Delta x)(v_{xxx})_1^m + (1+4k)\frac{(\Delta x)^2}{2}(v_{xxxx})_1^m + \\
&(1+8k)\frac{(\Delta x)^3}{6}(v_{xxxxx})_1^m + O((\Delta x)^4) = (k_1+k_2+k_3+k_4+k_5+k_6)\frac{1}{(\Delta x)^2}v_1^m \\
&+ (k_2+2k_3+3k_4+4k_5+5k_6)\frac{1}{(\Delta x)}(v_x)_1^m \\
&+ (k_2+2^2k_3+3^2k_4+4^2k_5+5^2k_6)\frac{1}{2}(v_{xx})_1^m \\
&+ (k_2+2^3k_3+3^3k_4+4^3k_5+5^3k_6)\frac{(\Delta x)}{6}(v_{xxx})_1^m
\end{aligned}$$

$$+ (k_2 + 2^4k_3 + 3^4k_4 + 4^4k_5 + 5^4k_6)\frac{(\Delta x)^2}{24}(v_{xxxx})_1^m$$
$$+ (k_2 + 2^5k_3 + 3^5k_4 + 4^5k_5 + 5^5k_6)\frac{(\Delta x)^3}{120}(v_{xxxxx})_1^m + O((\Delta x)^4).$$

Comparing the corresponding coefficients of $(\Delta x)^{-2}, (\Delta x)^{-1}$, $(\Delta x)^0$, $(\Delta x)^1$, $(\Delta x)^2$ and $(\Delta x)^3$ on both sides, we get,

$$\begin{aligned}
k_1 + k_2 + a_3 + k_4 + k_5 + k_6 &= 0,\\
k_2 + 2k_3 + 3k_4 + 4k_5 + 5k_6 &= 0,\\
k_2 + 2^2k_3 + 3^2k_4 + 4^2k_5 + 5^2k_6 &= 2 + 2k,\\
k_2 + 2^3k_3 + 3^3k_4 + 4^3k_5 + 5^3k_6 &= 6 + 12k,\\
k_2 + 2^4k_3 + 3^4k_4 + 4^4k_5 + 5^4k_6 &= 12 + 48k,\\
k_2 + 2^5k_3 + 3^5k_4 + 4^5k_5 + 5^5k_6 &= 20 + 160k.
\end{aligned}$$

The value of k being free, we choose $k = \frac{1}{2}$ to obtain

$$k_1 = \frac{19}{24}, \quad k_2 = -\frac{7}{12}, \quad k_3 = -\frac{19}{12}, \quad k_4 = \frac{11}{6}, \quad k_5 = -\frac{13}{24}, \quad k_6 = \frac{1}{12}.$$

Substituting these values in (5.1.13) we obtain,

$$(v_{xx})_2^m + \frac{1}{2}(v_{xx})_3^m = \frac{1}{(\Delta x)^2}\left(\frac{19}{24}v_1^m - \frac{7}{12}v_2^m - \frac{19}{12}v_3^m + \frac{11}{6}v_4^m - \frac{13}{24}v_5^m + \frac{1}{12}v_6^m\right). \tag{5.1.14}$$

At the right boundary (x_M, t^m) we have the *Neumann* boundary condition, $v_x(x_M, t^m) = e^{-r(T-t^m)}$. The following compact schemes are used to derive a fourth-order approximation to $(v_x)_{M-1}^m$,

$$d_2(v_x)_{M-2}^m + e_2(v_x)_{M-1}^m + f_2(v_x)_M^m = \frac{1}{(\Delta x)}\left(g_2v_{M-1}^m + h_2v_{M-2}^m\right), \tag{5.1.15}$$

where the constants d_2, e_2, f_2, g_2 and h_2 are to be determined. Multiplying both sides of (5.1.15) by Δx we get

$$d_2\Delta x(v_x)_{M-2}^m + e_2\Delta x(v_x)_{M-1}^m + f_2\Delta x(v_x)_M^m = \left(g_2v_{M-1}^m + h_2v_{M-2}^m\right). \tag{5.1.16}$$

By Taylor series, expansion of each of the terms about the point (x_M, t^m), we get,

$$v_{M-1}^m = v_M^m - (\Delta x)(v_x)_M^m + \frac{(\Delta x)^2}{2}(v_{xx})_M^m - \frac{(\Delta x)^3}{6}(v_{xxx})_M^m + O((\Delta x)^4),$$
$$v_{M-2}^m = v_M^m - (2\Delta x)(v_x)_M^m + \frac{(2\Delta x)^2}{2}(v_{xx})_M^m - \frac{(2\Delta x)^3}{6}(v_{xxx})_M^m + O((\Delta x)^4),$$

$$(v_x)^m_{M-1} = (v_x)^m_M - (\Delta x)(v_{xx})^m_M + \frac{(\Delta x)^2}{2}(v_{xxx})^m_M + O((\Delta x)^3),$$
$$(v_x)^m_{M-2} = (v_x)^m_M - (2\Delta x)(v_{xx})^m_M + \frac{(2\Delta x)^2}{2}(v_{xxx})^m_M + O((\Delta x)^3).$$

Substituting these expansions in (5.1.16) and after simplification we get

$$(f_2 + d_2 + e_2)(\Delta x)(v_x)^m_M - (2d_2 + e_2)(\Delta x)^2(v_{xx})^m_M + (4d_2 + e_2)\frac{(\Delta x)^3}{2}(v_{xxx})^m_M$$
$$+ O((\Delta x)^4) = (g_2 + h_2)v^m_M - (g_2 + 2h_2)(\Delta x)(v_x)^m_M + (g_2 + 4h_2)\frac{(\Delta x)^2}{2}(v_{xx})^m_M$$
$$- (g_2 + 8h_2)\frac{(\Delta x)^3}{6}(v_{xxx})^m_M + O((\Delta x)^4). \tag{5.1.17}$$

Comparing the corresponding coefficients of $(\Delta x)^0, (\Delta x)^1, (\Delta x)^2$ and $(\Delta x)^3$ on both sides, we get,

$$g_2+h_2 = 0,\ f_2+d_2+e_2 = -g_2-2h_2,\ -2d_2-e_2 = \frac{g_2+4h_2}{2},\ \frac{4d_2+e_2}{2} = -\frac{g_2+8h_2}{6},$$

which gives

$$d_2 = -(5/12)h_1, \quad f_2 = h_1/12, \quad g_2 = -h_2, \quad e_2 = -(2/3)h_2.$$

The value of h_2 being free, we choose $h_2 = -12$ to obtain

$$d_2 = 5, \quad e_2 = 8, \quad f_2 = -1, \quad g_2 = 12, \quad h_2 = -12.$$

Substituting these values in (5.1.15) we obtain,

$$5(v_x)^m_{M-2} + 8(v_x)^m_{M-1} = (v_x)^m_M + \frac{1}{\Delta x}\left(12v^m_{M-1} - 12v^m_{M-2}\right). \tag{5.1.18}$$

The following compact schemes are used to derive a fourth-order approximation to $(v_{xx})^m_{M-1}$,

$$d_3(v_{xx})^m_{M-2} + e_3(v_{xx})^m_{M-1} + \frac{1}{\Delta x}f_3(v_x)^m_M = \frac{1}{(\Delta x)^2}\left(g_3v^m_{M-1} + h_3v^m_{M-2}\right), \tag{5.1.19}$$

where the constants d_3, e_3, f_3, g_3 and h_3 are to be determined. Multiplying both sides of (5.1.19) by $(\Delta x)^2$ we get

$$d_3(\Delta x)^2(v_{xx})^m_{M-2} + e_3(\Delta x)^2(v_{xx})^m_{M-1} + f_3\Delta x(v_x)^m_M = \left(g_3v^m_{M-1} + h_3v^m_{M-2}\right). \tag{5.1.20}$$

By Taylor series expansion of each of the terms about the point (x_M, t^m), we get

$$v^m_{M-1} = v^m_M - (\Delta x)(v_x)^m_M + \frac{(\Delta x)^2}{2}(v_{xx})^m_M - \frac{(\Delta x)^3}{6}(v_{xxx})^m_M + O((\Delta x)^4),$$
$$v^m_{M-2} = v^m_M - (2\Delta x)(v_x)^m_M + \frac{(2\Delta x)^2}{2}(v_{xx})^m_M - \frac{(2\Delta x)^3}{6}(v_{xxx})^m_M + O((\Delta x)^4),$$
$$(v_{xx})^m_{M-1} = (v_{xx})^m_M - (\Delta x)(v_{xxx})^m_M + O((\Delta x)^2),$$
$$(v_{xx})^m_{M-2} = (v_{xx})^m_M - (2\Delta x)(v_{xxx})^m_M + O((\Delta x)^2).$$

Substituting these expansions in (5.1.20) and after simplification, we get,

$$\begin{aligned} & f_3\Delta x(v_x)_M^m + (d_3+e_3)(\Delta x)^2(v_{xx})_M^m - (2d_3+e_3)(\Delta x)^3(v_{xxx})_M^m + O((\Delta x)^4) \\ & = (g_3+h_3)v_M^m - (g_3+2h_3)(\Delta x)(v_x)_M^m + (g_3+4h_3)\frac{(\Delta x)^2}{2}(v_{xx})_M^m \\ & - (g_3+8h_3)\frac{(\Delta x)^3}{6}(v_{xxx})_M^m + O((\Delta x)^4). \end{aligned} \tag{5.1.21}$$

Comparing the corresponding coefficient of $(\Delta x)^0, (\Delta x)^1, (\Delta x)^2$ and $(\Delta x)^3$ on both sides, we get,

$$g_3+h_3=0, \quad f_3=-g_3-2h_3, \quad d_3+e_3=\frac{g_3+4h_3}{2}, \quad 2d_3+e_3=\frac{g_3+8h_3}{6}.$$

which gives,

$$d_3=-(1/3)h_3, \quad e_3=(11/6)h_3, \quad f_3=-h_3, \quad g_3=-h_3.$$

The value of h_3 being free we choose $h_3=1$ to obtain

$$d_3=-(1/3), \quad e_3=11/6, \quad f_3=-1, \quad g_3=-1.$$

Substituting these values in (5.1.19) we obtain,

$$(-4)(v_{xx})_{M-2}^m + 22(v_{xx})_{M-1}^m = \frac{12}{\Delta x}(v_x)_M^m + \frac{1}{(\Delta x)^2}\left(-12v_{M-1}^m + 12v_{M-2}^m\right). \tag{5.1.22}$$

Thus the set of schemes, consisting of (5.1.1), (5.1.5), (5.1.8), (5.1.12), (5.1.14), (5.1.18) and (5.1.22) has the overall order of $O\left((\Delta t)^2+(\Delta x)^4\right)$.

5.1.3 Matrix form

We now introduce a few notations prior to representing the numerical scheme (5.1.1) in the matrix form. At the time level $t^m, m=0,1,\ldots,N-1$, we have

$$\begin{aligned} (\vec{v})^m &= \left(v_2^m,\ldots,v_{M-1}^m\right)^\top, \\ (\vec{v}_x)^m &= \left((v_x)_2^m,\ldots,(v_x)_{M-1}^m\right)^\top, \\ (\vec{v}_{xx})^m &= \left((v_{xx})_2^m,\ldots,(v_{xx})_{M-1}^m\right)^\top \end{aligned}$$

$$A = \begin{bmatrix} 1 & \frac{1}{2} & & & \\ 1 & 10 & 1 & & \\ & \ddots & \ddots & \ddots & \\ & & 1 & 10 & 1 \\ & & & -4 & 22 \end{bmatrix}, \tag{5.1.23}$$

$$B = \begin{bmatrix} -7/24 & -19/24 & 11/12 & -13/48 & 1/24 & 0 & \dots & 0 \\ 6 & -12 & 6 & & & & & \\ & \ddots & \ddots & \ddots & & & & \\ & & \ddots & \ddots & \ddots & & & \\ & & & \ddots & \ddots & \ddots & & \\ & & & & \ddots & \ddots & \ddots & \\ & & & & & \ddots & \ddots & \ddots \\ & & & & & & 6 & -12 & 6 \\ & & & & & & & 6 & -6 \end{bmatrix}, \tag{5.1.24}$$

$$D = \begin{bmatrix} 4 & 2 & & & \\ 1 & 4 & 1 & & \\ & \ddots & \ddots & \ddots & \\ & & 1 & 4 & 1 \\ & & & 5 & 8 \end{bmatrix}, \tag{5.1.25}$$

$$E = \begin{bmatrix} -4 & 5 & & & \\ -3 & 0 & 3 & & \\ & \ddots & \ddots & \ddots & \\ & & -3 & 0 & 3 \\ & & & -12 & 12 \end{bmatrix}. \tag{5.1.26}$$

$$(\vec{C})^m = \left(\frac{19}{24(\Delta x)^2} v_1^m, 0, \dots, 0, \frac{12}{\Delta x} (v_x)_M^m \right)^\top, \tag{5.1.27}$$

$$(\vec{F})^m = \left(-\frac{1}{\Delta x} v_1^m, 0, \dots, 0, (v_x)_M^m \right)^\top. \tag{5.1.28}$$

Using these notations, the schemes in (5.1.8), (5.1.14) and (5.1.22) can be written as

$$A(\vec{v}_{xx})^m = \frac{2}{(\Delta x)^2} B(\vec{v})^m + (\vec{C})^m \tag{5.1.29}$$

Similarly, the schemes in (5.1.5), (5.1.12) and (5.1.18) can be written as

$$D(\vec{v}_x)^m = \frac{1}{\Delta x} E(\vec{v})^m + (\vec{F})^m. \tag{5.1.30}$$

The invertibility of matrices A and D shows the solvability of (5.1.29) and (5.1.30) which can be proved using the Gerschgorin Theorem [48]. Simplifying (5.1.29) and (5.1.30) we obtain

$$(\vec{v}_{xx})^m = \frac{2}{(\Delta x)^2} A^{-1} B(\vec{v})^m + A^{-1}(\vec{C})^m. \tag{5.1.31}$$

$$(\vec{v}_x)^m = \frac{1}{\Delta x} D^{-1} E(\vec{v})^m + D^{-1}(\vec{F})^m. \tag{5.1.32}$$

Using (5.1.31) and (5.1.32) in the CNIM (5.1.1) we obtain,

$$\begin{aligned}
&\frac{(\vec{v})^{m+1} - (\vec{v})^m}{\Delta t} + \frac{1}{2\Delta x} S^{m+1} D^{-1} E \left[(\vec{v})^{m+1} + (\vec{v})^m\right] \\
&+ \frac{1}{2} S^{m+1} D^{-1} \left[(\vec{F})^{m+1} + (\vec{F})^m\right] + \frac{1}{(\Delta x)^2} R^{m+1} A^{-1} B \left[(\vec{v})^{m+1} + (\vec{v})^m\right] \\
&+ \frac{1}{2} R^{m+1} A^{-1} \left[(\vec{C})^{m+1} + (\vec{C})^m)\right] = \frac{\gamma}{2} \left[(\vec{v})^{m+1} + (\vec{v})^m)\right],
\end{aligned} \tag{5.1.33}$$

where R and S are diagonal matrices given by

$$\begin{aligned}
S^{m+1} &= \text{diag}(\alpha_2^{m+1}, \alpha_3^{m+1}, \ldots \alpha_{M-1}^{m+1}),\ \alpha_j^{m+1} = \mathcal{A}\left(x_j, (u^*)_j^{m+1}\right), \\
R^{m+1} &= \text{diag}(\beta_2^{m+1}, \beta_3^{m+1}, \ldots \beta_{M-1}^{m+1}),\ \beta_j^{m+1} = \mathcal{B}\left(x_j, (u^*)_j^{m+1}\right).
\end{aligned} \tag{5.1.34}$$

Upon further simplification, (5.1.33) becomes

$$\begin{aligned}
&\left[\left(1 + \frac{\gamma \Delta t}{2}\right) I - \frac{1}{2} q S^{m+1} D^{-1} E - p R^{m+1} A^{-1} B\right] (\vec{v})^m \\
&= \left[\left(1 - \frac{\gamma \Delta t}{2}\right) I + \frac{1}{2} q S^{m+1} D^{-1} E + p R^{m+1} A^{-1} B\right] (\vec{v})^{m+1} \\
&+ \frac{\Delta t}{2} S^{m+1} D^{-1} \left[(\vec{F})^{m+1} + (\vec{F})^m\right] + \frac{\Delta t}{2} R^{m+1} A^{-1} \left[(\vec{C})^{m+1} + (\vec{C})^m)\right],
\end{aligned} \tag{5.1.35}$$

where I is the identity matrix of size $(M-2) \times (M-2)$, $p = \dfrac{\Delta t}{(\Delta x)^2}$ and $q = \dfrac{\Delta t}{\Delta x}$. The discretization of u^* in (1.2.4) using the HOC schemes is

$$(u^*)_j^m = \text{sign}\left(\frac{(r-\gamma)}{2} \left[(v_x)_j^{m+1} + (v_x)_j^m\right] - \frac{1}{2} x_j \sigma^2 \left[(v_{xx})_j^{m+1} + (v_{xx})_j^m\right]\right), \tag{5.1.36}$$

which upon further simplification using (5.1.31) and (5.1.32) results in

$$(\vec{u^*})^m = \text{sign}\left(\frac{(r-\gamma)}{2\Delta x}D^{-1}E\left[(\vec{v})^{m+1}+(\vec{v})^m\right]+\frac{(r-\gamma)}{2}D^{-1}\left[(\vec{F})^{m+1}+(\vec{F})^m\right]\right.$$
$$\left.-\sigma^2\frac{1}{(\Delta x)^2}TA^{-1}B\left[(\vec{v})^{m+1}+(\vec{v})^m\right]-\frac{\sigma^2}{2}TA^{-1}\left[(\vec{C})^{m+1}+(\vec{C})^m\right]\right), \tag{5.1.37}$$

where

$$(\vec{u^*})^m = ((u^*)_2^m,\ldots,(u^*)_{M-1}^m)^\top,$$

and T is diagonal matrix given by

$$T = \text{diag}(x_2, x_3, \ldots x_{M-1}). \tag{5.1.38}$$

Note that the compact stencil was used only in the spatial direction with Crank-Nicholson scheme being used for temporal discretization. Accordingly HOC scheme would mean HOC scheme in space and Crank-Nicholson scheme in time.

5.2 Grid stretching

The improved convergence observed for HOC scheme as compared to the Crank-Nicholson scheme is somewhat limited near the zero accumulated gain. Consequently with the goal of improving upon the convergence rate in addition to reduction in maximum error arising from the final condition being non-smooth, we need to a grid stretching transformation [49,50] and derive the HOC schemes with grid stretching (HOCGS). The aforesaid transformation using the transformed coordinate $y \in [0,1]$ is given by

$$x = \phi(y) = \frac{1}{\xi}\sinh(c_2 y + c_1(1-y)) + k, \tag{5.2.1}$$

where ξ is the stretching parameter, $c_1 = \sinh^{-1}(\xi(x_{\min}-k))$, $c_2 = \sinh^{-1}(\xi(x_{\max}-k))$ and k is the stretched coordinate (which for our problem is $k = 0$ *i.e.,* near the zero accumulated gain), Using the transformed variable $V(y,t) = v(x,t)$, the equations (1.2.3),(1.2.4),(2.2.1),(2.2.2) and (2.2.3) can be rewritten as,

$$\frac{\partial V}{\partial t} + \mathbb{A}(y,u^*)\frac{\partial V}{\partial y} + \mathbb{B}(y,u^*)\frac{\partial^2 V}{\partial y^2} = \gamma V, \tag{5.2.2}$$

$$u^*(y,t) = \text{sign}\left(\mathbb{P}(y)\frac{\partial V}{\partial y} - \mathbb{Q}(y)\frac{\partial^2 V}{\partial y^2}\right), \tag{5.2.3}$$

$$V(0,t) = 0, \tag{5.2.4}$$

$$V_y(1,t) = J(1)e^{-r(T-t)}, \tag{5.2.5}$$

$$V(y,T) = \max\left(\phi(y), 0\right). \tag{5.2.6}$$

with

$$\mathbb{A}(y,u^*) = \frac{(u^*-\phi(y))(r-\gamma)}{J(y)} - \frac{1}{2}(u^*-\phi(y))^2\sigma^2\frac{H(y)}{(J(y))^3}, \tag{5.2.7}$$

$$\mathbb{B}(y,u^*) = \frac{1}{2}\frac{(u^*-\phi(y))^2\sigma^2}{(J(y))^2}, \tag{5.2.8}$$

$$\mathbb{P}(y) = \frac{(r-\gamma)}{J(y)} + \frac{\sigma^2\phi(y)H(y)}{(J(y))^3}, \tag{5.2.9}$$

$$\mathbb{Q}(y) = \frac{\sigma^2\phi(y)}{(J(y))^2}. \tag{5.2.10}$$

$$J(y) = \frac{\partial\phi}{\partial y} = \frac{c_2-c_1}{\xi}\cosh(c_2y + c_1(1-y)), \tag{5.2.11}$$

$$H(y) = \frac{\partial^2\phi}{\partial y^2} = \frac{(c_2-c_1)^2}{\xi}\sinh(c_2y + c_1(1-y)), \tag{5.2.12}$$

In order to discretize (5.2.2) and (5.2.3) over the transformed domain $[0,1]$, we use $\Delta y = \dfrac{1}{M-1}$, $y_j = (j-1)\Delta y,\ j = 1,2,\ldots,M$ with Δt being the same as previously defined. The temporal semi-discretization of (5.2.2) using the CNIM is as follows,

$$\frac{V_j^{m+1}-V_j^m}{\Delta t} + \mathbb{A}\left(y_j,(u^*)_j^{m+1}\right)\left[\frac{(V_y)_j^{m+1}+(V_y)_j^m}{2}\right] + \mathbb{B}\left(y_j,(u^*)_j^{m+1}\right)\left[\frac{(V_{yy})_j^{m+1}+(V_{yy})_j^m}{2}\right] = \gamma\left[\frac{V_j^{m+1}+V_j^m}{2}\right]. \tag{5.2.13}$$

The fourth order approximation to V_y and V_{yy} (similar to that of v_x and v_{xx}) are as follows,

$$(\vec{V_{yy}})^m = \frac{2}{(\Delta y)^2}A^{-1}B(\vec{V})^m + A^{-1}(\vec{C_{gs}})^m. \tag{5.2.14}$$

$$(\vec{V_y})^m = \frac{1}{\Delta y}D^{-1}E(\vec{V})^m + D^{-1}(\vec{F_{gs}})^m. \tag{5.2.15}$$

where the matrices A, B,D, E are same as given in (5.1.23) – (5.1.26) and

$$(\vec{C_{gs}})^m = \left(\frac{19}{24(\Delta y)^2}V_1^m, 0, \ldots, 0, \frac{12}{\Delta y}(V_y)_M^m\right)^T,$$

$$(\vec{F_{gs}})^m = \left(-\frac{1}{\Delta y}V_1^m, 0, \ldots, 0, (V_y)_M^m\right)^T.$$

Using (5.2.14) and (5.2.15), equation (5.2.13) can be written as,

$$\frac{(\vec{V})^{m+1}-(\vec{V})^{m}}{\Delta t}+\frac{1}{2\Delta y}\mathbb{S}^{m+1}D^{-1}E\left[(\vec{V})^{m+1}+(\vec{V})^{m}\right]$$
$$+\frac{1}{2}\mathbb{S}^{m+1}D^{-1}\left[(\vec{F_{gs}})^{m+1}+(\vec{F_{gs}})^{m}\right]+\frac{1}{(\Delta y)^2}\mathbb{R}^{m+1}A^{-1}B\left[(\vec{V})^{m+1}+(\vec{V})^{m}\right]$$
$$+\frac{1}{2}\mathbb{R}^{m+1}A^{-1}\left[(\vec{C_{gs}})^{m+1}+(\vec{C_{gs}})^{m})\right]=\frac{\gamma}{2}\left[(\vec{V})^{m+1}+(\vec{V})^{m})\right], \tag{5.2.16}$$

where $\mathbb{S}$ and $\mathbb{R}$ are diagonal matrices given by

$$\begin{aligned}\mathbb{S}^{m+1} &= \text{diag}(\alpha_2^{m+1},\alpha_3^{m+1},\dots\alpha_{M-1}^{m+1}),\alpha_j^{m+1}=\mathbb{A}\left(y_j,(u^*)_j^{m+1}\right),\\ \mathbb{R}^{m+1} &= \text{diag}(\beta_2^{m+1},\beta_3^{m+1},\dots\beta_{M-1}^{m+1}),\beta_j^{m+1}=\mathbb{B}\left(y_j,(u^*)_j^{m+1}\right).\end{aligned}$$

Upon further simplification, (5.2.16) becomes

$$\left[\left(1+\frac{\gamma\Delta t}{2}\right)I-\frac{1}{2}q_1\mathbb{S}^{m+1}D^{-1}E-p_1\mathbb{R}^{m+1}A^{-1}B\right](\vec{V})^{m}$$
$$=\left[\left(1-\frac{\gamma\Delta t}{2}\right)I+\frac{1}{2}q_1\mathbb{S}^{m+1}D^{-1}E+p_1\mathbb{R}^{m+1}A^{-1}B\right](\vec{V})^{m+1}$$
$$+\frac{\Delta t}{2}\mathbb{S}^{m+1}D^{-1}\left[(\vec{F_{gs}})^{m+1}+(\vec{F_{gs}})^{m}\right]+\frac{\Delta t}{2}\mathbb{R}^{m+1}A^{-1}\left[(\vec{C_{gs}})^{m+1}+(\vec{C_{gs}})^{m})\right], \tag{5.2.17}$$

where I is the identity matrix of size $(M-2)\times(M-2)$, $p_1=\dfrac{\Delta t}{(\Delta y)^2}$ and $q_1=\dfrac{\Delta t}{\Delta y}$. The discretization of $u^*(y,t)$ using HOC is as follows

$$(u^*)_j^m=\text{sign}\left(\frac{1}{2}\mathbb{P}(y_j)\left[(V_y)_j^{m+1}+(V_y)_j^{m}\right]-\frac{1}{2}\mathbb{Q}(y_j)\left[(V_{yy})_j^{m+1}+(V_{yy})_j^{m}\right]\right), \tag{5.2.18}$$

which upon further simplification, by using (5.2.14) and (5.2.15) results in

$$(\vec{u^*})^m=\text{sign}\left(\left[\frac{\mathcal{P}D^{-1}E}{2\Delta y}-\frac{\mathcal{Q}A^{-1}B}{(\Delta y)^2}\right]\left[(\vec{V})^{m+1}+(\vec{V})^{m}\right]\right.$$
$$\left.+\frac{1}{2}\mathcal{P}D^{-1}\left[(\vec{F_{gs}})^{m+1}+(\vec{F_{gs}})^{m}\right]-\frac{1}{2}\mathcal{Q}A^{-1}\left[(\vec{C_{gs}})^{m+1}+(\vec{C_{gs}})^{m})\right]\right). \tag{5.2.19}$$

where

$$(\vec{u^*})^m=((u^*)_2^m,\dots,(u^*)_{M-1}^m)^\top,$$

and $\mathcal{P}$ and $\mathcal{Q}$ are diagonal matrices given by

$$\begin{aligned}\mathcal{P} &= \text{diag}(\mathbb{P}(y_2),\mathbb{P}(y_3),\dots\mathbb{P}(y_{M-1})),\\ \mathcal{Q} &= \text{diag}(\mathbb{Q}(y_2),\mathbb{Q}(y_3),\dots\mathbb{Q}(y_{M-1})).\end{aligned}$$

The pricing for American passport option is exercised through the following result which takes into account the fact that the American option can be exercised on or before the expiration date.

Proposition 5.2.1. *[3] The price of an American passport option, $\widehat{v}(x,t)$ satisfies (1.2.3)-(1.2.4) on the continuation region denoted by $\mathcal{R}^c$, where $\mathcal{R}^c = \{(x,t) \in \mathbb{R} \times [0,T) : \widehat{v}(x,t) > \max(x,0)\}$, subject to the free boundary condition and terminal condition,*

$$\widehat{v}(x,t) \geq \max(x,0), \ \forall (x,t) \in \mathcal{R}^c \tag{5.2.20}$$

and

$$\widehat{v}(x,T) = \max(x,0). \tag{5.2.21}$$

In order to determine the value of the American passport option numerically, the following early exercise condition

$$\widehat{v}_{i,j} = \max(v_{i,j}, \max(x,0)), \tag{5.2.22}$$

where $v_{i,j}$ is the solution of (5.1.35) and (5.2.17) in case of and HOC and HOCGS schemes respectively, is used.

5.3 Numerical results

The HOC and the HOCGS schemes derived in Sections 5.1 and 5.2 will be numerically illustrated in this section along with a comparative analysis involving both HOC and HOCGS as well as the CNIM. We will portray the advantages offered by the HOC scheme over CNIM along with even better results being obtained from the usage of HOCGS scheme.

We first look at the case $r = \gamma$ (symmetric) and use the analytic solution (available in this case) for the purpose of comparison. The parameters used are same as given in Section 2.2 of Chapter 2 [3]. As before, the simulation carried out in MatLab™ were for several values of M and N with the results being presented (in Table 5.1) for $M = 800$ and $N = 800$ only. It is observed that the HOC scheme offer slight improvement over CNIM scheme. The HOCGS scheme which includes grid stretching results in even more improved results, in terms of the values obtained being closely matched to the analytic values. These improvements are further evident from the log-log plot of the maximum error

versus M for each of the three scheme as illustrated in Figure 5.1. While the presentation in Figure 5.1 is only for $M = 800$. Evidently, while marginal maximum error reduction was seen for HOC scheme, significant reduction happened when HOCGS scheme was used. Table 5.2 lists the maximum error and the rate of convergence for all the three schemes. Further, both CNIM and HOC attain only second order convergence during numerical implementation while HOCGS was able to reach close to third order convergence (numerically). While this reflects that numerical implementation using HOCGS is unable to attain the theoretical fourth order accuracy, it still does indicate significantly better accuracy when compared to the HOC scheme and CNIM.

The existence of analytic solution being precluded in the $r \neq \gamma$ (non-symmetric) case, it becomes imperative to specify an alternate approach to calculate maximum error and the rate of convergence for this case. Accordingly, the maximum error and rate of convergence are computed using the double-mesh principle [51]. Let $U^M(x_i)$ and $U^{2M}(x_i)$ be the approximate numerical solutions in the computational domain $[x_{\min}, x_{\max}]$ obtained with M and $2M$ mesh intervals respectively. Also let

$$\overline{\Omega}^M = \{x_i : x_i = x_{\min} + (i-1)h,\ i = 1, 2, \ldots, M\}.$$

where $h = \dfrac{x_{\max} - x_{\min}}{M-1}$. The maximum error and the rate of convergence are determined by the double-mesh differences

$$E^M = \max_{x_i \in \overline{\Omega}^M} |U^M(x_i) - U^{2M}(x_i)|, \tag{5.3.1}$$

and

$$q = \log_2 \left(\frac{E^M}{E^{2M}} \right). \tag{5.3.2}$$

The numerical results for the European and American passport option for this case, using the parameter values in Section 2.3 of Chapter 2 [3] for all the three schemes for various accumulated gains are illustrated in Table 5.3 and 5.7 respectively.

Further, the log-log plot of the maximum error as given by (5.3.1) versus M (for European option), are presented in Figure 5.2. Finally, the maximum error and the rate of convergence for this case using three schemes are given in Table 5.4 and Table 5.8 respectively. Also, the maximum error and rate of convergence for several grid stretching parameter ξ and M are presented in Table 5.5 and

Table 5.6 for the symmetric and non-symmetric case respectively (for European option).

w	Analytic	CNIM	HOC	HOCGS
-20	5.887568	5.886553	5.886658	5.887572
-10	8.880836	8.879288	8.879603	8.880844
-5	10.830686	10.828835	10.829259	10.830680
-2	12.169565	12.168752	12.169237	12.169553
-1	12.646019	12.644768	12.645272	12.646016
0	13.138099	13.135937	13.136459	13.138079
1	13.646019	13.644768	13.645272	13.646016
2	14.169565	14.168752	14.169237	14.169553
5	15.830686	15.828835	15.829259	15.830680
10	18.880836	18.879288	18.879603	18.880844
20	25.887568	25.886553	25.886658	25.887572

Table 5.1: Price of the European passport option with $S(t) = 100$, $r = 0$, $\gamma = 0$, $\sigma = 30\%$, $T - t = 1$, $M = 800$ and $N = 800$ with $\xi = 13$.

.

Spatial nodes	CNIM error	CNIM order	HOC error	HOC order	HOCGS error	HOCGS order
21	3.203367	-	2.442399	-	0.568289	-
41	0.873704	1.874372	0.651655	1.906119	0.144473	1.975826
81	0.216691	2.011507	0.163756	1.992564	0.028900	2.321656
161	0.054095	2.002059	0.040994	1.998047	0.004692	2.622644
321	0.013519	2.000502	0.010252	1.999559	0.000673	2.800841

Table 5.2: Maximum error and rate of convergence for the European passport option with $S(t) = 100$, $r = 0$, $\gamma = 0$, $\sigma = 30\%$, $T - t = 1$ and $N = 800$ with $\xi = 13$.

5.4 Conclusion

In this chapter, we presented the HOC scheme for pricing both the European and American passport option. The HOC scheme when numerically implemented is second order accurate in space direction. This was improved upon by the

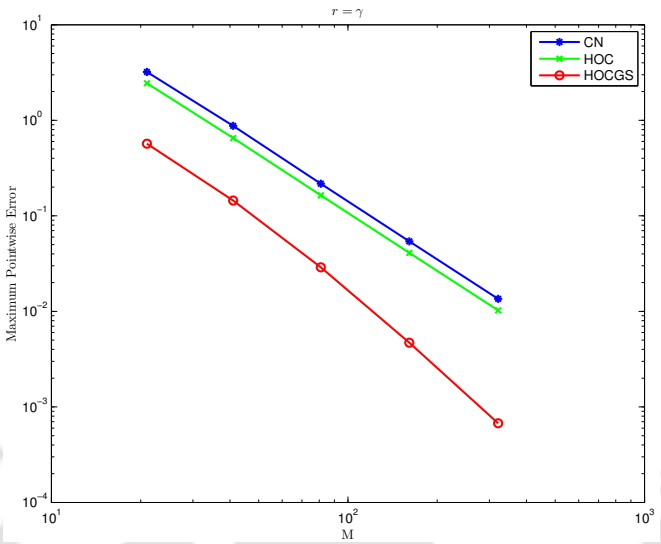

Figure 5.1: Log-log plot of the maximum error against M for the European passport option with $S(t) = 100$, $r = 0$, $\gamma = 0$, $\sigma = 30\%$, $T - t = 1$ and $N = 800$ with $\xi = 13$.

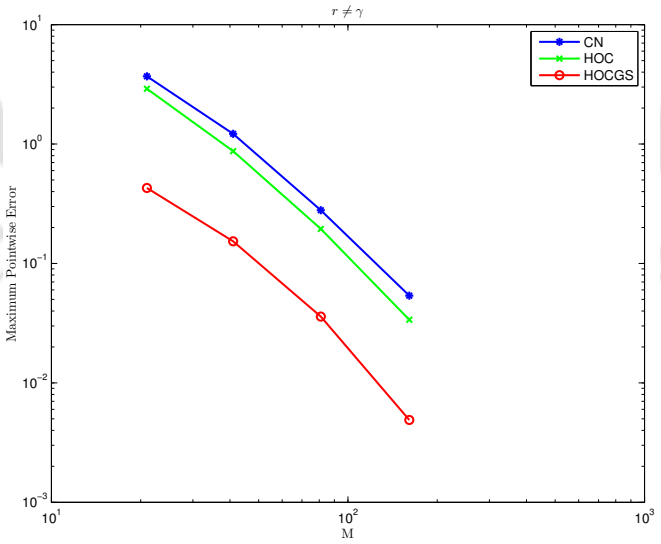

Figure 5.2: Log-log plot of the maximum error against M for the European passport option with $S(t) = 100$, $r = 5\%$, $\gamma = 4.5\%$, $\sigma = 30\%$, $T - t = 2$ and $N = 800$ with $\xi = 13$.

w	CNIM	HOC	HOCGS
-20	10.428911	10.430595	10.430803
-10	13.509960	13.512246	13.512163
-5	15.357743	15.360405	15.360103
-2	16.577444	16.580551	16.579883
-1	17.003622	17.006314	17.006092
0	17.439919	17.440792	17.442332
1	17.886523	17.889334	17.889046
2	18.343627	18.347030	18.346170
5	19.778782	19.781776	19.781271
10	22.372380	22.374982	22.374694
20	28.226310	28.228299	28.228294

Table 5.3: Price of the European passport option with $S(t) = 100$, $r = 5\%$, $\gamma = 4.5\%$, $\sigma = 30\%$, $T - t = 2$, $M = 800$ and $N = 800$ with $\xi = 13$.

.

Spatial nodes	CNIM error	CNIM order	HOC error	HOC order	HOCGS error	HOCGS order
21	3.692374	-	2.904958	-	0.429031	-
41	1.218312	1.599666	0.871569	1.736830	0.153247	1.485222
81	0.279163	2.125705	0.194817	2.161497	0.035894	2.094036
161	0.053758	2.376550	0.033796	2.527194	0.004895	2.874414

Table 5.4: Maximum error and rate of convergence for the European passport option with $S(t) = 100$, $r = 5\%$, $\gamma = 4.5\%$, $\sigma = 30\%$, $T - t = 2$ and $N = 800$ with $\xi = 13$.

application of grid stretching near the zero accumulated gain giving the HOCGS scheme which has third order accuracy in the spatial direction.

ξ	M=21	M=41	M=81	M=161	M=321
1	0.858980	0.217465	0.054529	0.013642	0.003411
	1.981842	1.995687	1.998968	1.999916	
2	0.393637	0.099603	0.024972	0.006247	0.001562
	1.982607	1.995885	1.999085	2.000152	
3	0.262586	0.059071	0.014811	0.003705	0.000926
	2.152258	1.995776	1.999125	2.000421	
4	0.316357	0.072677	0.013157	0.002502	0.000625
	2.121981	2.465625	2.394758	2.000752	
5	0.360326	0.084606	0.015630	0.002408	0.000456
	2.090476	2.436402	2.698680	2.400214	
6	0.397625	0.094951	0.017826	0.002774	0.000391
	2.066148	2.413170	2.684078	2.827118	
7	0.430080	0.104107	0.019807	0.003108	0.000439
	2.046534	2.394007	2.671740	2.822355	
8	0.458848	0.112334	0.021614	0.003417	0.000485
	2.030222	2.377773	2.661075	2.817996	
9	0.484714	0.119814	0.023278	0.003704	0.000527
	2.016338	2.363740	2.651695	2.814002	
10	0.508230	0.126679	0.024823	0.003973	0.000566
	2.004303	2.351414	2.643332	2.810328	
11	0.529804	0.133029	0.026266	0.004226	0.000604
	1.993717	2.340450	2.635792	2.806933	
12	0.549744	0.138940	0.027622	0.004465	0.000639
	1.984296	2.330594	2.628933	2.803781	
13	0.568289	0.144473	0.028900	0.004692	0.000673
	1.975826	2.321656	2.622644	2.800841	
14	0.585628	0.149675	0.030111	0.004909	0.000706
	1.968147	2.313491	2.616842	2.798089	
15	0.601915	0.154587	0.031261	0.005115	0.000737
	1.961136	2.305983	2.611457	2.795503	

Table 5.5: Maximum error and rate of convergence of the European passport option for various values of ξ and M, with $S(t) = 100$, $r = 0\%$, $\gamma = 0\%$, $\sigma = 30\%$, $T - t = 1$ and $N = 800$.

ξ	M=21	M=41	M=81	M=161
1	0.658137	0.143690	0.026107	0.006971
	2.195429	2.460436	1.905090	
2	0.252002	0.059186	0.014014	0.003056
	2.090101	2.078355	2.197110	
3	0.269837	0.077166	0.013052	0.002396
	1.806046	2.563666	2.445724	
4	0.303693	0.090864	0.016459	0.002862
	1.740837	2.464800	2.523634	
5	0.329496	0.101962	0.019449	0.003191
	1.692228	2.390271	2.607718	
6	0.349808	0.111354	0.022124	0.003498
	1.651409	2.331468	2.661031	
7	0.366531	0.119434	0.024553	0.003767
	1.617722	2.282261	2.704571	
8	0.380658	0.126579	0.026782	0.003973
	1.588455	2.240695	2.753014	
9	0.393092	0.132907	0.028847	0.004180
	1.564453	2.203930	2.786737	
10	0.403794	0.138755	0.030772	0.004379
	1.541075	2.172835	2.812973	
11	0.413034	0.143960	0.032579	0.004546
	1.520596	2.143658	2.841175	
12	0.421538	0.148877	0.034282	0.004724
	1.501543	2.118600	2.859329	
13	0.429031	0.153247	0.035894	0.004895
	1.485222	2.094036	2.874414	
14	0.436074	0.157517	0.037426	0.004989
	1.469064	2.073388	2.907113	
15	0.442243	0.161376	0.038886	0.005182
	1.454413	2.053086	2.907717	

Table 5.6: Maximum error and rate of convergence of the European passport option for various values of ξ and M, with $S(t) = 100$, $r = 5\%$, $\gamma = 4.5\%$, $\sigma = 30\%$, $T - t = 2$ and $N = 800$.

w	CNIM	HOC	HOCGS
-20	10.612413	10.614219	10.613976
-10	13.787373	13.789847	13.789170
-5	15.700414	15.703318	15.702323
-2	16.967035	16.970438	16.968990
-1	17.410351	17.413314	17.412324
0	17.864595	17.865597	17.866500
1	18.330000	18.333108	18.332004
2	18.806809	18.810562	18.808815
5	20.306628	20.309958	20.308561
10	23.027069	23.030020	23.028786
20	28.551988	29.213696	29.212595

Table 5.7: Price of the American passport option with $S(t) = 100$, $r = 5\%$, $\gamma = 4.5\%$, $\sigma = 30\%$, $T - t = 2$, $M = 800$ and $N = 800$ with $\xi = 13$.

.

Spatial nodes	CNIM error	CNIM order	HOC error	HOC order	HOCGS error	HOCGS order
21	3.692747	-	2.864784	-	0.003617	-
41	1.238479	1.576126	0.859610	1.736673	0.004003	-0.146441
81	0.284755	2.120778	0.186518	2.204366	0.000790	2.341362
161	0.054978	2.372786	0.029594	2.655934	0.000110	2.841505

Table 5.8: Maximum error and rate of convergence for the American passport option with $S(t) = 100$, $r = 5\%$, $\gamma = 4.5\%$, $\sigma = 30\%$, $T - t = 2$ and $N = 800$ with $\xi = 13$.

Chapter 6

Summary and future work

6.1 Summary of the results

The results of this thesis with some important observations are briefly described below:

The radial basis function approach was used to determine the price of the European passport option for both the symmetric and non-symmetric cases, with grid refinement being used near the zero accumulated gain in order to improve the accuracy. Further, improvement in the numerical option price and the Greeks was accomplished using three time level scheme for larger time steps for both the cases. The three time level scheme was then applied to price the American passport option with the corresponding discretized system being solved using the Brennan-Schwartz algorithm and the PSOR method. Finally, higher order compact schemes are applied to obtain the price for both the European and American Passport option with greater accuracy. In conclusion, the advantages and disadvantages of the methods proposed in the thesis are summarized in the Table below:

Scheme	Advantage	Diadvantage
RBPI	Better accuracy because of fully implicit scheme with non smooth payoff	Difficult to choose the appropriate shape parameter and optimal value for mesh refinement points
TTL	Spurious oscillations free and works well for the Greeks in case of larger time steps without loss of accuracy	Similar to classical Crank-Nicholson scheme for smaller time steps.
HOC	Better accuracy upto third order	Unable to achieve the fourth order accuracy and difficult to handle the non smooth coefficients

6.2 Future work

The possible extensions of the works carried out in this thesis are presented below:

1. Pricing of passport option with jump-diffusion

   The jump-diffusion models, which are an extension of the GBM were introduced in order to address the shortcomings of the latter model, such as non-normal properties of asset returns and volatility smile. The price of the option would typically lead to an extension of the Black-Scholes type equation, except that in this case, one will arrive at partial integro-differential equation. The problem for the risk-neutral pricing will be solved using the application of Fourier transform and the numerical implementation will be accomplished using the Fast-Fourier Transform.

2. Pricing of passport option with stochastic volatility

   In the formulation of the passport option problem, we assumed that the volatility, σ of the asset price is constant. In reality, a more accurate representation of the asset volatility would be through a separate SDE for the volatility. In particular, we will implement the passport option pricing making use of the Heston model [52]. Under this model the asset price (in the risk-neutral world) is assumed to be governed by the SDE:

$$dS(t) = rS(t)dt + \sqrt{\sigma(t)}S(t)dW_1(t),$$

where the risk-free rate r is constant and the volatility $\sigma(t)$ satisfies the SDE:

$$d\sigma(t) = (a - b\sigma(t))dt + \sigma_1\sqrt{\sigma(t)}dW_2(t).$$

The parameters a, b, σ_1 are constants and $W_1(t)$ and $W_2(t)$ are Wiener process with correlation $\rho \in (-1, 1)$.

3. Pricing of passport option using Monte-Carlo simulation

   In the real financial markets, especially with the advent of high-frequency trading, one has to resort to more efficient methods, even at the cost of some loss of accuracy. One of the classical and most widely used method is the Monte Carlo simulation. This method is based on simulation of a large number of realizable paths of the underlying asset. The resulting option price, however, is not unique but lies in a confidence interval, whose length is proportional to the sampling variance and inversely proportional to the number of simulations. This interval has to be shrunk in order to achieve more accurate pricing. One could resort to larger number of simulations, which in turn means that the method becomes less efficient defeating the very purpose of resorting to Monte-Carlo simulation. Thus one must make use of variance reduction techniques such as antithetic, control variates and stratified sampling. We propose to study the passport option using the Monte-Carlo approach as well as examine various efficient variance reduction techniques for the same.

4. Improvements in accuracy of the methods

   Some modifications such as exponential time differencing scheme (which very strict error tolerance), which have been observed to improve the accuracy of several higher order methods will be explored. In addition other classes of high accuracy methods, in particular, some spectral methods in spatial direction combined with higher order time integration schemes in the temporal direction is another possible direction of future work.

Bibliography

[1] J.C. Hull, Options, futures, and other derivatives, Pearson Education India, 2006.

[2] T. Hyer, A. Lipton-Lifschitz & D. Pugachevsky, Passport to success, Risk, vol. 10, no. 9, pp. 127-131, 1997.

[3] L. Andersen, J. Andreasen & R. Brotherton-Ratcliffe, The passport option, Journal of Computational Finance, vol. 1, no. 3, pp. 15-36, 1998.

[4] J. Topper, A finite element implementation of passport options, M.Sc. Thesis, University of Oxford, 2003.

[5] H. Malloch, The valuation of options on traded accounts: continuous and discrete time models, Ph.D. thesis, University of Sydney, 2010.

[6] I. Nagayama, Pricing of passport option, Journal of Mathematical Sciences University of Tokyo, vol. 5, no. 4, pp. 747-785, 1998.

[7] S-S. Chan, The valuation of American passport options, University of Wisconsin-Madison, Working Paper, 1999.

[8] S.P. Dirkse & M.C. Ferris, The PATH solver: A non-monotone stabilization scheme for mixed complementarity problems, Optimization Methods and Software, vol. 5, pp. 123-156, 1995.

[9] H. Ahn, A. Penaud & P. Wilmott, Various passport options and their valuation, Applied Mathematical Finance, vol. 6, no. 4, pp. 275-292, 1999.

[10] A. Penaud, P. Wilmott & H. Ahn, Exotic passport options, Asia-Pacific Financial Markets, vol. 6, no. 2, pp. 171-182, 1999.

[11] V. Henderson & D. Hobson, Local time, coupling and the passport option, Finance and Stochastics, vol. 4, no. 1, pp. 69-80, 2000.

[12] V. Henderson & D. Hobson, Passport options with stochastic volatility, Applied Mathematical Finance, vol. 8, no. 2, pp. 97-118, 2001.

[13] J. Hull & A. White, The pricing of options on assets with stochastic volatilities, Journal of Finance, vol. 42, no.2, pp. 281-300, 1987.

[14] E.M. Stein & J.C. Stein, Stock price distributions with stochastic volatility: An analytic approach, Review of Financial Studies, vol. 4, no. 4, pp. 727-752, 1991.

[15] S.E. Shreve & J. Vecer, Options on a traded account: vacation calls, vacation puts and passport options, Finance and Stochastics, vol. 4, no. 3, pp. 255-274, 2000.

[16] B. Hajek, Mean stochastic comparison of diffusions, Zeitschrift fr Wahrscheinlichkeitstheorie und Verwandte Gebiete, vol. 68, no. 3, pp. 315-329, 1985.

[17] F. Delbaen & M. Yor, Passport options, Mathematical Finance, vol. 12, no. 4, pp. 299-328, 2002.

[18] D. Pooley, Numerical methods for nonlinear equations in option pricing, Ph.D. Thesis, University of Waterloo, 2003.

[19] B. Baojun & W. Yang, A viscosity solution approach to valuation of passport options in a jump-diffusion model, Proceedings of the 27th Chinese Control Conference, Kunming, Yunnan, China, pp. 606-608, 2008.

[20] B. Baojun, W. Yang & Z. Jizhou, Viscosity solutions of HJB equations arising from the valuation of European passport options, Acta Mathematica Scientia, vol. 30, no. 1, pp. 187-202, 2010.

[21] J. Kampen, Optimal strategies of passport options, Mathematics in Industry, vol. 12, pp. 666-670, 2008.

[22] H. Malloch & P.W. Buchen, Passport option: continuous and binomial models, Finance and Corporate Governance Conference, 2011.

[23] B. Oksendal, Stochastic differential equations: an introduction with application, Springer-Verlag, Berlin-Heidelberg, 2003.

[24] A. Kanaujiya & S.P. Chakrabarty, Pricing European passport option with radial basis function, International Journal of Applied and Computational Mathematics, vol.3, no. 3, pp. 1589-1604, 2017.

[25] W. Chen, Z-J. Fu & C.S. Chen, Recent advances in radial basis function collocation methods, Springer Briefs in Applied Sciences and Technology, 2014.

[26] S. Chen, C.F.N. Cowan & P.M. Grant, Orthogonal least squares learning algorithm for radial basis function networks, IEEE Transactions on Neural Networks, vol. 2, no. 2, pp. 302-309, 1991.

[27] A. Iske, Scattered data modelling using radial basis functions, Tutorials on Multiresolution in Geometric Modelling, Springer, pp. 205-242, 2002.

[28] G.R. Liu & Y.T. Gu, A point interpolation method for two-dimensional solids, International Journal for Numerical Methods in Engineering, vol. 50, no. 4, pp. 937-951, 2001.

[29] G.R. Liu, L. Yan, J.G. Wang & Y.T. Gu, Point interpolation method based on local residual formulation using radial basis functions, Structural Engineering and Mechanics, vol. 14, no. 6, pp. 713-732, 2002.

[30] G.R. Liu & Y.T. Gu, An introduction to meshfree methods and their programming, Springer, 2005.

[31] J.A. Rad, K. Parand & L.V. Ballestra, Pricing European and American options by radial basis point interpolation, Applied Mathematics and Computation, vol. 251, pp. 363-377, 2015.

[32] A. Kumar, L.P. Tripathi & M.K. Kadalbajoo, A numerical study of Asian option with radial basis functions based finite differences method, Engineering Analysis with Boundary Elements, vol. 50, pp. 1-7, 2015.

[33] M.D. Buhmann, Radial basis functions: theory and implementations, Cambridge Monograms on Applied and Computational Mathematics, vol. 12, 2004.

[34] G.E. Fasshauer, Meshfree approximation methods with Matlab, World Scientific, vol. 6, 2007.

[35] A. Kanaujiya & S.P. Chakrabarty, Pricing and estimates of Greeks for passport option: a three time level approach, Journal of Computational and Applied Mathematics, vol. 315, pp. 49-64, 2017.

[36] R.D. Richtmyer & K.W. Morton, Difference method for initial-value problem, Interscience Tracts in Pure and Applied Mathematics, 1967.

[37] W.T. Shaw, Modelling financial derivatives with Mathematica, Cambridge University Press, 1998.

[38] G.D. Smith, Numerical solution of partial differential equations: finite difference methods, Oxford Applied Mathematics and Computing Science Series, 1985.

[39] A. Borici & H. Luthi, Fast solutions of complementarity formulations in American put pricing, Journal of Computational Finance, vol. 9, no. 1, 2005.

[40] R. Seydel, Tools for computational finance, Springer Science & Business Media, 2012.

[41] P. Jaillet, D. Lamberton & B. Lapeyre, Variational inequalities and the pricing of American options, Acta Applicandae Mathematicae, vol. 21, no.3, pp. 263-289, 1990.

[42] R.C. Merton, M.J. Brennan & E.S. Schwartz, The valuation of American put options, The Journal of Finance, vol. 32, no.2, pp. 449-462, 1977.

[43] C.W. Cryer, The solution of a quadratic programming problem using systematic over relaxation, SIAM Journal on Control, vol. 9, no. 3, pp. 385-392, 1971.

[44] J. Zhao, W. Dai & T. Niu, Fourth-order compact schemes of a heat conduction problem with Neumann boundary conditions, Numerical Methods for Partial Differential Equations, vol. 23, no. 5, pp. 949-959, 2007.

[45] D. Yambangwai & N. Moshkin, Deferred correction technique to construct high-order schemes for the heat equation with Dirichlet and Neumann boundary conditions, Engineering Letters, vol. 21, no. 2, pp. 61-67, 2013.

[46] S. Lele, Compact finite difference schemes with spectral like resolution, Journal of Computational Physics, vol. 103, pp. 16-42, 1992.

[47] L. Collatz, The numerical treatment of differential equations, Springer, Berlin Heidelberg, 1960.

[48] K.E. Atkinson, An introduction to numerical analysis, John Wiley & Sons, New York, 1988.

[49] D.Y. Tangman, A. Gopaul & M. Bhuruth, Numerical pricing of options using high-order compact finite difference schemes, Journal of Computational and Applied Mathematics, vol. 218, no. 2, pp. 270-280, 2008.

[50] C.W. Oosterlee, C.C.W. Leentvaar & X. Huang, Accurate American option pricing by grid stretching and high order finite differences, Delft University of Technology, The Netherlands, Technical Report, 2005.

[51] R.K. Bawa & S. Natesan, An efficient hybrid numerical scheme for convection-dominated boundary-value problems, International Journal of Computer Mathematics, vol. 86, no. 2, pp. 261-273, 2009.

[52] S.E. Shreve, Stochastic calculus for finance II: continuous-time models, Springer Science & Business Media, 2004.

List of Published or Communicated Papers

Based on the work in this thesis, the following research articles have been published or communicated.

1. Ankur Kanaujiya and Siddhartha P. Chakrabarty, Pricing European passport option with radial basis function, *International Journal of Applied and Computational Mathematics*, vol. 3, no. 3, pp. 1589-1604, 2017.
2. Ankur Kanaujiya and Siddhartha P. Chakrabarty, Pricing and estimates of Greeks for passport option: A three time level approach, *Journal of Computational and Applied Mathematics*, vol. 315, pp. 49-64, 2017.
3. Ankur Kanaujiya and Siddhartha P. Chakrabarty, Valuation of American passport option using a three time level scheme, communicated.
4. Ankur Kanaujiya and Siddhartha P. Chakrabarty, Higher order compact schemes with grid stretching in the numerical pricing of passport option, communicated.